Morfologische eigenschappen van trochleodysplasie en hun biomechanische impact op het patellofemorale gewricht

Morphological Characteristics of Trochlear Dysplasia and Their Biomechanical Impact on the Patellofemoral Joint

Annemieke Van Haver

Promotoren: prof. dr. P. Verdonk, dr. ir. M. De Beule, prof. dr. ir. T. Claessens
Proefschrift ingediend tot het behalen van de graad van
Doctor in de Ingenieurswetenschappen

Vakgroep Fysiotherapie en Orthopedie
Voorzitter: prof. dr. J. Victor
Faculteit Geneeskunde en Gezondheidswetenschappen

Vakgroep Elektronica en Informatiesystemen
Voorzitter: prof. dr. ir. J. Van Campenhout
Faculteit Ingenieurswetenschappen en Architectuur

Vakgroep Industriële Technologie en Constructie
Voorzitter: prof. dr. M. Vanhaelst
Faculteit Ingenieurswetenschappen en Architectuur

Academiejaar 2013 - 2014

UNIVERSITEIT GENT

ISBN 978-90-8578-633-7
NUR 954
Wettelijk depot: D/2013/10.500/66

Promoters:

Prof. dr. Peter Verdonk
Ghent University
Faculty of Medicine
Department of Physical medicine and orthopaedic surgery

Dr. ir. Tom Claessens
Ghent University
Faculty of Engineering and Architecture
Department of Industrial Technology and Construction

Dr. ir. Matthieu De Beule
Ghent University
Faculty of Engineering and Architecture
IBiTech-bioMMeda, Department of Electronics and Information Systems, iMinds
Future Health Department

Examination Committee:

Prof. dr. ir. R. Van de Walle (Chairman)	Ghent University
Prof. dr. ir. P. De Baets (Secretary)	Ghent University
Prof. dr. P. Verdonk	Ghent University
Dr. ir. T. Claessens	Ghent University
Dr. ir. M. De Beule	Ghent University
Prof. dr. ing. L. Cardon	Ghent University
Prof. dr. J. Bellemans	Katholieke Universiteit Leuven
Dr. ir. L. Labey	Katholieke Universiteit Leuven
Prof. dr. ir. B. Innocenti	Université libre de Bruxelles
Prof. dr. ir. B. Verhegghe	Ghent University

Research Institute:

Ghent University
Department of Mechanical Construction and Production
Technologiepark 903
B-9052 Gent
Belgium

Samenvatting

Introductie (hoofdstuk 1)

Luxatie van de patella (of knieschijf) is een aandoening die een grote impact kan hebben op het leven van de patiënt. Instabiliteit van de knieschijf treedt namelijk niet alleen op tijdens het beoefenen van sportactiviteiten, maar vaak ook tijdens activiteiten van het dagelijkse leven. Deze aandoening doet zich typisch voor bij jonge actieve personen. Wanneer deze patiënten ouder worden, neemt het aantal luxaties af, maar hebben ze een verhoogd risico om artrose te ontwikkelen, wat op zich weer leidt tot een toename van pijn, fysieke beperking en in sommige gevallen ook het vroegtijdig plaatsen van een patellofemorale prothese.

Het ontstaansmechanisme van patella luxatie is multifactorieel en heel complex. Als een gevolg hiervan zijn meer dan 100 verschillende chirurgische ingrepen beschreven in de literatuur. De belangrijkste risicofactor in het ontstaansmechanisme is trochleodysplasie; een morfologische afwijking van het contactvlak op de femur (dijbeen), waarop de patella op en neer glijdt bij het buigen en strekken van de knie.

Dit werk is gericht op de morfologie en de biomechanische impact van trochleodysplasie. Trochleodysplasie doet zich voor in veel vormvariaties, die moeilijk te classificeren zijn. Classificatie is echter noodzakelijk om onderzoek te kunnen doen naar patellofemorale biomechanica en behandelingsresultaten in functie van deze vormvariaties. Op basis van dit soort onderzoek kan men vervolgens goed gefundeerde chirurgische aanbevelingen doen.

Het doel van dit proefschrift is om:

- een grondige morfologische beschrijving te geven van de trochleodysplastische femur, inclusief de regio's buiten de trochlea (hoofdstukken 2 en 3).

- een methode te ontwikkelen om verschillende types trochleodysplasie te simuleren voor experimenteel kadaveronderzoek (hoofdstuk 4)

- het biomechanisch effect van verschillende types trochleodysplasie te evalueren (hoofdstuk 5)

Dit inleidend hoofdstuk beschrijft eerst de anatomie en functie van het patellofemorale gewricht. Vervolgens wordt een beschrijving gegeven van het ontstaansmechanisme en behandelingsmethoden van patella luxatie. Het derde deel van de inleiding bevat een summier overzicht van experimentele onderzoeksmethoden om de impact van risicofactoren op de patellastabiliteit te onderzoeken. Dit inleidende hoofdstuk eindigt met het uiteenzetten van het doel en de organisatie van dit proefschrift.

Morfologisch deel (hoofdstukken 2 en 3)

Traditioneel worden de morfologische kenmerken van de trochleodysplastische femur geëvalueerd op conventionele laterale of axiale röntgenfoto's. Diagnostische cut-off waarden van trochleodysplasie zijn eveneens gebaseerd op deze röntgenfoto's. Dergelijke metingen en cut-off waarden gebaseerd op röntgenfoto's hebben echter enkele belangrijke nadelen:

(1) ze houden geen rekening met de kraakbeendikte, terwijl het algemeen bekend is dat de vorm van het kraakbeen sterk kan afwijken van de vorm van het bot, vooral bij patiënten met trochleodysplasie

(2) ze kunnen leiden tot onjuiste metingen, veroorzaakt door positioneringsfouten van het been tijdens de beeldacquisitie

(3) ze houden geen rekening met de grootte van de knie, waardoor de cut-off waarden sneller bereikt worden door grote patiënten

Tegenwoordig wordt de morfologie van de trochlea meestal geëvalueerd op een selectie van axiale of laterale CT of MRI coupes. Hoewel kraakbeen kan gevisualiseerd worden op arthro-CT-scans en MRI-scans, werden de diagnostische cut-off waarden hier niet aan aangepast. Ook positioneringsfouten tijdens het scannen en grootteverschillen tussen patiënten kunnen niet in rekening gebracht worden met deze meetmethoden.

In het morfologisch luik van dit onderzoeksproject werden 3D modellen inclusief het kraakbeen gecreëerd van normale en trochleodysplastische distale femurs. Deze modellen werden vervolgens uniform herschaald om grootteverschillen uit te sluiten. De vorm van deze 3D modellen werd onderzocht met een landmark-gebaseerde analyse (hoofdstuk 2) en een statistical shape analyse (hoofdstuk 3).

Beide methoden werden toegepast om de geometrische verschillen tussen de normale en trochleodysplastische femurs te onderzoeken. Principiële componentenanalyse werd uitgevoerd om belangrijkste bronnen van variatie in de trochleodysplastische 3D modellen te beschrijven. Vervolgens werd ook een geautomatiseerde classificatie uitgevoerd om de diagnose van trochleodysplasie te faciliteren en er werd getracht om de trochleodysplastische femurs te clusteren.

Deze studies toonden aan dat de verschillen in kniegrootte opliepen tot meer dan 30%, wat een impact heeft op de cut-off waarden die gebruikt worden om trochleodysplasie te diagnosticeren.

De landmark-gebaseerde studie repliceerde reeds gekende verschillen tussen normale en trochleodysplastische knieën. De statistical shape analyse toonde tevens aan dat de trochleaire groeve niet alleen meer anterieur georiënteerd is, maar ook meer proximaal en meer lateraal. Naast de verschillen in de trochleaire regio, toonden beide analyses ook aan dat de mediolaterale breedte en de notch breedte kleiner waren in de trochleodysplastische knieën in vergelijking met de normale knieën.

De 3 belangrijkste bronnen van variatie in de trochleodysplastische 3D modellen zijn verschillen in grootte, sulcus hoek en notch breedte. Bovendien bleek dat een smallere notch breedte gepaard ging met een grotere sulcus hoek.

Automatische classificatie van normale en trochleodysplastische modellen was mogelijk met een sensitiviteit van 85% en een specificiteit van 95%. Gezien het kleine aantal geïncludeerde 3D modellen kon geen adequate clustering van trochleodysplasie bekomen worden.

Biomechanisch deel (hoofdstukken 4 en 5)

Trochleodysplasie treedt gewoonlijk op in associatie met andere afwijkingen aan de beenderen of weke delen. Daarom is het moeilijk om de biomechanische impact van trochleodysplasie op de functie van het patellofemorale gewricht te onderzoeken in een patiëntenpopulatie.

In het biomechanische deel van dit onderzoek wordt een nieuwe onderzoeksmethode gevalideerd die vervolgens wordt toegepast om het effect na te gaan van verschillende types trochleodysplasie op de patellofemorale biomechanica. Deze nieuwe methode maakt gebruik van rapid prototyping om prothesen te ontwikkelen die verschillende vormen van trochleodysplasie kunnen simuleren. Deze prothesen

kunnen vervolgens in kadaver knieën geïmplanteerd worden voor experimenteel onderzoek.

Voor de validatiestudie (hoofdstuk 4) werden 4 prothesen gemaakt die de oorspronkelijke vorm van de kadaver trochlea repliceren. Deze replica prothesen werden geïmplanteerd in de kadavers met behulp van kadaver-specifieke instrumenten. De prothesen werden geprint in 2 verschillende materialen zodat de kraakbeenlaag in een zachter materiaal kon geprint worden om vormaanpassing van het articulatievlak toe te laten. De instrumenten werden geprint in een transparant materiaal, wat toelaat om de positionering van het instrument te controleren. In deze validatiestudie werd de nauwkeurigheid van de instrumenten geëvalueerd en werden de patellofemorale kinematica, contact drukken en contact oppervlakken voor en na plaatsing van de prothesen geëvalueerd. De nauwkeurigheid van de instrumenten was vergelijkbaar met die van standaard instrumenten beschreven in de literatuur. De patellofemorale kinematica, contactoppervlakte en -druk toonden kleine gemiddelde verschillen. De invloed van de materiaaleigenschappen en nauwkeurigheidsfouten van de instrumenten kunnen uitgesloten worden door gebruik te maken van een replica prothese als controle conditie in plaats van de intacte knie.

Om het effect van trochleodysplasie te onderzoeken werden trochleodysplastische prothesen ontworpen voor 4 kadaverknieën (hoofdstuk 5). Elke kadaverknie werd getest met 4 trochleodysplastische prothesen en 1 replica prothese, welke dienst deed als controleconditie. De 3D modellen van de gewijzigde kadaver knieën (kadaverfemur + prothese) werden geclassificeerd volgens de Dejour classificatie. De patellofemorale kinematica, contact drukken, contact oppervlakten en stabiliteit warden vervolgens geanalyseerd in functie van het type trochleodysplasie.

Deze experimentele studie toonde aan dat trochleodysplasie een significante impact heeft op de patellofemorale biomechanica. De trochleodysplastische prothesen veroorzaakten toegenomen laterale tracking, toegenomen laterale tilt, interne rotatie, afgenomen contactoppervlakten, toegenomen contactdrukken en afgenomen stabiliteit van de patella. De 4 Dejour types toonden geen 4 afzonderlijke patronen in patellofemorale biomechanica. Maar trochleodysplastische types met een uitgesproken anterieure offset toonden voor alle metingen de grootste afwijkingen, wat overeenkomt met studies die een hogere incidentie van artrose en een beter resultaat van trochleoplastie aantonen in trochleodysplastische types met een uitgesproken anterieure offset.

Discussie en toekomstig onderzoek (hoofdstuk 6)

Het laatste hoofdstuk geeft een overzicht van de belangrijkste bevindingen in dit werk en beschrijft enkele suggesties voor toekomstig onderzoek.

Tot slot zijn 2 appendices toegevoegd. Appendix 1 beschrijft een pilootstudie waarin kadaver knieën getest worden in een knieproefstand die aan de UGent ontwikkeld werd. Deze studie beschrijft de knieproefstand en test de herhaalbaarheid. Appendix 2 bevat de definities van de landmarks, vlakken en metingen die gebruikt worden in hoofdstuk 2.

Summary

Introduction (chapter 1)

Patellar dislocation is a very disabling condition for the patient because instability symptoms do not only appear during sports activities but can also be experienced during activities of daily living. It is a condition that typically appears in young active people. With increasing age, patients suffer less from patellar dislocations but are at increased risk to develop isolated patellofemoral osteoarthritis, which can in turn lead to pain, disability and early patellofemoral implants.

The aetiology of patellar dislocation is multifactorial and complex, which is reflected in over 100 different surgical procedures described in literature. The main predisposing factor of patellar dislocation is trochlear dysplasia, which is a morphological abnormality of the femoral articular surface.

This work will be focussing on the morphology and biomechanical impact of trochlear dysplasia. Trochlear dysplasia is presented in many variations which are difficult to capture in a classification system. Yet, classification is necessary to evaluate the patellofemoral biomechanics and treatment outcome in function of the trochlear shape variations. In compliance with these evaluations, well-founded treatment recommendations can be achieved.

This dissertation aims to:

- Provide a profound morphological description of the trochlear dysplastic distal femur, including the regions outside the anterior trochlea (chapters 2 and 3).

- Develop a method to simulate different types of trochlear dysplasia in cadaveric knees for experimental testing (chapter 4)

- Evaluate the biomechanical effect of different types of trochlear dysplasia (chapter 5)

This introducing chapter first describes the anatomy and function of the patellofemoral joint, followed by a description of the aetiology and treatment methods of patellar dislocation. The third part of this introduction consists of a brief overview of experimental research methods employed to investigate the impact of predisposing factors on the patellar stability.

Morphological part (chapters 2 and 3)

Traditionally, the morphological characteristics of the trochlear dysplastic femur are evaluated on lateral or axial radiographs. Diagnostic cut-off values of trochlear dysplasia are based on such radiographs as well. Important disadvantages of these radiographs include that (1) they do not take the cartilage thickness into account, while it is well established that the cartilage anatomy can differ markedly from the osseous anatomy, particularly in patients with trochlear dysplasia and (2) they can lead to incorrect measurements due to positioning errors of the legs during image acquisition and (3) the size of the knee is not taken into account, therefore cut off values will more easily be reached by large patients compared to small patients.

Nowadays, evaluation of the trochlear shape is usually done on selected axial or lateral CT or MRI slices. Though cartilage can be visualised on arthro-CT scans and in MRI scans, the diagnostic cut-off values were not adjusted to take cartilage into account. In addition, positioning errors and size differences are still not taken into account.

In the morphological part of this research project, 3D surface models of normal and trochlear dysplastic distal femurs, including the cartilage, were created. Consequently, these models were uniformly scaled to rule out size differences. The shape of these 3D surface models was investigated with a landmark-based analysis (chapter 2) and a statistical shape analysis (chapter 3).

Both methods were used to evaluate the geometrical differences between normal and trochlear dysplastic femurs. PCA was applied to describe the main modes of variation in trochlear dysplastic femurs, to perform automated classification to facilitate diagnosis of trochlear dysplasia and in addition, clustering was attempted to facilitate classification of trochlear dysplasia.

The studied population showed knee size differences up to 30%, affecting the cut-off values which are commonly used to diagnose trochlear dysplasia. The landmark-based morphology study replicated well-established differences between normal and trochlear dysplastic knees. The statistical shape analysis also showed that the trochlear groove was not only elevated but also proximalized and lateralised. In addition, both analyses showed that the mediolateral width and the notch width were reduced in the trochlear dysplastic femurs. PCA demonstrated that the first 3 PCs mainly concerned size, sulcus angle and notch width and that a smaller notch width was accompanied by an increased sulcus angle. Automated classification could be

achieved with a sensitivity of 85% and a specificity of 95%. Given the small number of included samples, no adequate clustering could be obtained.

Biomechanical part (chapters 4 and 5)

Trochlear dysplasia occurs usually in association with other osseous or soft-tissue abnormalities. Therefore it is difficult to investigate the biomechanical impact of trochlear dysplasia on the patellofemoral function in patients.

In the biomechanical part of this research project, a new research method was first validated and then applied to investigate the effect of different types of trochlear dysplasia on the patellofemoral biomechanics. This new method implemented the use of rapid prototyped implants to simulate trochlear shape variations in cadaver knees.

For the validation study (chapter 4), the trochlear shape of 4 cadaver knees was replicated. These trochlear replicas were implanted in the cadaver knees with the help of cadaver-specific guiding instruments. Both the implants and guiding instruments were based on the arthro-CT scans of the cadaver knees and were manufactured with rapid prototyping. The implants were printed with a multi-material 3D printer. This permitted printing the cartilage layer in a softer material, allowing for articular shape adaptation. The guiding instruments were printed in a translucent material to allow monitoring of the position of the guiding instrument. In the validation study, the accuracy of the guiding instruments was evaluated and the patellofemoral kinematics, contact areas and contact pressures before and after placing the replica implants were evaluated. The accuracy of the guiding instruments was found comparable with the accuracy of standard guiding instruments reported in literature. The patellofemoral kinematics and contact area and pressure showed small mean differences. The influence of the material properties and rotational errors of the implants can be countered by using a replica implant as a control condition instead of the native condition.

To investigate the effect of trochlear dysplasia, trochlear dysplastic implants were designed for four cadaver specimen (chapter 5). Each knee was tested with 4 trochlear dysplastic implants and 1 replica implant, which served as the native condition. The 3D models of the modified cadavers (cadaver femur + implant) were graded with the 4-grade Dejour classification. The patellofemoral kinematics, contact pressure, contact area and stability were then analysed in function of the type of trochlear dysplasia. The experimental study demonstrated that trochlear dysplasia had a significant impact on patellofemoral biomechanics. Trochlear dysplasia

showed increased lateral tracking, increased lateral tilt, increased internal rotation, decreased contact areas, increased contact pressures and decreased patellar stability. The 4 Dejour types did not demonstrate 4 different patterns in patellofemoral biomechanics. However, trochlear dysplastic types with a pronounced trochlear bump demonstrated the largest deviations for all parameters, which is in line with studies showing a higher incidence of osteoarthritis and a better outcome of trochleoplasty in trochlear dysplastic types with a pronounced trochlear bump.

Discussion and future prospects (chapter 6)

The final chapter gives an overview of the major findings of this dissertation and provides some suggestions for further research.

In addition, 2 appendices are included. The first appendix describes a pilot cadaver study on an Oxford-like knee rig developed at Ghent University. This study described the knee rig and investigated its repeatability. The second appendix lists the details of the landmarks, planes and measurements applied in chapter 2.

TABLE OF CONTENTS

Abbreviations

2D	two-dimensional
3D	three-dimensional
AP	anteroposterior
aTEA	anatomical transepicondylar axis
CT	computed tomography
CV	coefficient of variation
F_{GR}	ground reaction force
FLCEP	femoral lateral condyle external point
FLCIP	femoral lateral condyle internal point
FLCP	femoral lateral condyle posterior
FLCPP	femoral lateral condyle posterior proximal
FLE	femoral lateral epicondyle
FLTA	femoral lateral trochlea anterior
FMCD	femoral medial condyle distal
FMCEP	femoral medial condyle external point
FMCIP	femoral medial condyle internal point
FMCP	femoral medial condyle posterior
FMCPP	femoral medial condyle posterior proximal
FME	femoral medial epicondyle
FMS	femoral medial sulcus
FMTA	femoral medial trochlea anterior
F_{PFJR}	patellofemoral joint reaction force
F_{Q}	quadriceps force
ITB	iliotibial band

l_{femur}	length of the femur
LPFL	lateral patellofemoral ligament
l_{tibia}	length of the tibia
ML	mediolateral
MPFL	medial patellofemoral ligament
MRI	magnetic resonance imaging
PCA	principal component analysis
PC	principal component
PCL	posterior condylar line
PD	proximodistal
PE	proximal edge of the trochlear cartilage
PF	patellofemoral
PIP	patella inferior point
PLP	patella lateral point
PMP	patella medial point
PSP	patella superior point
PT	patellar tendon
RF	rectus femoris
RMS	root mean square
RPT	rapid prototyping technology
SD	standard deviation
SSA	statistical shape analysis
SSM	statistical shape modelling
sTEA	surgical transepicondylar axis
TD	trochlear dysplasia
TT-TG	tibial tubercle–trochlear groove

VI	vastus intermedius
VLL	vastus lateralis longus
VLO	vastus lateralis obliquus
VML	vastus medialis longus
VMO	vastus medialis obliquus

Chapter 1

Introduction

Recurrent dislocations of the patella (knee cap) can be very disabling to the patient because instability symptoms do not only appear during sports activities but can also be experienced during activities of daily living (Andrish 2008). With increasing age, patients suffer less from patellar dislocations (Crosby and Insall 1976), but are at increased risk to develop isolated patellofemoral osteoarthritis (Grelsamer et al. 2008).

The aetiology of patellar dislocation is multifactorial and complex. Predisposing factors of patellar dislocation include osseous as well as soft tissue abnormalities and if present, they can cause patellar dislocations in one knee and patellofemoral pain without instability or dislocation in the contralateral knee (Feller et al. 2007). Of these predisposing factors, trochlear dysplasia –a morphological abnormality of the femoral articular surface- is identified as the most important factor (Dejour et al. 1994).

More than 100 different procedures have been described to prohibit patellar dislocations and to repair the knee damage caused by the dislocation (Fithian et al. 2001). Preventing redislocation however is no guarantee for success. On long term some studies have even reported an increased risk of developing patellofemoral osteoarthritis after surgery, despite the reduction in dislocations (Andrish 2008).

Patellofemoral disorders have received a lot of attention in literature to properly diagnose its exact aetiology and focus on a proper treatment regime (Arendt and Dejour 2013). Still, the patellofemoral joint and its pathology is probably the least understood field in the knee joint (Dejour et al. 2013).

In this work, the shape variations of the distal femur and their impact on patellofemoral biomechanics are investigated.

In this introducing chapter, the anatomy and function of the patellofemoral joint is briefly described, followed by a description of the aetiology and treatment methods of patellar dislocation. The third part of this introduction consists of a brief overview of experimental research methods employed to investigate the impact of predisposing factors on the patellar stability. At the end of the introduction, the aim of this research project and the organisation of the dissertation are explained.

1. 1. The patellofemoral joint

1. 1. 1. Anatomy

The patellofemoral (PF) joint is composed by the patella and the femoral trochlea, which have a low degree of congruency by nature, making the PF joint susceptible to dislocation.

The patella is a sesamoid bone situated at the anterior side of the knee. It is enclosed within the quadriceps muscle. The posterior side of the patella has two main articular facets (medial and lateral facet) which are covered with cartilage and articulate with the femoral trochlea (Figure 1.1). On close inspection, multiple articulating facets can be distinguished in patterns that are unique to each individual (Kwak et al. 1997).

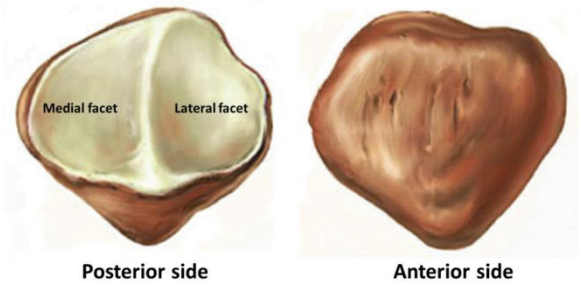

Figure 1.1 Posterior (left) and anterior view (right) on the patella (Source: Sobotta Atlas of Human Anatomy, 1994)

The femoral trochlea, also covered with articular cartilage, is located at the anterior aspect of the distal femur. The trochlea is composed of two facets, the medial and lateral facet, which are divided by the trochlear groove (Figure 1.2).

Distally, this groove deepens and becomes the intercondylar notch In the normal PF joint, the lateral facet is extending more proximally and anteriorly compared to the smaller medial facet (Amis 2007, Shih et al. 2004).

In the axial plane, the trochlea is generally V-shaped. The opposing articular cartilage surfaces of the patella and trochlea are congruent at different knee flexion angles, while the corresponding subchondral osseous contours do not necessarily do so (Staubli et al. 1999).

In the sagittal view, the PF articulation is incongruent with only a minority of the patella in contact with the trochlea at any given knee flexion angle (Grelsamer and Weinstein 2001).

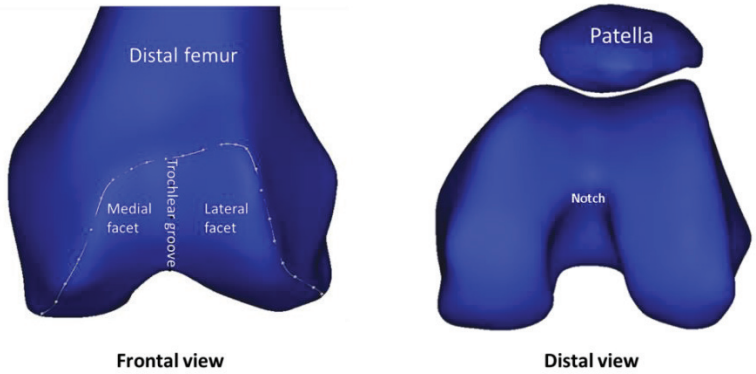

Figure 1.2 Frontal and distal view of the distal femur showing the femoral trochlea

Smooth interaction of these complex geometries is essential for the PF joint function. Small shape variations of the patella or trochlea can be tolerated as long as the articular surfaces of the patella and trochlea are congruent (Grelsamer et al. 2008). Larger trochlear shape variations, however, cannot be compensated by a matching patella. These variations include unusual steep, shallow, flat or even convex trochlea's (Figure 1.3) (Grelsamer et al. 2008).

In such cases of shallow, flat or convex trochlea's (trochlear dysplasia), it has been found that the patella frequently has a distal medial facet, which is smaller than normal and which does not articulate with the trochlea (Fucentese et al. 2006).

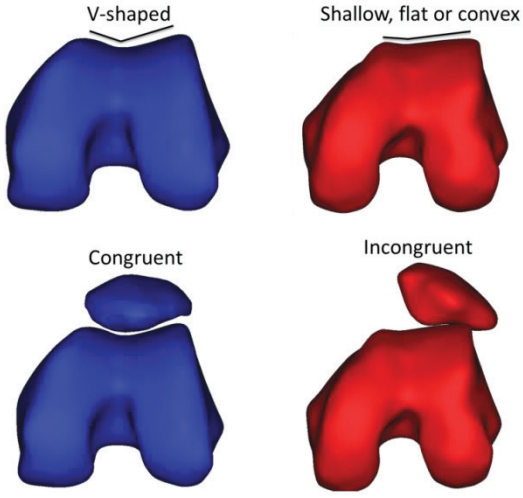

Figure 1.3 Distal view on 3D models of femur and patella, including the cartilage. The blue models show a normal knee with a V-shaped trochlea, congruent with the patella. The red models show an abnormal knee with a shallow trochlea, incongruent with the patella.

The patella is surrounded by a cruciform soft tissue system (Figure 1.4).

- Proximal pole of the patella: the quadriceps tendon connects the patella to the quadriceps muscle. The quadriceps muscle is composed by six components which apply forces on the patella in the proximal, medial and lateral side direction: VLL, VLO, VML, VMO, RF and VI (Farahmand et al. 1998).

- Distal pole of the patella: the PT connects the patella to the tibia (tuberositas tibiae).

- Medial pole of the patella: the MPFL connects the patella to the medial condyle of the femur.

- Lateral pole of the patella: the LPFL connects the patella to the lateral condyle of the femur.

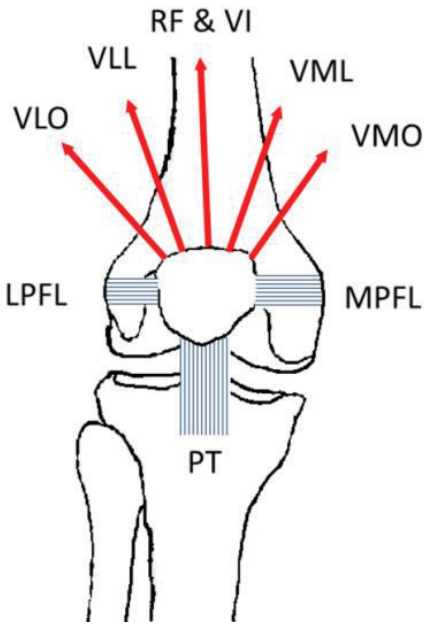

Figure 1.4 Cruciform soft tissues system surrounding the patella: Proximally: vastus lateralis obliquus (VLO), vastus lateralis longus (VLL), rectus femoris (RF) and vastus intermedius (VI) vastus medialis longus (VML), vastus medialis obliquus (VMO). Distally: patellar tendon (PT). Medially: medial patellofemoral ligament (MPFL). Laterally: lateral patellofemoral ligament (LPFL).

In addition, the patella is also connected medially and laterally to the tibia by the medial and lateral patellotibial band and to the medial meniscus by the patellomeniscal ligament. Together with the MPFL and LPFL, these structures form the deep retinacular layer. This deep layer is covered by the superficial retinacular layers, which connect the fasciae of the vastus lateralis and medialis to the patella. Together, the deep and superficial layers are referred to as the medial and lateral retinaculum (Powers et al. 2006). In severe cases of TD, the lateral retinaculum can be thickened and foreshortened (Arendt and Dejour 2013)

1. 1. 1. Function

The PF joint acts as a lever which transmits the force of the quadriceps muscle to the lower leg (Hehne 1990). The patella acts as a fulcrum to increase the moment arm of the quadriceps. As a consequence the patella needs to withstand great compressive loads. To cope with these high loads, the patella has some efficient characteristics:

- The patellar articular cartilage is thicker, softer and more permeable than any other human articular cartilage, including that of the trochlea (Grelsamer et al. 2008), providing the patella with an optimal cushioning effect and low friction coefficient.

- When the PF contact pressures are maximal (at around 90° of knee flexion), the PF joint shows a maximal contact area and maximal cartilage thickness (Huberti and Hayes 1984, Luyckx et al. 2009).

Figure 1.5 schematically shows hypothetic forces acting on the PF joint in a nearly extended knee and in a flexed knee, demonstrating that for a given quadriceps muscle force, the PF joint reaction force increases as the knee flexion angle increases.

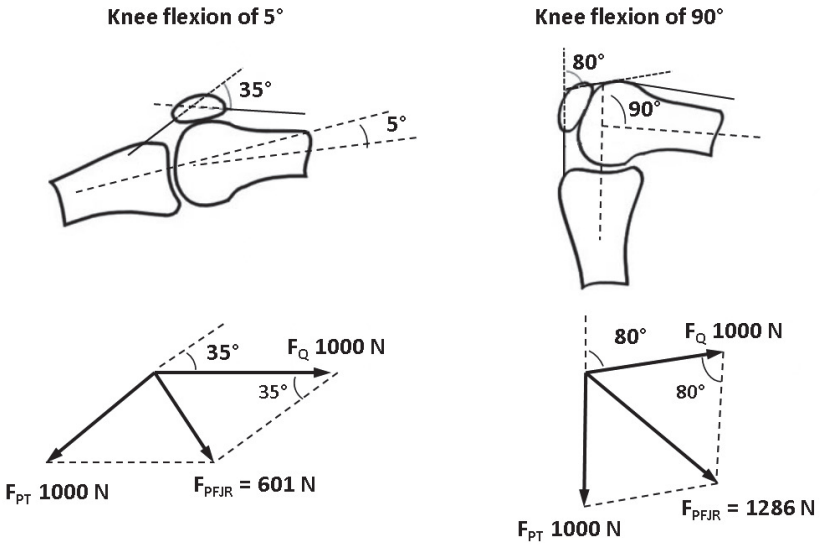

Figure 1.5 Schematic representation of the quadriceps force (F_Q), patellar tendon force (FPT) and patellofemoral joint reaction force (FPFJR) at 5° and 90° of knee flexion

1. 1. 2. Stability

When the knee is viewed in the frontal plane, the quadriceps muscle tends to displace the patella laterally because of the laterally oriented Q-angle (angle between the axis of the F_Q and the axis of the PT).

When the knee is in extension, this Q-angle is maximized because of the accompanied external rotation of the tibia, which moves the tuberositas tibiae laterally (Figure 1.6). The patellar stability is assured by bony constraints (passive) due to congruity between the patella and the femoral trochlea (Merchant et al. 1974) and by soft tissue constraints, which can be subdivided in active and passive stabilisers (Farahmand et al. 1998). The quadriceps muscle is considered as the active stabilizer and the MPFL together with the retinacula as main passive stabilisers (Farahmand et al. 1998).

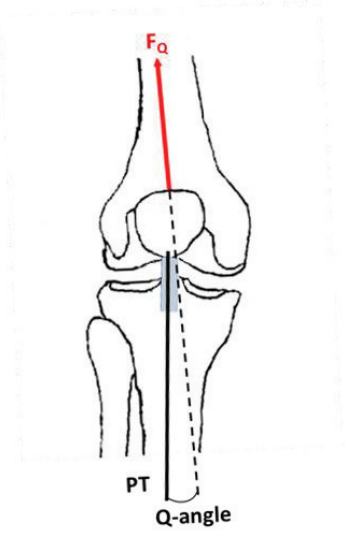

Figure 1.6 Intersection of axis of the quadriceps force (F_Q) and axis of patellar tendon (PT), forming the Q-angle

The relative contributions of these stabilisers vary in function of the knee angle:

In extension and early flexion the patellar stability is mainly ensured by the medial PF ligament. When the quadriceps is contracted, the MPFL is tight in full knee extension, it stabilizes the patella during early flexion (until 30°) and brings the patella into the trochlear groove to ensure normal further tracking of the patella (Amis et al. 2003, Philippot et al. 2012). In addition, the VMO has also been reported to contribute to patellar alignment during early knee flexion (Sakai et al. 2000). However, this contribution remains controversial (Philippot et al. 2012).

In deeper knee flexion (>30°) the MPFL is relaxed and the patella has entered the trochlear groove. The patella is now stabilised by the PF joint congruity and the PF joint compression caused by the increasing force vectors of the quadriceps tendon and PT (Farahmand et al. 1998). While the patella is tracking within the trochlea, the slope of the lateral trochlear facet provides resistance to lateral patellar translation (Carrillon et al. 2000).

Experimental patellar stability studies on cadaver specimens have demonstrated that the lowest lateral patellar stability occurs at 20° of knee flexion (Amis et al. 2003, Senavongse and Amis 2005). This supports observations in patients showing that lateral maltracking and dislocation of the patella occurs during the last 20-30° of knee extension (Doucette and Child 1996, Powers 2000, Varadarajan et al. 2010).

1. 2. Patellar dislocation

1. 2. 1. Definitions

In literature, patient inclusion is often based on different criteria, which are not always clearly defined. Patellar instability is a general term and can range from a subjective feeling of giving-way of the patella to recurrent true dislocations of the patella and even permanent or habitual dislocations in knee flexion. In this research project only knees with recurrent dislocations of the patella are included. To avoid confusion of terminology, a list with definitions of frequently used terms is provided.

Terms referring to instability:

- *Objective patellar instability*: At least one documented patellar dislocation which involves a total loss of contact between the patellar and femoral articular surfaces (Dejour 1987).

- *Symptomatic patellar instability*: All patellar instabilities characterized by a true dislocation of the patella which involves a total loss of contact between the patellar and femoral articular surfaces (Dejour et al. 1994).

- *Potential Patellar Instability*: No patellar dislocation, but pain and one or more instability factors (Dejour 1987).

Terms referring to dislocation:

- *Dislocation or "True dislocation"*: A total loss of contact between the patellar and femoral articular surfaces (Dejour et al. 1994).

- *Acute patellar dislocation* or "Primary/ first-time/ first episode patellar dislocation": A clinical entity that usually causes a traumatic disruption of the previously uninjured medial peripatellar structures. A traumatic injury disrupts normal or previously uninjured confinement of the patella within the femoral groove (Arendt et al. 2002, Atkin et al. 2000).

- *Recurrent or episodic patellar dislocation*: A minimum of two true patellar dislocations (Dejour 1987).

- *Permanent and habitual patella dislocation*: The patella dislocates systematically when the knee is flexed (Dejour 1987).

Patellar subluxation:

> The term "subluxation" can refer to either a radiographic sign (displacement of the patella), a finding on the physical examination (mediolateral hypermobility), or a patient's symptoms (feeling of giving-way) (Grelsamer 2005).

1. 2. 2. Epidemiology

Acute patellar dislocation is the second most common cause of traumatic hemarthrosis of the knee and accounts for approximately 3% of all knee injuries (Stefancin and Parker 2007). Primary dislocations usually occur during sports or dancing activities (Fithian et al. 2004). The mechanism of injury is typically with the foot planted and the tibia externally rotated (Hayes et al. 2000). Primary dislocation generally causes hemarthrosis, MPFL injury and medial retinacular disruption (Sillanpaa et al. 2008).

Children aged 10-17 years are most at risk to dislocate their patella (Andrish 2008, Fithian et al. 2004, Nietosvaara et al. 1994) and in this high-risk age range girls were found to be 33% more at risk for primary dislocations and 300% more at risk for recurrent patellar dislocation compared to boys of the same age (Table 1.1) (Fithian et al. 2004).

Table 1.1 Average annual risk for first time patellar dislocation per 100.000 members ± 95% Confidence interval. Based on (Fithian et al. 2004).

Age (years)	Female	Male	Both
10-17	33 ± 11	25 ± 9	29 ± 8
18-29	7 ± 4	10 ± 8	9 ± 6
≥ 30	1 ± 1	1 ± 1	1 ± 1
Overall			5.8 ± 1

After the primary dislocation, young age at the time of the primary dislocation, female sex, familial history of patellar instability and TD have been reported as risk factor for recurrent patellar dislocations (Andrish 2008, Atkin et al. 2000, Dejour et al. 1994, Fithian et al. 2004, Nietosvaara et al. 1994).

Predisposing factors for both primary and recurrent patella dislocations are TD, patella alta, increased tibial tubercle–trochlear groove (TT-TG) distance and patella tilt (Dejour et al. 1994).

1. 2. 3. Predisposing factors

Four principal factors are associated with primary and recurrent patellar dislocations with statistical threshold: TD (trochlear bump ≥ 3 mm and/or trochlear depth ≤ 4 mm), patella alta (>1.2 as defined by the Caton/Deschamps index), increased tuberositas tibiae – trochlear groove distance (TT-TG >20 mm) and excessive lateral patellar tilt (>20°) (Dejour et al. 1994). In more than 96% of the patients with patellar dislocations radiographic examination will detect at least one of the four following factors:

Trochlear dysplasia

TD is identified as the main predisposing factor of patellar dislocation. It is defined as a trochlea with a shallow, flat or convex articular zone of variable length, which is situated proximally and is associated with a shallow groove distally (Dejour et al. 1994).

H. Dejour defined TD by one qualitative and two quantitative signs of the femoral trochlea: the crossing sign, the trochlear depth and the trochlear bump measured on a true lateral radiograph with perfect superimposition of the medial and lateral posterior condyles (Figure 1.7):

- Crossing sign: present in 96% of the patients with objective patellar instability compared to 3% in the reference normal group. The line of the trochlear floor crosses the anterior contour of the lateral femoral condyle (subjective sign).

- Trochlear depth ≤ 4 mm: present in 85% of the patients with objective patellar compared to 3% in the reference normal group. The trochlear depth is measured as the distance between the trochlear floor (contour of the trochlea on a midsagittal section, figure 1.7, point B) and the most anterior point of the trochlea (figure 1.7, point A) along a line subtended 15° from the perpendicular to the tangent of the posterior femoral cortex (Figure 1.7, distance AB)

- Trochlear bump ≥ 3 mm: present in 66% of the patients with objective patellar instability compared to 6.5% in the reference normal group. The bump is measured between a tangential line to the anterior cortex and the trochlear floor (Figure 1.7, Distance BC).

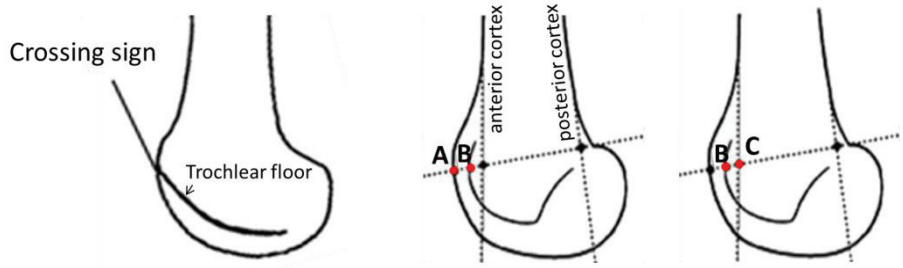

Figure 1.7 Assessment of the crossing sign, trochlear depth and trochlear bump, according to H. Dejour (Dejour et al. 1994)

H. Dejour proposed a three-grade classification based on the (proximodistal) level of the crossing sign and on the presence of asymmetry of the lateral and medial condyle (Dejour et al. 1994) (Figure 1.8):

- Type I (minor dysplasia): The condyles are symmetrical and single crossing sign on the superior portion of the trochlear floor
- Type II (moderate dysplasia): The condyles are asymmetrical and double crossing sign at a variable level
- Type III (major dysplasia): The condyles are symmetrical, single crossing sign low in the groove

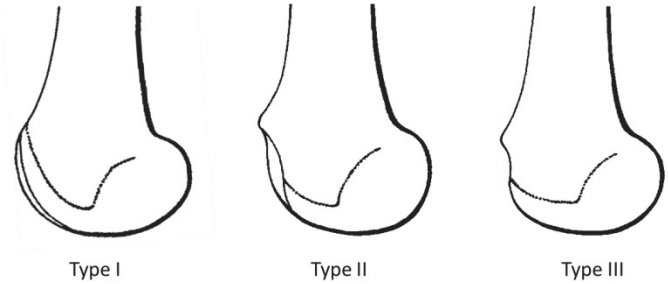

Figure 1.8 Three-grade classification according to H. Dejour (Dejour et al. 1994)

This three-grade classification however showed a poor intra- and interobserver agreement (Remy et al. 1998). Later, D. Dejour introduced two new signs on lateral radiographs (Dejour et al. 1998):

- Supratrochlear spur: global prominence of the trochlea, acts as a “ski jump” when the patella engages the trochlea.

- Double contour: radiographic line ending below the crossing sign; it represents the projection of the hypoplastic medial facet on the lateral view.

D. Dejour proposed a four-grade classification on 2-dimensional true lateral radiographs and 3-dimensional CT scans (on the first proximodistal axial image, where the complete cartilaginous trochlea can be seen) (Dejour et al. 1998) (Figure 1.9):

- Type A: fairly shallow trochlea on an axial view; crossing sign on a lateral view

- Type B: flat or convex trochlea on an axial view; supratrochlear bump on a lateral view

- Type C: asymmetry of trochlear facets, hypoplastic medial condyle on an axial view; crossing sign, a double contour on a lateral view

- Type D: asymmetry of trochlear facets, vertical join, cliff pattern on an axial view; crossing sign, double contour, supratrochlear bump on a lateral view

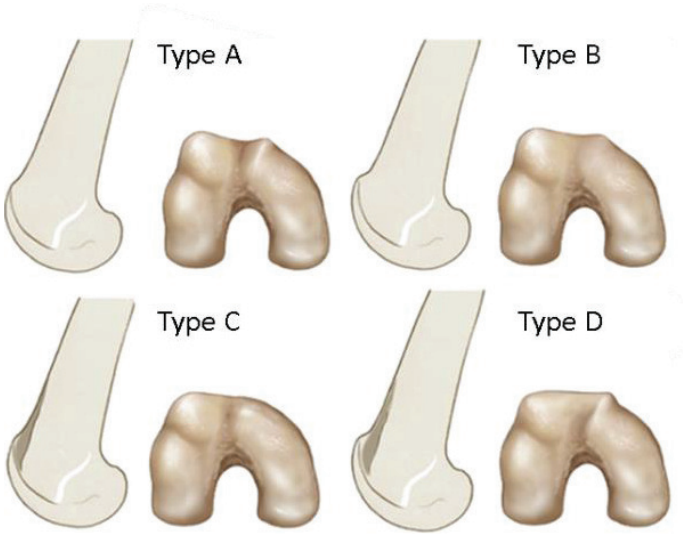

Figure 1.9 Four-grade Dejour classification: Trochlear dysplasia type A, B, C, D. (Reprinted with permission from Springer-Link (Zaffagnini et al. 2010))

In patients with objective patellar dislocation the prevalence of these different types of TD is estimated to be 54% for type A, 17% for type B, 9% for type C and 11% for type D.

This four-grade classification is widely in use to assess the severity of TD and to decide which treatment is best suited for the patient. This classification demonstrated improved reproducibility compared to the three-grade classification (Remy et al. 2002). However distinguishing type B, C and D recently showed a poor intra- and interobserver agreement (Lippacher et al. 2012).

Besides the measurements described by H. Dejour, many other measurements have been described to assess the shape of the femoral trochlea. Important measurements include the sulcus angle (Merchant et al. 1974), medial and lateral inclination angle of the trochlea (Stefanik et al. 2012), asymmetry of the trochlear facets (Pfirrmann et al. 2000) and height of the trochlear cartilage (Yamada et al. 2007) (Figure 1.10).

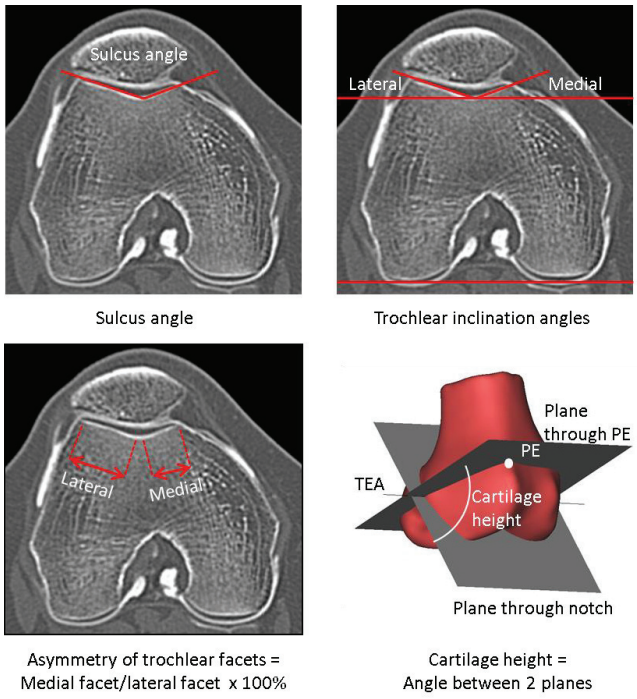

Figure 1.10 Measurements of the femoral trochlea: Sulcus angle, medial and lateral trochlear inclination angle, asymmetry of the trochlear facets (expressed as a percentage of the medial to the lateral facet length), cartilage height (defined as the angle between a plane through the transepicondylar axis (TEA) and the notch and a plane through the TEA and the proximal edge of the cartilage (PE)).

Consequently, other systems to identify or classify TD have been proposed as well. Biedert described two morphologic types of TD; a trochlea with a decreased lateral condylar height and, more commonly, a trochlea with an increased central/medial height (Biedert and Bachmann 2009). Pfirrmann et al. found that measuring the trochlear depth and trochlear facet asymmetry were most successful to diagnose TD (Pfirrmann et al. 2000). Carrillon et al. found that the lateral trochlear inclination angle was the most successful parameter to identify knees with patellar instability (Carrillon et al. 2000).

Patella alta

Patella alta is defined as a superior patellar position relative to the trochlear groove of the femur (Insall and Salvati 1971). Patella alta is reported in 24% of the patients with objective patellar instability. Of these patients, 77% have bilateral patella alta even if the contralateral knee is asymptomatic (Dejour et al. 1994). Patella alta is frequently associated with TD and rarely occurs in isolation (Caton et al. 1990, Dejour et al. 1990). In some patients with patella alta and patellar instability, the length of the PT is increased while the proximodistal position of the tibial tubercle was within normal limits (Neyret et al. 2002).

In patients with patella alta, the patella engages the trochlea at a greater knee flexion angle. As a consequence, the patella is mediolaterally less constrained and lateral patellar maltracking may occur in extension and early knee flexion (Colvin and West 2008, Pal et al. 2013). In addition, patella alta causes disturbed contact areas between the patella and trochlea, resulting in increased PF pressures and potentially increased rates of PF osteoarthritis (Stefanik et al. 2010, Ward et al. 2007).

Patella alta can be assessed in many ways. Most used indexes are performed on lateral radiographs with a knee flexion angle of $\geq 20°$ to ensure tension of the PT to show the full length of the tendon (Figure 1.11):

- Caton-Deschamps index = distance from the inferior part of the patellar articular surface to the antero-superior angle of the tibia outline (AT) / length of the articular surface of the patella (AP). AT/AP ≥ 1.2 indicates patella alta (Caton et al. 1982)

- Insall-Salvati index = length of the PT (LT) / longest sagittal diameter of the patella (LP). LT/LP > 1.2 indicates patella alta (Insall and Salvati 1971)

- Blackburne and Peel index = distance measured from a line projected tangential to the tibial plateau to the inferior part of the patellar articular surface (AB) / the length of the patellar articular surface (AP). AB/AP > 1 indicates patella alta (Blackburne and Peel 1977)

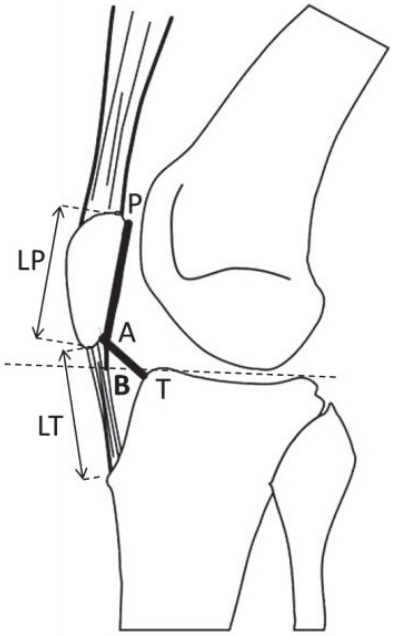

Figure 1.11 Indexes to assess patellar height: Caton-Deschamps index (AT/AP), Insall-Salvati index (LT/LP), Blackburne and Peel index (AB/AP)

Patellar tilt

Excessive lateral patellar tilt is highly associated with TD and with patella dislocations. H. Dejour found lateral patellar tilt ≥ 20° in 83% of the knees with objective patellar instability compared to 3% in the reference normal group (Dejour et al. 1994). More recently, a direct relation between patellar tilt and the type of TD was demonstrated: higher grades of TD show higher lateral patellar tilt (Arendt and Dejour 2013).

The aetiology of patella tilt remains uncertain. H. Dejour first hypothesized that external patellar tilt is a consequence of muscular disequilibrium (weakness of the vastus medialis combined with a contracture or hypertonicity of the vastus lateralis)

(Dejour et al. 1994). Recently, it was stated that lateral tilt may represent lateral tightness, but always represents medial laxity (Arendt and Dejour 2013).

Patellar tilt is measured using two axial cuts; on the first cut a line is drawn going through the transverse axis of the patella and on the second cut a line is drawn tangential to the posterior femoral condyles. The angle formed between these two lines is the patellar tilt angle (Figure 1.12) (Dejour et al. 1994).

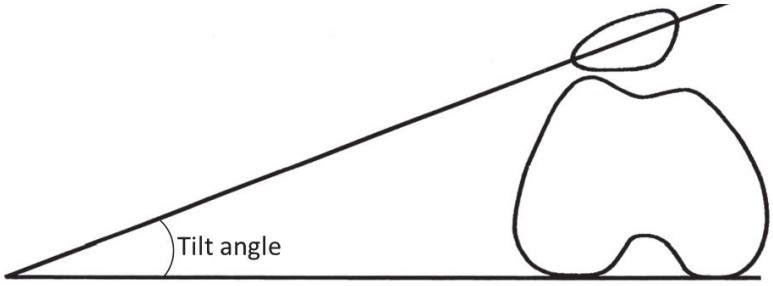

Figure 1.12 Measurement of the patellar tilt angle. Based on (Dejour et al. 1994)

Increased tuberositas tibiae – trochlear groove distance (TT-TG distance)

The pathologic threshold of the TT-TG distance is set at 20 mm. In objective patellar instability, 56% of the patients showed TT-TG values > 20 mm, compared to only 3.5% of control patients. 24% of the contralateral asymptomatic knees showed a TT-TG displacement ≥ 20 mm (Dejour et al. 1994).

A large TT-TG distance increases the Q-angle and hereby induces a large lateral tracking vector (as explained in section 1.1.2.). Measurement of the TT-TG groove has been reported not very precise and should therefore not be used as an isolated factor (Arendt and Dejour 2013).

TT-TG distance is measured on a CT image in 0°-15° knee flexion with a superimposition of the central point of the proximal part of the tibial tuberosity and the deepest point of the trochlear groove (Figure 1.13) (Dejour et al. 1994).

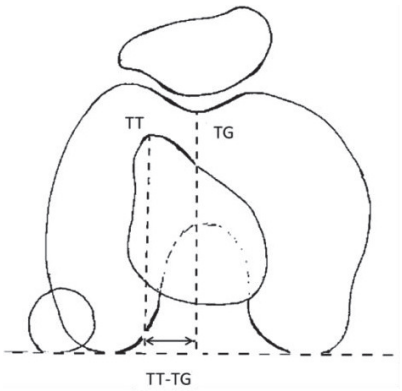

Figure 1.13 Measurement of the tuberositas tibiae-trochlear groove distance (superimposition of 2 axial slices). Based on (Dejour et al. 1994)

1. 2. 4. Surgical treatment methods

Surgical interventions for PF instability can vary considerably between centres and orthopaedic surgeons apply often only 1 or 2 procedures (Feller et al. 2007). However, the general idea about PF joint surgery is that the main cause of the instability should be identified to select the appropriate treatment regime. This concept 'menu à la carte' was proposed by Henri Dejour in 1987 (Table 1.2) (Dejour 2013).

Table 1.2 Overview of the main factors of patellar instability and the appropriate treatment according to H. Dejour (1987)

Main factors of patellar instability			
Trochlear dysplasia	Patella Alta	TT-TG distance	Patellar tilt
	Index > 1.2	> 20 mm	> 20°
96% True dislocation	30% True dislocation	56% True dislocation	83% True dislocation
3% Control	0% Control	12 mm Control	
"Menu à la carte" - H. Dejour, 1987			
Trochleoplasty ?	tibial tubercle distalization	tibial tubercle medialization	vastus medialis plasty

Despite numerous studies, there is still no consensus on the aetiological factors of patellar dislocation and at which thresholds these factors need to be corrected (Arendt and Dejour 2013, Dejour et al. 2013).

As a consequence, a high number of surgical techniques has been proposed to address the soft tissues, osseous tissues or both (Dejour et al. 2013). These surgical techniques attempt to improve congruity and stability of the PF joint by correcting the trochlear shape (trochleoplasty) and the patellar position relative to the trochlea. The latter can be subdivided in proximal realignment techniques (reconstruction of the MPFL or lateral release) and distal realignment techniques (repositioning of the tuberositas tibiae).

Deepening trochleoplasty

Two main types of trochleoplasty have been described to modify the shape of the trochlear groove: the lateral facet of the trochlea can be lifted or the central trochlea can be deepened to create a new trochlear groove. Trochleoplasty is only performed by a small number of surgeons (Beaufils et al. 2012), which is probably due the technical difficulty of the operation, the lack of agreement on the inclusion criteria and the wide variety of surgical methods (Dejour et al. 2013).

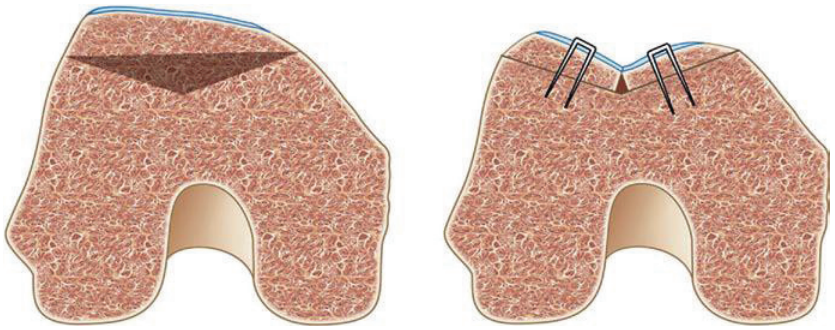

Figure 1.14 Deepening trochleoplasty (Reprinted with permission from Springer-Link (Zaffagnini et al. 2010))

During the sulcus deepening trochleoplasty cancellous bone is removed from underneath the trochlear groove (Figure 1.14). After removing the cancellous bone, the medial and lateral facets of the trochlear groove are created by fixing the cartilage layer with staples to each side of the groove. This way, a new groove with normal depth is created, which will correct patellar tracking. Trochleoplasty requires

outstanding surgical skill and the capacity to ‘‘see’’ and recreate trochlear anatomy (Arendt and Dejour 2013).

To date, the debate remains in what clinical settings the trochlear anatomy should be altered (Arendt and Dejour 2013). Currently, sulcus deepening trochleoplasty is only indicated in high grade TD with patellar instability and/or abnormal tracking (Arendt and Dejour 2013). This patient population frequently shows additional abnormalities which need to be addressed as well. Trochleoplasty is therefore commonly performed in combination with other corrections like MPFL reconstruction or correction of increased patellar height or increased TT-TG distance (Dejour and Saggin 2010, Fithian et al. 2004, Servien et al. 2007).

Reconstruction of medial patellofemoral ligament

Acute lateral patellar dislocation is commonly associated with medial retinacular injury (Arendt et al. 2002). Previously, a vastus medialis plasty was used to be performed, but the efficacy of this procedure is now found questionable (Fithian et al. 2004, Matthews and Schranz 2010). Instead, a MPFL reconstruction has become more popular to restore the patellar tracking in extension and early flexion.

MPFL reconstruction has a relatively low risk and low difficulty and has a high success rate with only 3.7% patients experiencing additional subluxation or dislocation after the reconstruction (Shah et al. 2012). However, isolated MPFL reconstruction is not considered the best solution for patellar dislocation if other factors contributing to instability are present like TD and patella alta (Dejour et al. 2013). Moreover, a normal trochlea with a deep groove and an elevated lateral facet is necessary for the MPFL to provide stability (Arendt et al. 2002, Bicos et al. 2007)

Lateral retinaculum release

Lateral release is a rather controversial procedure. It can be performed if the lateral retinaculum is tightened, thickened and/or foreshortened, which might contribute to lateral tilt of the patella. Lateral retinaculum release reduces the tension on the lateral side of the PF joint (Henry et al. 1986). Therefore, this procedure can address excessive lateral pressure and elective location of pain on the lateral retinaculum (Panni et al. 2005). For patellar instability however isolated lateral retinaculum release showed little or no benefit (Christoforakis et al. 2006, Lattermann et al. 2007).

Medial tuberositas tibiae transfer

Medialization of the tuberositas tibiae can be performed if the tuberositas is lateralised (Tuberositas tibiae – trochlear groove distance > 20 mm). As a result of the lateralised tuberositas the patella is pulled laterally (Q-angle). Traditionally, surgical approaches attempted to reduce this Q-angle. Medialization of the tuberositas changes the direction of the pulling force applied on the patella by the extensor mechanism.

Biomechanical studies however have suggested that medial tuberositas transfers do not accomplish patellar stability (Mani et al. 2011, Ostermeier et al. 2006). Moreover, moving the tuberositas may even have negative consequences. Medialization of the tuberositas tibiae significantly increases the PF contact pressures and the contact pressures in the medial tibiofemoral compartment (Elias et al. 2004, Kuroda et al. 2001). Overmedialization is a commonly observed error and should especially be avoided in varus knees, knees with medial meniscectomy, and knees with preexisting degenerative arthritis of the medial compartment (Kuroda et al. 2001). In addition, medialization of the tuberositas may cause a significant increase in external tibial rotation (Kelman et al. 1989). Pure medial transfer is now less performed (Feller 2012). Instead, it is more often combined with an anterior transfer of the tuberositas tibiae (Fulkerson osteotomy) or with a lateral release (Elmslie-Trillat procedure).

Distal tuberositas tibiae transfer

Patella alta currently receives increased attention as a predisposing factor to recurrent patellar dislocation, which has resulted in an increased popularity of distalization of the tuberositas tibiae to correct patella alta (Caton-Deschamps index > 1.2) (Feller 2012). As a result, the patella will engage the trochlear groove earlier in knee flexion, which will in turn increase the PF stability. The objective is to bring the tuberositas tibiae to a more distal position in order to obtain a Caton-Deschamps index of 1.

Anterior tuberositas tibiae transfer (Maquet procedure)

Anteriorization of the tuberositas tibiae is performed to decrease the posterior orientation of the PT and increase the moment arm about the centre of rotation of the knee, both decreasing PF compression (Saranathan et al. 2012). In a Maquet procedure a 1 cm thick bone block is placed underneath the tuberositas tibiae to attempt patellar decompression (Leach and Schepsis 1981). Pure anteriorization of

the tuberositas however has shown inadequate results (Buuck and Fulkerson 2000, Radin and Pan 1993).

1. 3. Experimental research in patellar dislocation

The underlying problem of PF instability is that the aetiology is multi-factorial.

Because of the lack of information about the relative importance of different predisposing factors, it is difficult to choose the most appropriate treatment. To better understand the relative contributions of predisposing factors to PF instability, experimental research has been performed on cadaver specimens with simulated abnormalities.

1. 3. 1. Simulation of anatomical abnormalities

Simulation of trochlear dysplasia in cadaver specimens

The first experimental simulation of trochlear dysplasia was achieved by removing a wedge of bone underneath the lateral trochlea (Figure 1.15) (Senavongse and Amis 2005).

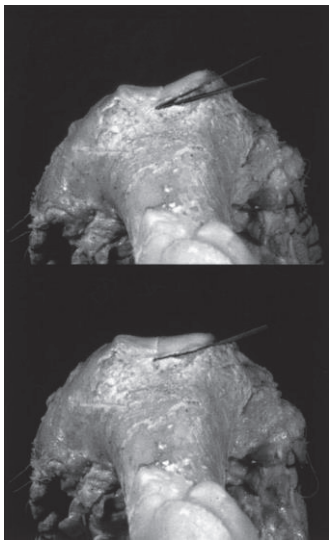

Figure 1.15 The procedure for flattening the lateral femoral trochlea by removal of a wedge of bone (Senavongse and Amis 2005)

PF joint stability was evaluated in a patellar stability rig with the quadriceps tensed to 175N (distributed over the different vasti) and with the knee positioned in knee flexion angles from 0° to 90°. The patella was displaced 10 mm laterally and medially and the required force was measured.

Flattening the lateral trochlear facet reduced the lateral restraining force significantly and had a larger pathological effect on patellar stability than vastus medialis insufficiency and rupture of the medial retinaculum. Abnormal trochlear geometry reduced the lateral stability by 70% at 30° flexion.

A few years later, the same research group simulated TD by elevating the central anterior trochlea (Amis et al. 2008). This was done by undermining the anterior trochlea and elevating the osteochondral shell. The underlying cavity was packed with bone fragments and bone cement until the anterior surface was flat in its mediolateral aspect (Figure 1.16).

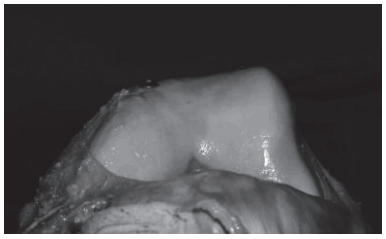

Figure 1.16 The geometry of the 'dysplastic' femoral trochlea after elevation of the central groove (Amis et al. 2008)

The newly formed trochlea approximated the shape of severe TD and the patellar stability was evaluated by the same method as described in 2005. In addition, PF kinematics were measured with an electromagnetic system with the cadaver knees mounted in a wooden test rig. The vasti of the quadriceps were loaded in their physiological directions, pulling the knee into full extension. Flexion was accomplished by pushing against the tibial intramedullary rod.

TD resulted in significantly reduced patellar stability and a more medial patellar tracking. The latter was not expected and the authors hypothesized that it might have resulted from tightening of the medial retinacular restraints as a consequence of the patella being elevated anteriorly by the dysplastic trochlea.

Simulation of vastus medialis insufficiency

The VMO fibres are oriented both medially and posteriorly, especially in deeper knee flexion (Farahmand et al. 1998, Lieb and Perry 1968). Different cadaver studies have demonstrated that the VMO can indeed contribute to resist lateral patellar motion (Bose et al. 1980, Goh et al. 1995, Lieb and Perry 1968, Senavongse and Amis 2005).

Vastus medialis insufficiency can be simulated by relaxing the VMO muscle during experimental test (Senavongse and Amis 2005). Senavongse and colleagues relaxed the VMO completely and distributed the total quadriceps tension over the other parts of the quadriceps tendons. The largest reduction in lateral restraint by vastus medialis insufficiency was found at 20-90° knee flexion with approximately 30% reduction.

Simulation of ruptured medial retinaculum

The effect of medial retinacular ruptures has been studied by multiple authors (Conlan et al. 1993, Desio et al. 1998, Hautamaa et al. 1998, Nomura et al. 2000, Senavongse and Amis 2005). Simulation of ruptured medial retinacular structures (MPFL, superficial medial patellar retinaculum, medial patellotibial ligament, medial patellomeniscal ligament) could be achieved in cadaver specimens by selective cutting of the retinacular structures or by pulling the patella laterally.

The contribution of the medial retinacular structures to PF stability is generally quantified by measuring lateral patellar translation during the application of a laterally directed force on the patella or by measuring the force required to cause a predefined mediolateral PF displacement.

These selective cutting studies showed that the MPFL is the most important ligamentous restraint to lateral displacement of the patella. In force controlled experiments, cutting the MPFL increased lateral patellar displacement with 50% compared to intact knees (Hautamaa et al. 1998, Nomura et al. 2000) and the MPFL was found to contribute between 41% and 80% of the restraining force against lateral PF displacement (Conlan et al. 1993, Desio et al. 1998). In a displacement-controlled study, medial retinaculum rupture reduced the restraining force throughout flexion with a maximal reduction when the knee approached full extension (Senavongse and Amis 2005).

Very recently, a study demonstrated that the MPFL has an aponeurotic nature (Zaffagnini et al. 2013). According to this study, the ligament only has a small

contribution during neutral knee flexion, but during motion, especially under high stress on lateral side of the patella, the MPFL functions as a restraint. During static stability tests, the patellar stability was significantly decreased by MPFL resection, mainly at 30° and 60° of knee flexion.

In addition to investigating the impact of ruptured medial retinacular structures on the PF stability, the PF kinematics were also studies by several authors, but the results appear variable (Zaffagnini et al. 2013).

Simulation of patella alta

Patella alta has been simulated on cadaver specimen by performing an osteotomy of the tibial tubercle, followed by a reattachment of the tubercle 5 and 10 mm superiorly (Singerman et al. 1994). The knee specimens were mounted in a test rig, simulating a flexion-extension movement from 20° to 110° of knee flexion, similar to a sitting-rising movement from a chair. The PF contact force was measured by a force transducer, inserted in the retropatellar surface. Patella alta significantly increased the resultant contact force, this increase was on average 3% per mm of change in patellar height. In addition, patella alta also increased the medial force acting on the retropatellar surface, indicating a tendency for lateral subluxation in patella alta (Singerman et al. 1994). Singerman and colleagues explained this tendency by the association between the delayed tendofemoral contact in patella alta and the mediolateral component of the contact force.

Later, this explanation was confirmed by an experimental study with a mechanical knee (Luyckx et al. 2009). The mechanical knee was composed by custom-made rigid fixtures to simulate the tibia and femur and a posteriorly stabilised total knee replacement. Five different predetermined patellar heights were studied in a knee rig simulating a squat movement from 30° to 120° of knee flexion. Patella alta caused disturbed contact areas, resulting in increased PF pressures and potentially increased rates of PF osteoarthritis (Luyckx et al. 2009).

1. 3. 2. Test devices

Testing devices have been developed in several biomechanical research labs to investigate the PF stability, kinematics and contact pressures and areas. For the current research project it was chosen to investigate the PF biomechanics experimentally on an Oxford-like knee rig. The rationale behind this choice is that

the Oxford knee rig has been validated and has been used for numerous other studies. Furthermore, the Oxford knee rig simulates a rather simple movement (flexion-extension squat movement) which facilitates analysis of the already very complex PF joint biomechanics.

Oxford knee rig

The most widely known type of knee rig is probably the Oxford knee rig (Figure 1.17) (Zavatsky 1997). In this type of knee rig the flexion-extension position of the knee can be controlled by applying a load on the quadriceps tendon. Alternatively flexion-extension can also be controlled by a second actuator which translates the hip assembly along vertical rails. During this flexion-extension movement, the PF kinematics can be measured with the use a motion capture system (e.g. Vicon infrared cameras, Vicon Motion Systems, Los Angeles, CA, USA). The PF contact area and pressure can be measured with the use of a pressure sensitive film (e.g. Tekscan, South Boston, MA, USA).

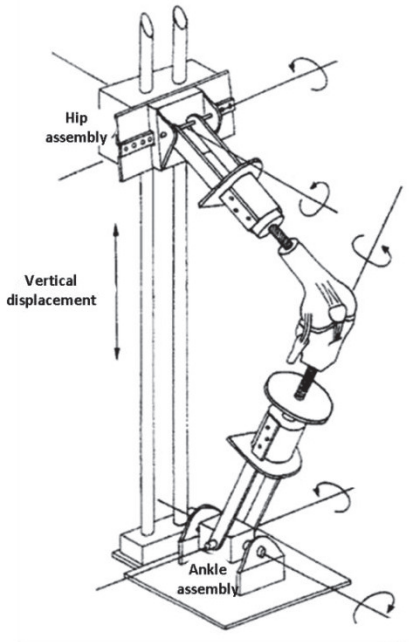

Figure 1.17 Oxford knee rig (Zavatsky 1997)

Many variations of the Oxford knee rig are in use. At Ghent University a quasi-static knee rig, based on the Oxford knee rig was developed. Though this knee rig demonstrated a good repeatability (Van Haver et al. 2013), it was decided not to use this knee rig for the current biomechanical studies (described in chapter 4 and 5). The main reasons for this decision were the lack of a motion capture system to reliably evaluate the PF kinematics and the ongoing modifications of the knee rig to further optimise its functionality. A pilot study on this knee rig is detailed in Appendix A.

Patellar stability rig

To evaluate the PF stability, Amis and colleagues developed a knee rig in which the cadaver knees were mounted horizontally in well-defined knee flexion angles ranging from 0º to 90º flexion (Figure 1.18) (Senavongse and Amis 2005). The vasti of the quadriceps muscle were loaded in their physiological directions. The patella was consequently displaced 10 mm in the mediolateral direction and the force required to cause this displacement was accepted as a measure of PF stability.

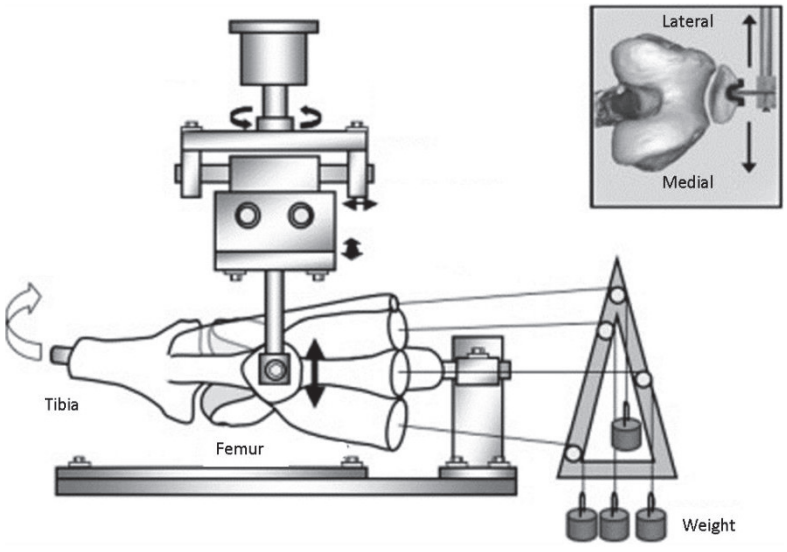

Figure 1.18 Patellar stability rig (Merican et al. 2009)

At Ghent University a similar patellar stability rig was built. An important difference with the rig developed by Amis and colleagues is that the mediolateral forces are force-controlled and that the displacement is a measure of stability.

1. 4. Problem statement and aim of dissertation

1. 4. 1. Problem statement

It is universally agreed that TD is the primary factor in patellar dislocation. Because of the large variation in trochlear shape, TD is commonly subdivided into classes. The 4-grade Dejour classification is widely used in clinical research and in clinical practice. Several studies have been performed to evaluate to what extent the Dejour classification can predict the outcome of trochleoplasty and the risk to develop PF osteoarthritis. Consequently, this classification is used to decide which treatment is most appropriate for the patient.

The Dejour classification however has recently demonstrated a rather low reliability. More specifically, type B, C and D appeared difficult to distinguish, leading to a proposal to apply a 2-grade classification (grade A versus grade B, C and D) instead of a 4-grade classification. This proposal however does not meet study results on the outcome of trochleoplasty and the risk to develop osteoarthritis (grade B and D seem more at risk to develop osteoarthritis and show a better outcome of trochleoplasty).

PF osteoarthritis has a strong relation with TD and patellar dislocation. However, surgical treatment has mainly focussed on restoring the stability of the PF joint, while the long term effects of patellar dislocation (osteoarthritis) have been reported to be more likely a consequence of increased pressures rather than a consequence of the dislocations themselves.

Despite the importance of both the Dejour classification and the contact pressures, their relation has not been investigated yet. Nor was the relation between the Dejour classes and the PF kinematics and stability investigated.

1. 4. 2. Aim of the dissertation

This dissertation aims to:

- Provide a profound morphological description of the TD distal femur, including the regions outside the anterior trochlea (chapter 2 and 3).
- Develop a method to simulate different types of TD in cadaveric knees for experimental testing (chapter 4)
- Evaluate the effect of different types of TD on the PF kinematics, contact area, contact pressure and stability (chapter 5)

This work aspires to contribute to understanding the complex mechanisms of patellar dislocation and the outcome of surgical treatment.

1. 5. Organization of dissertation

The dissertation includes 4 research chapters (chapter 2-5), which are self-contained and can be read independently of the others. Following the research chapters, a general discussion is organised in which the main ideas, conclusions and directions for future research and practice are discussed (chapter 6).

The thesis is organised as follows:

- In chapter 2, the morphology of the distal TD femur is evaluated with a landmark-based analysis. To exclude the effect of size differences, the 3D femur models were first isotropically scaled. Discrete parameters are measured to quantify the differences between normal and TD knees.

- To take the full geometrical complexity of TD into account statistical shape analysis (SSA) of TD knees is performed in chapter 3. This chapter includes description of pointwise distances and principal components and assessment of automated classification and clustering.

- Chapter 4 describes the methodology to design and manufacture rapid prototyped implants and guiding instruments for experimental testing on cadaver specimens. Replica implants (replicating the native trochlea) are tested to investigate the accuracy of the guiding instruments and the impact of the implants on the biomechanical behaviour of the PF joint.

- In chapter 5 this method is applied to investigate the effect of different types of TD on the PF kinematics, contact pressure, contact area and stability.

- Finally, in chapter 6 the major findings of this research project are discussed and further research is suggested.

References

1. Amis AA. 2007. Current concepts on anatomy and biomechanics of patellar stability. Sports Med Arthrosc. 15:48-56.

2. Amis AA, Firer P, Mountney J, Senavongse W, Thomas NP. 2003. Anatomy and biomechanics of the medial patellofemoral ligament. Knee. 10:215-220.

3. Amis AA, Oguz C, Bull AMJ, Senavongse W, Dejour D. 2008. The effect of trochleoplasty on patellar stability and kinematics - A biomechanical study in vitro. J Bone Joint Surg Br. 90B:864-869.

4. Andrish J. 2008. The management of recurrent patellar dislocation. Orthop Clin N Am. 39:313-+.

5. Arendt EA, Dejour D. 2013. Patella instability: building bridges across the ocean a historic review. Knee Surg Sport Tr A. 21:279-293.

6. Arendt EA, Fithian DC, Cohen E. 2002. Current concepts of lateral patella dislocation. Clin Sport Med. 21:499-+.

7. Atkin DM, Fithian DC, Marangi KS, Stone ML, Dobson BE, Mendelsohn C. 2000. Characteristics of patients with primary acute lateral patellar dislocation and their recovery within the first 6 months of injury. Am J Sport Med. 28:472-479.

8. Beaufils P, Thaunat M, Pujol N, Scheffler S, Rossi R, Carmont M. 2012. Trochleoplasty in major trochlear dysplasia: current concepts. Sports Med Arthrosc Rehabil Ther Technol. 4:7.

9. Bicos J, Fulkerson JP, Amis A. 2007. Current concepts review - The medial patellofemoral ligament. Am J Sport Med. 35:484-492.

10. Biedert RM, Bachmann M. 2009. Anterior-posterior trochlear measurements of normal and dysplastic trochlea by axial magnetic resonance imaging. Knee Surg Sport Tr A. 17:1225-1230.

11. Blackburne JS, Peel TE. 1977. New Method of Measuring Patellar Height. J Bone Joint Surg Br. 59:241-242.

12. Bose K, Kanagasuntheram R, Osman MBH. 1980. Vastus Medialis Oblique - an Anatomic and Physiologic Study. Orthopedics. 3:880-883.

13. Buuck DA, Fulkerson JP. 2000. Anteromedialization of the tibial tubercle: A 4- to 12-year follow-up. Oper Techn Sport Med. 8:131-137.

14. Carrillon Y, Abidi H, Dejour D, Fantino O, Moyen B, Tran-Minh VA. 2000. Patellar instability: Assessment on MR images by measuring the lateral trochlear inclination-initial experience. Radiology. 216:582-585.

15. Caton J, Deschamps G, Chambat P, Lerat JL, Dejour H. 1982. The Low Patellas - Report of 128 Cases - Patella-Inferae. Rev Chir Orthop. 68:317-325.

16. Caton J, Mironneau A, Walch G, Levigne C, Michel CR. 1990. Adolescent Idiopathic Patella Alta - a Review of 61 Operated Cases. Rev Chir Orthop. 76:253-260.

17. Christoforakis J, Bull AMJ, Strachan RK, Shymkiw R, Senavongse W, Amis AA. 2006. Effects of lateral retinacular release on the lateral stability of the patella. Knee Surg Sport Tr A. 14:273-277.

18. Colvin AC, West RV. 2008. Patellar Instability. J Bone Joint Surg Am. 90A:2751-2762.

19. Conlan T, Garth WP, Lemons JE. 1993. Evaluation of the Medial Soft-Tissue Restraints of the Extensor Mechanism of the Knee. J Bone Joint Surg Am. 75A:682-693.

20. Crosby EB, Insall J. 1976. Recurrent Dislocation of Patella - Relation of Treatment to Osteoarthritis. J Bone Joint Surg Am. 58:9-13.

21. Dejour D. 2013. The patellofemoral joint and its historical roots: the Lyon School of Knee Surgery. Knee surgery, sports traumatology, arthroscopy : official journal of the ESSKA.

22. Dejour D, Byn P, Ntagiopoulos PG. 2013. The Lyon's sulcus-deepening trochleoplasty in previous unsuccessful patellofemoral surgery. Int Orthop. 37:433-439.

23. Dejour D, Reynaud P, Lecoultre B. 1998. Douleurs et instabilité rotulienne. Essai de classification. Médecin et Hygiène. 56:1466-1471.

24. Dejour D, Saggin P. 2010. The sulcus deepening trochleoplasty-the Lyon's procedure. Int Orthop. 34:311-316.

25. Dejour H. 1987. Terminologie classification des affections femoro-patellairet. Journees Lyonnaise de chirurgie du Genou.

26. Dejour H, Walch G, Neyret P, Adeleine P. 1990. Dysplasia of the Femoral Trochlea. Rev Chir Orthop. 76:45-54.

27. Dejour H, Walch G, Nove-Josserand L, Guier C. 1994. Factors of patellar instability: an anatomic radiographic study. Knee surgery, sports traumatology, arthroscopy : official journal of the ESSKA. 2:19-26.

28. Desio SM, Burks RT, Bachus KN. 1998. Soft tissue restraints to lateral patellar translation in the human knee. Am J Sport Med. 26:59-65.

29. Doucette SA, Child DD. 1996. The effect of open and closed chain exercise and knee joint position on patellar tracking in lateral patellar compression syndrome. J Orthop Sport Phys. 23:104-110.

30. Elias JJ, Cech JA, Weinstein DM, Cosgrea AJ. 2004. Reducing the lateral force acting on the patella does not consistently decrease patellofemoral pressures. Am J Sport Med. 32:1202-1208.

31. Farahmand F, Senavongse W, Amis AA. 1998. Quantitative study of the quadriceps muscles and trochlear groove geometry related to instability of the patellofemoral joint. J Orthopaed Res. 16:136-143.

32. Feller JA. 2012. Distal Realignment (Tibial Tuberosity Transfer). Sports Med Arthrosc. 20:152-161.

33. Feller JA, Amis AA, Andrish JT, Arendt EA, Erasmus PJ, Powers CM. 2007. Surgical biomechanics of the patellofemoral joint. Arthroscopy-the Journal of Arthroscopic and Related Surgery. 23:542-553.

34. Fithian DC, Nomura E, Arendt E. 2001. Anatomy of patellar dislocation. Oper Techn Sport Med. 9:102-111.

35. Fithian DC, Paxton EW, Cohen AB. 2004. Indications in the treatment of patellar instability. The journal of knee surgery. 17:47-56.

36. Fithian DC, Paxton EW, Stone ML, Silva P, Davis DK, Elias DA, White LM. 2004. Epidemiology and natural history of acute patellar dislocation. Am J Sport Med. 32:1114-1121.

37. Fucentese SF, von Roll A, Koch PP, Epari DR, Fuchs B, Schottle PB. 2006. The patella morphology in trochlear dysplasia - A comparative MRI study. Knee. 13:145-150.

38. Goh JCH, Lee PYC, Bose K. 1995. A Cadaver Study of the Function of the Oblique Part of Vastus Medialis. J Bone Joint Surg Br. 77B:225-231.

39. Grelsamer RP. 2005. Patellar nomenclature the tower of babel revisited. Clin Orthop Relat R. 60-65.

40. Grelsamer RP, Dejour D, Gould J. 2008. The pathophysiology of patellofemoral arthritis. Orthop Clin N Am. 39:269-+.

41. Grelsamer RP, Weinstein CH. 2001. Applied biomechanics of the patella. Clin Orthop Relat R. 9-14.

42. Hautamaa PV, Fithian DC, Kaufman KR, Daniel DM, Pohlmeyer AM. 1998. Medial soft tissue restraints in lateral patellar instability and repair. Clin Orthop Relat R. 174-182.

43. Hayes CW, Brigido MK, Jamadar DA, Propeck T. 2000. Mechanism-based pattern approach to classification of complex injuries of the knee depicted at MR imaging. Radiographics. 20:S121-S134.

44. Hehne HJ. 1990. Biomechanics of the Patellofemoral Joint and Its Clinical Relevance. Clin Orthop Relat R. 73-85.

45. Henry JH, Goletz TH, Williamson B. 1986. Lateral Retinacular Release in Patellofemoral Subluxation - Indications, Results, and Comparison to Open Patellofemoral Reconstruction. Am J Sport Med. 14:121-129.

46. Huberti HH, Hayes WC. 1984. Patellofemoral Contact Pressures - the Influence of Q-Angle and Tendofemoral Contact. J Bone Joint Surg Am. 66A:715-724.

47. Insall J, Salvati E. 1971. Patella Position in Normal Knee Joint. Radiology. 101:101-&.

48. Kelman G, Focht L, Drakauer J, Colwell C. 1989. A cadaveric study of patello-femoral kinematics using a biomechanical testing rig and gait laboratory motion analysis. Orthop Trans. 13:248-249.

49. Kuroda R, Kambic H, Valdevit A, Andrish JT. 2001. Articular cartilage contact pressure after tibial tuberosity transfer - A cadaveric study. Am J Sport Med. 29:403-409.

50. Kwak SD, Colman WW, Ateshian GA, Grelsamer RP, Henry JH, Mow VC. 1997. Anatomy of the human patellofemoral joint articular cartilage: Surface curvature analysis. J Orthopaed Res. 15:468-472.

51. Lattermann C, Toth J, Bach BR. 2007. The role of lateral retinacular release in the treatment of patellar instability. Sports Med Arthrosc. 15:57-60.

52. Leach R, Schepsis A. 1981. Anterior displacement of the tibial tubercle: the Maquet procedure. Contemp Orthop. 3:199–204.

53. Lieb FJ, Perry J. 1968. Quadriceps Function - an Anatomical and Mechanical Study Using Amputated Limbs. J Bone Joint Surg Am. A 50:1535-&.

54. Lippacher S, Dejour D, Elsharkawi M, Dornacher D, Ring C, Dreyhaupt J, Reichel H, Nelitz M. 2012. Observer Agreement on the Dejour Trochlear Dysplasia Classification A Comparison of True Lateral Radiographs and Axial Magnetic Resonance Images. Am J Sport Med. 40:837-843.

55. Luyckx T, Didden K, Vandenneucker H, Labey L, Innocenti B, Bellemans J. 2009. Is there a biomechanical explanation for anterior knee pain in patients with patella alta? Influence of patellar height on patellofemoral contact force, contact area and contact pressure. J Bone Joint Surg Br. 91B:344-350.

56. Mani S, Kirkpatrick MS, Saranathan A, Smith LG, Cosgarea AJ, Elias JJ. 2011. Tibial Tuberosity Osteotomy for Patellofemoral Realignment Alters Tibiofemoral Kinematics. Am J Sport Med. 39:1024-1031.

57. Matthews JJ, Schranz P. 2010. Reconstruction of the medial patellofemoral ligament using a longitudinal patellar tunnel technique. Int Orthop. 34:1321-1325.

58. Merchant AC, Mercer RL, Jacobsen RH, Cool CR. 1974. Roentgenographic Analysis of Patellofemoral Congruence. J Bone Joint Surg Am. A 56:1391-1396.

59. Merican AM, Kondo E, Amis AA. 2009. The effect on patellofemoral joint stability of selective cutting of lateral retinacular and capsular structures. J Biomech. 42:291-296.

60. Neyret P, Robinson AHN, Le Coultre B, Lapra C, Chambat P. 2002. Patellar tendon length - the factor in patellar instability? Knee. 9:3-6.

61. Nietosvaara Y, Aalto K, Kallio PE. 1994. Acute Patellar Dislocation in Children - Incidence and Associated Osteochondral Fractures. J Pediatr Orthoped. 14:513-515.

62. Nomura E, Horiuchi Y, Kihara M. 2000. Medial patellofemoral ligament restraint in lateral patellar translation and reconstruction. Knee. 7:121-127.

63. Ostermeier S, Stukenborg-Colsman C, Hurschler C, Wirth CJ. 2006. In vitro investigation of the effect of medial patellofemoral ligament reconstruction and medial tibial tuberosity transfer on lateral patellar stability. Arthroscopy-the Journal of Arthroscopic and Related Surgery. 22:308-319.

64. Pal S, Besier TF, Beaupre GS, Fredericson M, Delp SL, Gold GE. 2013. Patellar maltracking is prevalent among patellofemoral pain subjects with patella alta: An upright, weightbearing MRI study. J Orthopaed Res. 31:448-457.

65. Panni AS, Tartarone M, Patricola A, Paxton EW, Fithian DC. 2005. Long-term results of lateral retinacular release. Arthroscopy-the Journal of Arthroscopic and Related Surgery. 21:526-531.

66. Pfirrmann CWA, Zanetti M, Romero J, Hodler J. 2000. Femoral trochlear dysplasia: MR findings. Radiology. 216:858-864.

67. Philippot R, Boyer B, Testa R, Farizon F, Moyen B. 2012. The role of the medial ligamentous structures on patellar tracking during knee flexion. Knee Surg Sport Tr A. 20:331-336.

68. Powers CM. 2000. Patellar kinematics, part II: The influence of the depth of the trochlear groove in subjects with and without patellofemoral pain. Phys Ther. 80:965-973.

69. Powers CM, Chen YJ, Farrokhi S, Lee TQ. 2006. Role of peripatellar retinaculum intransmission of forces within the extensor mechanism. J Bone Joint Surg Am. 88A:2042-2048.

70. Radin EL, Pan HQ. 1993. Long-Term Follow-up-Study on the Maquet Procedure with Special Reference to the Causes of Failure. Clin Orthop Relat R. 253-258.

71. Remy F, Chantelot C, Fontaine C, Demondion X, Migaud H, Gougeon F. 1998. Inter- and intraobserver reproducibility in radiographic diagnosis and classification of femoral trochlear dysplasia. Surg Radiol Anat. 20:285-289.

72. Remy F, Gougeon F, Ala Eddine T, Migaud H, Fontaine C, Duquennoy A. 2002. Reproducibility of the new classification of femoral trochlea dysplasia proposed by Dejour: predictive value for severity of femoropatellar instability in 47 knees. J Bone Joint Surg Br. 84:1.

73. Sakai N, Luo ZP, Rand JA, An KN. 2000. The influence of weakness in the vastus medialis oblique muscle on the patellofemoral joint: an in vitro biomechanical study. Clin Biomech. 15:335-339.

74. Saranathan A, Kirkpatrick MS, Mani S, Smith LG, Cosgarea AJ, Tan JS, Elias JJ. 2012. The effect of tibial tuberosity realignment procedures on the patellofemoral pressure distribution. Knee Surg Sport Tr A. 20:2050-2057.

75. Senavongse W, Amis AA. 2005. The effects of articular, retinacular, or muscular deficiencies on patellofemoral joint stability - A biomechanical study in vitro. J Bone Joint Surg Br. 87B:577-582.

76. Servien E, Verdonk PC, Neyret P. 2007. Tibial tuberosity transfer for episodic patellar dislocation. Sports Med Arthrosc. 15:61-67.

77. Shah JN, Howard JS, Flanigan DC, Brophy RH, Carey JL, Lattermann C. 2012. A Systematic Review of Complications and Failures Associated With Medial Patellofemoral Ligament Reconstruction for Recurrent Patellar Dislocation. Am J Sport Med. 40:1916-1923.

78. Shih YF, Bull AM, Amis AA. 2004. The cartilaginous and osseous geometry of the femoral trochlear groove. Knee surgery, sports traumatology, arthroscopy : official journal of the ESSKA. 12:300-6.

79. Sillanpaa P, Mattila VM, Iivonen T, Visuri T, Pihlajamaki H. 2008. Incidence and risk factors of acute traumatic primary patellar dislocation. Med Sci Sport Exer. 40:606-611.

80. Singerman R, Davy DT, Goldberg VM. 1994. Effects of Patella Alta and Patella Infera on Patellofemoral Contact Forces. J Biomech. 27:1059-1065.

81. Staubli HU, Durrenmatt U, Porcellini B, Rauschning W. 1999. Anatomy and surface geometry of the patellofemoral joint in the axial plane. J Bone Joint Surg Br. 81B:452-458.

82. Stefancin JJ, Parker RD. 2007. First-time traumatic patellar dislocation - A systematic review. Clin Orthop Relat R. 93-101.

83. Stefanik JJ, Roemer FW, Zumwalt AC, Zhu YY, Gross KD, Lynch JA, Frey-Law LA, Lewis CE, Guermazi A, Powers CM, Felson DT. 2012. Association between measures of trochlear morphology and structural features of patellofemoral joint osteoarthritis on MRI: The MOST study. J Orthopaed Res. 30:1-8.

84. Stefanik JJ, Zhu Y, Zumwalt AC, Gross KD, Clancy M, Lynch JA, Law LAF, Lewis CE, Roemer FW, Powers CM, et al. 2010. Association Between Patella Alta and the Prevalence and Worsening of Structural Features of Patellofemoral Joint Osteoarthritis: The Multicenter Osteoarthritis Study. Arthrit Care Res. 62:1258-1265.

85. Van Haver A, De Roo K, Claessens T, De Beule M, Verdonk P, De Baets P. 2013. Pilot validation study on a quasi-static weight-bearing knee rig. P I Mech Eng H. 227:229-233.

86. Varadarajan KM, Freiberg AA, Gill TJ, Rubash HE, Li GA. 2010. Relationship Between Three-Dimensional Geometry of the Trochlear Groove and In Vivo

Patellar Tracking During Weight-Bearing Knee Flexion. J Biomech Eng-T Asme. 132:

87. Ward SR, Terk MR, Powers CM. 2007. Patella alta: Association with patellofemoral alignment and changes in contact area during weight-bearing. J Bone Joint Surg Am. 89A:1749-1755.

88. Yamada Y, Toritsuka Y, Yoshikawa H, Sugamoto K, Horibe S, Shino K. 2007. Morphological analysis of the femoral trochlea in patients with recurrent dislocation of the patella using three-dimensional computer models. J Bone Joint Surg Br. 89B:746-751.

89. Zaffagnini S, Colle F, Lopomo N, Sharma B, Bignozzi S, Dejour D, Marcacci M. 2013. The influence of medial patellofemoral ligament on patellofemoral joint kinematics and patellar stability. Knee surgery, sports traumatology, arthroscopy : official journal of the ESSKA. 21:2164-71.

90. Zaffagnini S, Dejour D, Arendt EA. 2010. Patellofemoral pain, instability, and arthritis clinical presentation, imaging, and treatment. Springer-Verlag. xii, 331 p.

91. Zavatsky AB. 1997. A kinematic-freedom analysis of a flexed-knee-stance testing rig. J Biomech. 30:277-280.

Chapter 2

Landmark-based 3D analysis reveals new morphometric characteristics in the trochlear dysplastic femur[1]

The authors hypothesize that the trochlear dysplastic distal femur is not only characterized by morphological changes to the trochlea. To investigate the characteristics of the trochlear dysplastic knee, a landmark based 3D analysis was performed on 20 trochlear dysplastic and 20 normal knees. Arthro-CT scans were used to generate 3D models including the cartilage. To rule out size differences, a set of landmarks was defined on the distal femur to isotropically scale the 3D models to a standard size. A predefined series of landmark-based reference planes was applied on the distal femur. With these landmarks and reference planes a series of previously described characteristics associated with trochlear dysplasia as well as a series of morphometric characteristics were measured. For the previously described characteristics, the analysis replicated highly significant differences between trochlear dysplastic and normal knees. Furthermore, the analysis showed that, when knee size is taken into account, trochlear bump and depth are allowed to be 1 mm larger in the largest knees compared to the smallest knees. For the morphometric characteristics, the analysis revealed that the trochlear dysplastic femur is also characterised by a 10% smaller intercondylar notch, 6-8% larger posterior condyles (lateral-medial) in the anteroposterior direction and a 6% larger medial condyle in the proximodistal direction compared to a normal femur. This study shows that knee size is important in the application of absolute metric cut-off values and that the posterior femur also shows a significantly different morphology.

[1] This study is accepted for publication: Annemieke Van Haver, Karel De Roo, Matthieu De Beule, Sofie Van Cauter, Emmanuel Audenaert, Tom Claessens, Peter Verdonk. Semi-automated landmark-based 3D analysis reveals new morphometric characteristics in the trochlear dysplastic femur. Knee Surgery, Sports Traumatology, Arthroscopy.

2. 1. Introduction

TD is the most important morphological abnormality associated with patellar dislocation. The lateral border of the trochlea normally acts as a restraint against the lateral pull of the quadriceps muscle. In a trochleodysplastic knee, the trochlea is shallow, flat or convex (Dejour et al. 1998). As a result, the patella is unable to engage properly in the trochlear groove and tends to dislocate laterally in early flexion of the knee joint (Chhabra et al. 2011).

Many variations in TD exist and several authors have tried to capture these variations in a classification system (Biedert and Bachmann 2009, Dejour et al. 1998, Dejour et al. 1994, Pfirrmann et al. 2000). H. Dejour was the first to describe three types of TD based on conventional lateral radiographs, on which he evaluated the crossing sign, the trochlear bump and the trochlear depth (Dejour et al. 1994). Later, D. Dejour implemented the use of CT scans in the Dejour classification and proposed a four-grade classification which is now widely used to grade the severity of TD and to help in the selection of the appropriate surgical treatment (Dejour and Le Coultre 2007, Dejour et al. 1998, Dejour and Saggin 2010). This four-grade Dejour classification is still considered insufficient to quantify the dysplasia and to predict the severity of the PF instability (Fucentese et al. 2011, Remy et al. 1998, Remy et al. 2002). Currently, there is an important tendency to reduce the four-grade classification to a two-grade classification (Lippacher et al. 2012, Nelitz et al. 2013); low-grade TD (type A) can successfully be distinguished from high-grade TD (type B, C, D), while distinguishing type B, C and D was found difficult due to the high variability of the trochlear geometry (Lippacher et al. 2012).

Lately, 3D computer models have also been used to analyse the morphology of TD knees (Biedert et al. 2011, Yamada et al. 2007). Indeed, 3D models provide an accurate and more realistic representation of the complex shape of the trochlea, whereas single cuts have been reported to be unable to fully describe the true morphology of the trochlea (Nelitz et al. 2013).

Despite the extensive and profound research on the characteristics of TD, certain interesting questions are still not fully explored.

From a biomechanical point of view, the actual stability of the PF joint is not only defined by the subchondral bone, but more importantly also by the shape of the articular cartilage. For many years now, authors have indicated that subchondral osseous anatomy of the patella and the femoral trochlea can differ markedly from the corresponding surface geometry of the articular cartilage, particularly in patients

with TD (Shih et al. 2004, Staubli et al. 1999, Toms et al. 2009, van Huyssteen et al. 2006). Consequently, the cartilage should be included in the 3D models, e.g. using arthro-CT scans. To date, absolute metric cut-off values are frequently used to define the TD knee, although it has been reported that knee size can influence these measurements (Chhabra et al. 2011). Recent population scale studies have shown that size is the principal mode of variation between subjects, making up for 50-60% of variation between individuals (Bredbenner et al. 2010, Fitzpatrick et al. 2011). Standardization of size is therefore crucial to allow for objective quantification of morphological differences between subjects. Such can easily be performed by means of generalized Procrustes analysis (Goodall 1991).

The aim of this study is to apply a new method that takes cartilage-bone mismatch and size differences into account to investigate the overall morphology of the distal femur in addition to previously described characteristics associated with TD. The authors hypothesize that the TD distal femur is not only characterized by morphological changes to the trochlea.

2. 2. Materials and methods

A landmark-based 3D analysis was performed on the distal femur to quantify the knee joint geometry, including the cartilage. Based on a set of manually identified landmarks, the knees are isotropically scaled and captured in a set of reference planes. This method allows quantification of the widely accepted characteristics associated with TD and at the same time it may reveal morphometric differences between normal and trochleodysplastic knees which have, to our knowledge, not been reported before.

The TD group (TD group) included retrospectively 20 patients (12 females and 8 males; mean age 29 ± 13 years, mean BMI 22.6) with a history of recurrent patellar dislocation. All patients were diagnosed with TD and were classified as type A, B, C or D by a senior orthopaedic surgeon (PV) according to the Dejour classification (5 patients in each class) (Dejour and Le Coultre 2007, Dejour et al. 1998, Dejour and Saggin 2010). None of these patients underwent a surgical treatment for patellar dislocation prior to imaging.

As a control group 20 patients with a normal anatomy of the PF joint were selected (11 females and 9 males, mean age 30 ± 8 years, mean BMI 22.3). The control group consulted the orthopaedic surgeon for a complaint unrelated to the PF area.

The TD and control group showed no significant differences in gender, age and BMI.

2. 2. 1. Generation and isotropic scaling of 3D computer models

To visualize the cartilage in the knee joint, unloaded arthro-CT scans were performed, which have been shown to be more accurate than MR arthrography to estimate the cartilage thickness (El-Khoury et al. 2004, Wyler et al. 2009). All patients were scanned on a multidetector CT (Definition Flash, Siemens, Erlangen, Germany) after intra-articular injection of 10 to 15 cc iohexol 240 mg/ml (Omnipaque 240, GE Healthcare, Diegem, Belgium) under fluoroscopic guidance. Slice thickness was 1 mm. Patients were fixed in a supine position with 15° of knee flexion and the toes pointing straight up.

The arthro-CT images were loaded in a 3D image processing software system (Mimics 14.12, Materialise, Haasrode, Belgium) to create 3D models of the knee bones including the cartilage.

Because differences in knee size can significantly affect the metric measurements in the TD knee (Chhabra et al. 2011), the 3D models were isotropically sized to match the standard size prior to the analyses. A generalised Procrustes transformation of the surface models was applied in a custom developed code in Matlab (Matlab 7.8.0, R2009a, Mathworks, Natick, MA) to minimize the total size variance between the knees, while preserving the shape of the knees (Gower 1975). The standard size was determined by non-rigid point set registration of the surface meshes of the 20 normal femurs (Myronenko and Song 2010). Twelve anatomical landmarks, covering the extremes of the distal femur in the anteroposterior, proximodistal and mediolateral direction, were defined to calculate a rescaling factor for each knee. This factor was considered as a measure of the femoral size.

2. 2. 2. Definition of the landmarks

All landmarks were defined in Mimics. For precise location of the landmarks on the femur, tibia and patella both the 3D models and the arthro-CT images were used.

Intra-and inter observer precision of landmarks defined on 3D models of the femur and tibia have been reported in a range of 0.4-1.4 mm and 0.3-3.5 mm respectively (Victor et al. 2009). Since the landmarks in the current study were also verified on the CT images, it is assumed that the landmark precision in the current study achieves an equivalent or higher level. In the current study two observers defined the

landmarks on 20 knees to assess the inter-observer precision. Twelve anatomical landmarks were defined on the femur to rescale the bone models (Figure 2.1, Appendix B). Additionally, 11 other landmarks on the femur, five landmarks on the patella and two landmarks on the tibia (Appendix B) were defined to create the reference planes and to measure the characteristics associated with TD.

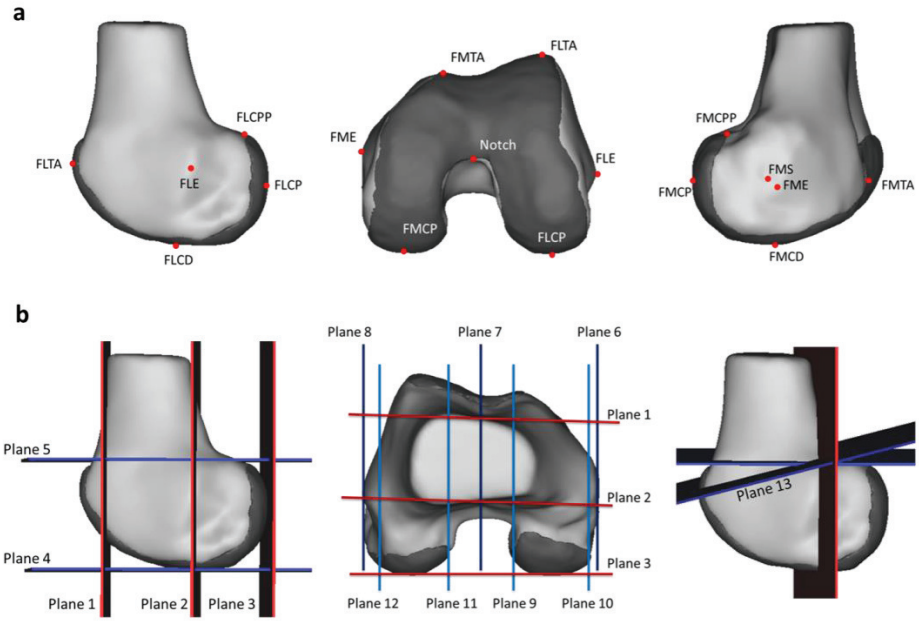

Figure 2.1 3D model of a distal femur composed of bone (light grey) and cartilage (dark grey). Panel a: Location of the 12 landmarks used for Procrustes rescaling: lateral, distal and medial view on the femur. Panel b: Reference planes to evaluate the morphometric parameters in the anteroposterior (left and middle figure), mediolateral (middle figure) and proximodistal (left figure) direction and an auxiliary plane (right figure) to evaluate trochlear depth (details on the landmarks and planes are listed in Appendix B)

2. 2. 3. Definition of the reference planes

The reference planes are predefined by the authors in Mimics in the anteroposterior (AP), proximodistal (PD) and mediolateral (ML) direction (Figure 2.1, Appendix B). By identifying the landmarks, the reference planes are automatically fitted on the geometry of the distal femur.

To evaluate the femur size in the AP direction three planes were defined: a plane tangent to the anterior cortex of the femur and parallel with the surgical

transepicondylar axis (sTEA) (plane 1), a plane tangent to the posterior cortex of the femur and parallel with sTEA (plane 2) and a plane tangent to the PCL and parallel with the longitudinal axis of the femur (plane 3). To evaluate the femur size in the PD direction two other planes were defined: a distal plane tangent to the distal condyles (plane 4) and a proximal plane on top of the medial and lateral condyles (plane 5). Finally, seven planes were required to evaluate the proportions in the ML direction: a medial, central and lateral plane, respectively through the medial epicondyle, the centre of the notch and the lateral epicondyle (resp. planes 6-8), a plane tangent to the internal and external side of the medial and lateral condyle (planes 9-12).

In addition to these reference planes, an auxiliary plane subtended 15° from the perpendicular plane to the tangent plane of the posterior femoral cortex was defined to measure the trochlear depth as described by Dejour et al (plane 13) (Dejour et al. 1994).

2. 2. 4. Measurements

Based on this set of landmarks and reference planes, the 3D models were evaluated for a series of well-known characteristics of TD (hereafter referred to as conventional parameters). These characteristics address the trochlear region as well as the relation of the patella to the trochlea. Furthermore, novel characteristics describing the geometry of the distal femur in its ML, AP and PD aspect (hereafter referred to as morphometric parameters) were also introduced.

Eleven conventional parameters were measured (trochlear depth (Dejour et al. 1994), sulcus angle (Merchant et al. 1974), medial and lateral inclination angle of the trochlea (Sasaki and Yagi 1986, Stefanik et al. 2012), trochlear bump (Dejour et al. 1994), height of the trochlear cartilage (Yamada et al. 2007), Caton-Deschamps index (Caton et al. 1982), lateral patellar displacement (Laurin et al. 1978), patellar tilt (Grelsamer et al. 1993), asymmetry of the trochlear facets (Pfirrmann et al. 2000), and asymmetry of the patellar facets (Endo et al. 2007)). Because most of these parameters were intended to be measured on 2D images without cartilage, the measurement procedure was slightly different (the details of the measurement method are listed in appendix B). In contrast to the original 2D measurements previously published, the current 3D measurements are not flawed by differences in cartilage thickness, differences in knee size, and alignment errors, which can considerably affect the measurements in 2D.

Additionally, a series of morphometric parameters of the distal femur were measured in three directions; the ML direction (width of the femur, width of the medial and lateral condyle and the notch), the PD direction (the PD size of the medial and lateral posterior condyle) and AP direction (AP size of the medial and lateral condyle, the medial, lateral and central trochlea and the medial and lateral posterior condyle). And in the axial plane, the angle between the PCL and the sTEA was measured (PCL-sTEA angle).

2. 2. 5. Statistical analysis

All data were analysed using IBM SPSS Statistics 20. To analyse the inter-observer reliability two observers (AVH and KDR) defined the landmarks on a set of 20 knees (four knees of the control group and 16 knees of the TD group, equally divided over the four Dejour types). The inter-observer reliability of the landmarks was then determined by calculating the intra-class correlation coefficient of the x, y, and z coordinate. The intra-class correlation coefficient and the mean error ± SD are reported. The rescaling factor of the control group and the TD group are reported as mean ± SD. A Mann-Whitney U-test was performed on the rescaling factor to evaluate if the actual knee size was different in the TD group compared to the control group. The measurements of the conventional and morphometric parameters are reported as mean ± SD. A Mann-Whitney U-Test was performed to compare the data in the TD group with the data in the control group. To facilitate visualisation of the parameters, the results of the TD group are expressed as a percentage with respect to the results of the control group. In the TD group, a Spearman's correlation test was also performed to investigate which parameters correlate with each other and with the order of the applied classification (Dejour type A, B, C and D).

For all statistical tests, a p-value less than 0.05 was considered statistically significant.

2. 3. Results

The knees in the control group (N=20) were rescaled with a mean rescaling factor of 1.00 ± 0.08 and the knees in the TD group (N=20) with a mean rescaling factor of 1.03 ± 0.07. The rescaling factor did not show a difference between both groups (n.s.). In this study population (N=40), the largest knee was 35% larger than the smallest knee.

Two observers defined all landmarks on 20 knees (4 of the control group and 16 of the TD group) with an intra-class correlation coefficient of 0.99 (mean error 1.0 mm ± 1.5 mm).

The results of all the conventional parameters show significant differences between the TD group and the control group ($p < 0.05$) (Table 2.1, Figure 2.2).

Within the TD group, the lateral inclination angle correlated with the trochlear depth ($r = 0.583$, $p = 0.007$) and the medial inclination angle with the trochlear sulcus angle ($r = - 0.674$, $p = 0.001$). The assigned four-grade Dejour classification showed a correlation with an increased trochlear sulcus angle ($r = 0.636$, $p = 0.003$) and patellar tilt ($r = 0.465$, $p = 0.039$).

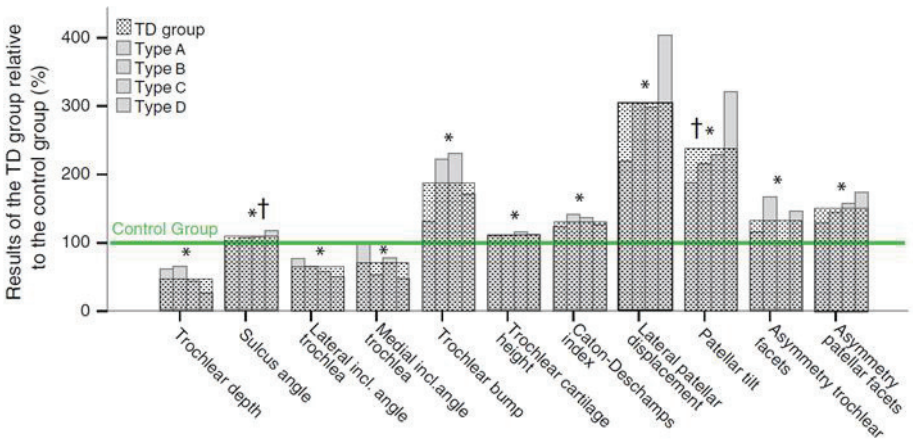

Figure 2.2 Results of 11 conventional parameters in the TD group, expressed as their ratio to the control group (%). The mean value of the control group is presented as 100%. For each parameter, the four thin bars represent the results of TD type A, B, C and D (in this order), the gridded bars represents the mean results of the TD group. A significant difference between the TD group and the control group is indicated by (*). A significant correlation ($p < 0.05$) with the Dejour classification is indicated by (†)

Table 2.1 Overview of 11 conventional parameters

Characteristics of trochlear dysplasia	Control	Trochlear Dysplasia	p-value
Trochlear depth (mm)	5.6 ± 1.5	2.7 ± 2.3	<0.001
Sulcus angle (°)	150.3 ± 4.4	164.3 ± 12.6	<0.001
Lateral inclination angle of the trochlea (°)	16.3 ± 2.8	10.2 ± 5.1	<0.001
Medial inclination angle of the trochlea (°)	13.4 ± 2.6	9.3 ± 4.9	0.005
Trochlear bump (mm)	2.6 ± 1.2	4.9 ± 2.1	<0.001
Trochlear cartilage height (mm)	33.7 ± 3.4	37.8 ± 3.0	<0.001
Caton-Deschamps index (-)	1.0 ± 0.1	1.3 ± 0.2	<0.001
Lateral patellar displacement (mm)	2.7 ± 2.6	8.1 ± 8.9	0.004
Patellar tilt (°)	10.5 ± 4.9	25.1 ± 10.0	<0.001
Asymmetry trochlear facets (%)	62.0 ± 10.2	52.3 ± 25.8	0.004
Asymmetry patellar facets (%)	93.4 ± 9.3	67. 8 ± 22.9	0.001

For the morphometric measurements there were significant differences between the TD group and the control group in the three directions (Table 2.2, Figure 2.3., Figure 2.4). In the AP direction, the distal femur was larger at three locations in the TD group; the medial posterior condyle was 6 % larger ($p = 0.048$), the lateral posterior condyle was 8% larger ($p = 0.013$) and the total medial condyle was 3% larger ($p = 0.009$) compared to the control group. In the ML direction, the distal femur was smaller at two measured levels in the TD group; the total width was 1% smaller ($p = 0.045$) and the notch was 10% smaller ($p = 0.037$). In the PD direction, the medial posterior condyle was 4% larger in the TD group ($p = 0.021$).

Within the TD group, the size of the lateral trochlea correlated with the trochlear depth ($r = 0.684$, $p = 0.001$) and with the lateral inclination angle ($r = 0.492$, $p = 0.028$), while the size of the medial trochlea correlated with the trochlear bump ($r = 0.839$, $p < 0.001$).

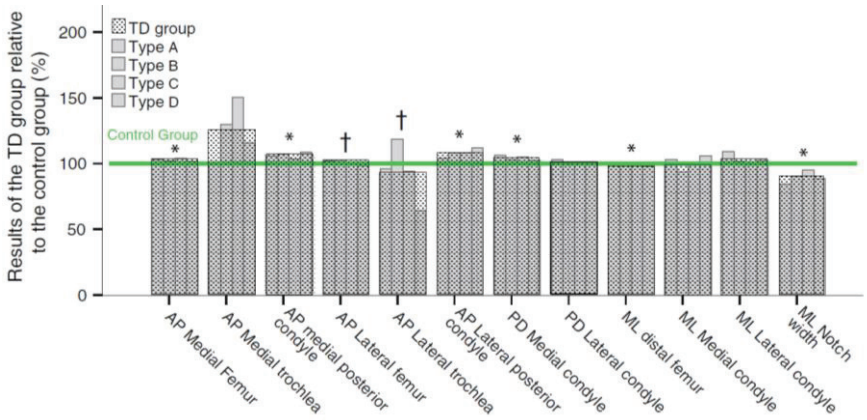

Figure 2.3 Results of 12 morphometric parameters in the AP, PD and ML direction in the TD group, expressed as their ratio to the control group (%). The mean value of control group is presented as 100%. For each parameter, the four thin bars represent the results of TD type A, B, C and D (in this order), the gridded bars represents the mean results of the TD group. A significant difference between the TD group and the control group is indicated by (*). A significant correlation ($p < 0.05$) with the Dejour classification is indicated by (†).

Table 2.2 Overview of the morphometric parameters on the distal femur

	Morphometric parameters (mm)	Control	TD	p-value
AP	Medial femur	64.3 ± 1.9	66.1 ± 2.4	0.009
	Medial trochlea	4.2 ± 1.7	5.2 ± 2.2	0.245
	Medial posterior condyle	27.6 ± 2.2	29.3 ± 2.5	0.048
	Lateral femur	67.1 ± 1.7	67.8 ± 2.4	0.433
	Lateral trochlea	8.3 ± 1.7	7.8 ± 2.6	0.176
	Lateral posterior condyle	25.5 ± 2.3	27.6 ± 2.6	0.013
PD	Medial condyle	39.7 ± 1.5	41.3 ± 2.8	0.021
	Lateral condyle	38.6 ± 1.6	38.6 ± 2.7	0.482
ML	Distal femur	79.1 ± 1.7	78.2 ± 1.5	0.045
	Medial condyle	23.3 ± 2.1	23.5 ± 2.1	0.829
	Lateral condyle	25.3 ± 2.1	26.2 ± 2.5	0.213
	Notch width	21.3 ± 3.2	19.2 ± 2.6	0.037

The assigned four-grade Dejour classification correlated negatively with the AP size of the lateral condyle (r = -0.504, p = 0.023) and the lateral trochlea (r = -0.465, p = 0.039).

The PCL-sTEA angle did not differ between the control group (2.6 ± 1.6°) and the TD group (2.6 ± 2.3°) (p = 0.626).

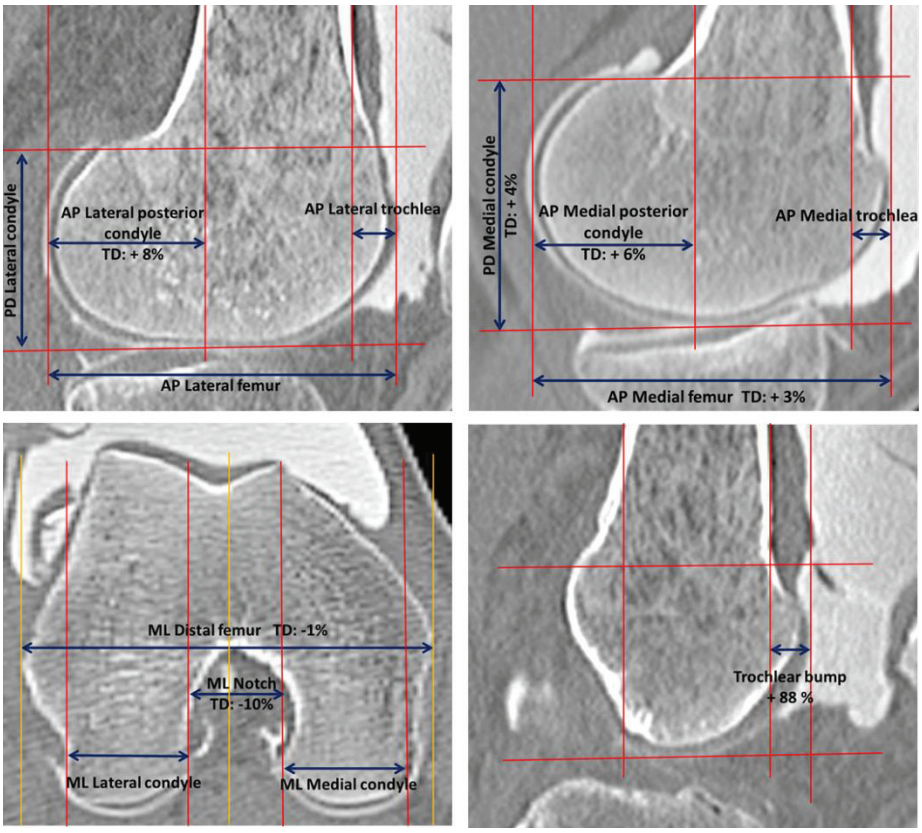

Figure 2.4 Representation of the morphometric measurements in the AP, PD and ML direction. Significant differences between the control group and the TD group are accompanied by the % deviation of the TD group from the control group.

2. 4. Discussion

The most important finding in this study is the evidence that dysplasia of the trochlea is accompanied by abnormalities in the posterior condylar morphology, which was demonstrated by applying a novel landmark-based analysis on a set of normal and TD rescaled knee bones. As such, it can be stated that isolated TD does not exist; the affected knees are also characterised by a smaller intercondylar notch, larger posterior condyles in the AP direction and a larger medial condyle in the PD direction.

Rescaling is particularly important in the interpretation of metric parameters used for diagnostic purposes. The current population of 40 subjects showed up to 35% difference in knee size. This difference in size is based on the rescaling factor, which takes the size in the AP, PD and ML direction into account (e.g. the ML size prior to rescaling showed a range of 66.8 mm to 94.5 mm). Alternatively, metric parameters can also be expressed as a percentage of the ML size, as done by Biedert and Bachmann for the AP size (Biedert and Bachmann 2009). However, given the variability in the AP-ML ratio, the resulting percentages would be influenced by this ratio, while sizing takes the full size of the distal femur into account

In this study the rescaled distal femur models were investigated by applying a predefined set of reference planes to measure a series of conventional parameters together with a set of overall morphometric characteristics.

Regarding the conventional parameters, this study replicates the highly significant differences between TD knees and normal knees, which confirms that the proposed method is suitable for measuring these parameters. An important difference, however, between the current study and most previous studies is that the cartilage was included in the current analyses. Because the cartilage tends to be thicker at the deepest point of the trochlea (Toms et al. 2009), the trochlear depth was smaller, the sulcus angle was larger and the medial and lateral inclination angle were smaller in the current study compared to measurements in previous studies (Dejour et al. 1994, Stefanik et al. 2012). Trochlear bump, which is a measure of trochlear floor elevation, is traditionally measured between the anterior cortex and the deepest point of the trochlear floor (Dejour et al. 1994). Obviously, if the cartilage on the trochlear floor is taken into account, a larger trochlear bump will be measured. Arthro-CT is proven to be an appropriate imaging method to generate 3D bone-cartilage models (Allen et al. 2010).

For the morphometric parameters, to date, limited research results were published focussing on the AP and ML size of the distal femur affected by TD. In 2000, Pfirrmann et al. found no significant differences in terms of the AP size of the medial and lateral femoral condyles and their ratio, the absolute and relative ML width of the distal femur and the trochlea, and the distance between the deepest point of the trochlear floor and the PCL (Pfirrmann et al. 2000). These findings do not correspond with the current study and with the findings of Biedert and Bachmann (Biedert and Bachmann 2009). This might be due to the smaller population size in the first study, to the inclusion criteria or to the location of the axial slice where the measurement took place. In 2009, Biedert and Bachmann investigated the AP size of the distal femur in relation to the ML size to detect if a decreased trochlear depth is caused by a heightened trochlear floor or by a flattened lateral and/or medial trochlea. In line with the current results, they found that the ratio was not altered at the level of the lateral trochlea and that it was increased at the level of the centre and medial trochlea. With the use of the reference planes, it was possible to look into these measurements in more detail. In the TD group, the posterior part of the lateral condyle was 8% longer while the lateral trochlea tended to be 7% shorter (not significant) compared to the control group. So even in knees in which the total lateral condyle is unaltered, it is possible that a difference in the posterior part compensates for a difference in the anterior part. At the level of the medial trochlea, the current data suggest that the enlarged medial condyle in the TD group is at least partially due to an increase of the posterior condyle. The mean medial trochlea was also increased by 24 % but this increase was not significant. At the level of the centre of the trochlea, the anterior offset (trochlear bump) was substantially increased in the TD group, which is in agreement with earlier findings of numerous other authors (Biedert et al. 2011, Biedert et al. 2011, Dejour et al. 1994).

In the ML direction, the overall width of the trochleodysplastic knees was slightly smaller compared to the normal group, while the size of the medial and lateral condyles shows no significant differences. This small difference in the overall width of the distal femur can be explained by the narrow intercondylar notch in the TD group. Intercondylar notch size and shape are known to be related to ACL damage and osteoarthritis (Anderson et al. 1987, Shepstone et al. 2001, Sonnery-Cottet et al. 2011), but has not yet been reported in association with TD.

Limitations of this study include the relatively small number of subjects and the use of a four-grade classification system which has recently been shown to be insufficient to distinguish type B, C and D from one another (Lippacher et al. 2012). In the current study, only one senior surgeon evaluated the arthro-CT scans to classify the patients and the intra-observer agreement was not tested. So it could be argued that the reliability of the patient group classification is insufficient. Testing the repeatability of the Dejour classification or assigning new characteristics to the classification, however, was beyond the scope of this study. The Dejour classification was only used to evaluate if the measured parameters correlated with the assigned classification. The focus of this study was on the morphological differences between normal and TD knees.

A Procrustes rescaling procedure was performed to rule out absolute knee size differences from the analysis. It must be noted that gender, femoral size and to a lesser extent somatotype (endo-, meso- and ectomorph type) are also known to influence the geometry of the distal femur in general, and more specifically the ML/AP ratio of the distal femur (Bellemans et al. 2010, Biedert and Bachmann 2009). In the current study, the control group and TD group were controlled for sex as well as size differences while somatotype was not analysed.

In clinical settings generating and rescaling 3D models sets rather high technical requirements, and is considerably more time-consuming than conventional measurements on axial or lateral slices. Technological evolution however might improve the cost, time-efficiency and complexity of these processes. In anticipation of such developments, this study shows that size differences irrespective of the type of measurement, can considerably affect the interpretation of measurements. For example, knees are found pathological if the trochlear bump is equal to or greater than 3 mm or if the trochlear depth is less than or equal to 4 mm (Dejour et al. 1994). If these cut-off values would be adjusted for the size differences observed in the current data set, these values would be 1 mm larger in the largest knees compared to the smallest knees. This difference is of clinical importance, since clinicians might rely on these absolute cut-off values to diagnose or grade TD. Since the Dejour classification is not only applied to grade the severity but also to assist in the treatment decision, over-or underestimation of morphological characteristics might indirectly lead to inappropriate treatment. Moreover, the presence of a trochlear bump (Dejour type B and D) is a key factor to decide if trochleoplasty is designated (Dejour et al. 2013, Dejour and Saggin 2010, Fucentese et al. 2011). A

recent study by Dejour et al. brought the problem of undiagnosed or underestimated TD to the attention (Dejour et al. 2013). Dejour and colleagues indicated that missed high grade dysplasia (defined as type B and D) may lead to inadequate treatment of patellar dislocation. Sizing the knees, as applied in the current study, provides a more reliable measure of the morphological characteristics, such as the trochlear bump, which can improve identification of high grade dysplasia and consequently improve treatment decision. To date, 3D modelling and sizing sets high technological and time-consuming requirements, but with the vast evolution of technology these processes might become more accessible in clinical settings.

2. 5. Conclusions

With this landmark-based 3D analysis of rescaled bones evidence was found that not only the trochlear region is affected in the trochleodysplastic femur, but that the posterior femur also has a significantly different morphology. The proposed method successfully excluded differences in cartilage thickness, differences in knee size and alignment errors from the analysis.

References

1. Allen BC, Peters CL, Brown NAT, Anderson AE. 2010. Acetabular Cartilage Thickness: Accuracy of Three-Dimensional Reconstructions from Multidetector CT Arthrograms in a Cadaver Study. Radiology. 255:544-552.

2. Anderson AF, Lipscomb AB, Liudahl KJ, Addlestone RB. 1987. Analysis of the Intercondylar Notch by Computed-Tomography. Am J Sport Med. 15:547-552.

3. Bellemans J, Carpentier K, Vandenneucker H, Vanlauwe J, Victor J. 2010. The John Insall Award: Both morphotype and gender influence the shape of the knee in patients undergoing TKA. Clin Orthop Relat Res. 468:29-36.

4. Biedert R, Sigg A, Gal I, Gerber H. 2011. 3D representation of the surface topography of normal and dysplastic trochlea using MRI. Knee. 18:340-346.

5. Biedert RM, Bachmann M. 2009. Anterior-posterior trochlear measurements of normal and dysplastic trochlea by axial magnetic resonance imaging. Knee surgery, sports traumatology, arthroscopy : official journal of the ESSKA. 17:1225-30.

6. Biedert RM, Netzer P, Gal I, Sigg A, Tscholl PM. 2011. The lateral condyle index: a new index for assessing the length of the lateral articular trochlea as predisposing factor for patellar instability. Int Orthop. 35:1327-1331.

7. Bredbenner TL, Eliason TD, Potter RS, Mason RL, Havill LM, Nicolella DP. 2010. Statistical shape modeling describes variation in tibia and femur surface

geometry between Control and Incidence groups from the Osteoarthritis Initiative database. J Biomech. 43:1780-1786.

8. Caton J, Deschamps G, Chambat P, Lerat JL, Dejour H. 1982. The Low Patellas - Report of 128 Cases - Patella-Inferae. Rev Chir Orthop. 68:317-325.

9. Chhabra A, Subhawong TK, Carrino JA. 2011. A systematised MRI approach to evaluating the patellofemoral joint. Skeletal Radiol. 40:375-387.

10. Dejour D, Byn P, Ntagiopoulos PG. 2013. The Lyon's sulcus-deepening trochleoplasty in previous unsuccessful patellofemoral surgery. Int Orthop. 37:433-439.

11. Dejour D, Le Coultre B. 2007. Osteotomies in patello-femoral instabilities. Sports Med Arthrosc. 15:39-46.

12. Dejour D, Reynaud P, Lecoultre B. 1998. Douleurs et instabilité rotulienne. Essai de classification. Médecin et Hygiène. 56:1466-1471.

13. Dejour D, Saggin P. 2010. The sulcus deepening trochleoplasty-the Lyon's procedure. Int Orthop. 34:311-316.

14. Dejour H, Walch G, Nove-Josserand L, Guier C. 1994. Factors of patellar instability: an anatomic radiographic study. Knee surgery, sports traumatology, arthroscopy : official journal of the ESSKA. 2:19-26.

15. El-Khoury GY, Alliman KJ, Lundberg HJ, Rudert MJ, Brown TD, Saltzman CL. 2004. Cartilage thickness in cadaveric ankles: Measurement with double-contrast multi-detector row CT arthrography versus MR imaging. Radiology. 233:768-773.

16. Endo Y, Schweitzer ME, Bordalo-Rodrigues M, Rokito AS, Babb JS. 2007. MRI quantitative morphologic analysis of patellofemoral region: Lack of correlation with chondromalacia patellae at surgery. Am J Roentgenol. 189:1165-1168.

17. Fitzpatrick CK, Baldwin MA, Laz PJ, FitzPatrick DP, Lerner AL, Rullkoetter PJ. 2011. Development of a statistical shape model of the patellofemoral joint for investigating relationships between shape and function. J Biomech. 44:2446-52.

18. Fucentese SF, Zingg PO, Schmitt J, Pfirrmann CW, Meyer DC, Koch PP. 2011. Classification of trochlear dysplasia as predictor of clinical outcome after trochleoplasty. Knee surgery, sports traumatology, arthroscopy : official journal of the ESSKA. 19:1655-61.

19. Goodall C. 1991. Procrustes Methods in the Statistical-Analysis of Shape. J Roy Stat Soc B Met. 53:285-339.

20. Gower JC. 1975. Generalized Procrustes Analysis. Psychometrika. 40:33-51.

21. Grelsamer RP, Bazos AN, Proctor CS. 1993. Radiographic Analysis of Patellar Tilt. J Bone Joint Surg Br. 75:822-824.

22. Laurin CA, Levesque HP, Dussault R, Labelle H, Peides JP. 1978. Abnormal Lateral Patello-Femoral Angle - Diagnostic Roentgenographic Sign of Recurrent Patellar Subluxation. J Bone Joint Surg Am. 60:55-60.

23. Lippacher S, Dejour D, Elsharkawi M, Dornacher D, Ring C, Dreyhaupt J, Reichel H, Nelitz M. 2012. Observer Agreement on the Dejour Trochlear Dysplasia Classification A Comparison of True Lateral Radiographs and Axial Magnetic Resonance Images. Am J Sport Med. 40:837-843.

24. Merchant AC, Mercer RL, Jacobsen RH, Cool CR. 1974. Roentgenographic Analysis of Patellofemoral Congruence. J Bone Joint Surg Am. A 56:1391-1396.

25. Myronenko A, Song XB. 2010. Point Set Registration: Coherent Point Drift. Ieee T Pattern Anal. 32:2262-2275.

26. Nelitz M, Lippacher S, Reichel H, Dornacher D. 2013. Evaluation of trochlear dysplasia using MRI: correlation between the classification system of Dejour and objective parameters of trochlear dysplasia.

27. Pfirrmann CWA, Zanetti M, Romero J, Hodler J. 2000. Femoral trochlear dysplasia: MR findings. Radiology. 216:858-864.

28. Remy F, Chantelot C, Fontaine C, Demondion X, Migaud H, Gougeon F. 1998. Inter- and intraobserver reproducibility in radiographic diagnosis and classification of femoral trochlear dysplasia. Surg Radiol Anat. 20:285-289.

29. Remy F, Gougeon F, Ala Eddine T, Migaud H, Fontaine C, Duquennoy A. 2002. Reproducibility of the new classification of femoral trochlea dysplasia proposed by Dejour: predictive value for severity of femoropatellar instability in 47 knees. J Bone Joint Surg Br. 84:1.

30. Sasaki T, Yagi T. 1986. Subluxation of the Patella - Investigation by Computerized-Tomography. Int Orthop. 10:115-120.

31. Shepstone L, Rogers J, Kirwan JR, Silverman BW. 2001. Shape of the intercondylar notch of the human femur: a comparison of osteoarthritic and non-osteoarthritic bones from a skeletal sample. Ann Rheum Dis. 60:968-973.

32. Shih YF, Bull AM, Amis AA. 2004. The cartilaginous and osseous geometry of the femoral trochlear groove. Knee surgery, sports traumatology, arthroscopy : official journal of the ESSKA. 12:300-6.

33. Sonnery-Cottet B, Archbold P, Cucurulo T, Fayard JM, Bortolletto J, Thaunat M, Prost T, Chambat P. 2011. The influence of the tibial slope and the size of the intercondylar notch on rupture of the anterior cruciate ligament. J Bone Joint Surg Br. 93B:1475-1478.

34. Staubli HU, Durrenmatt U, Porcellini B, Rauschning W. 1999. Anatomy and surface geometry of the patellofemoral joint in the axial plane. J Bone Joint Surg Br. 81B:452-458.

35. Stefanik JJ, Roemer FW, Zumwalt AC, Zhu YY, Gross KD, Lynch JA, Frey-Law LA, Lewis CE, Guermazi A, Powers CM, Felson DT. 2012. Association between measures of trochlear morphology and structural features of patellofemoral joint osteoarthritis on MRI: The MOST study. J Orthopaed Res. 30:1-8.

36. Toms AP, Cahir J, Swift L, Donell ST. 2009. Imaging the femoral sulcus with ultrasound, CT, and MRI: reliability and generalizability in patients with patellar instability. Skeletal Radiol. 38:329-338.

37. van Huyssteen AL, Hendrix MRG, Barnett AJ, Wakeley CJ, Eldridge JDJ. 2006. Cartilage-bone mismatch in the dysplastic trochlea - An MRI study. J Bone Joint Surg Br. 88B:688-691.

38. Victor J, Van Doninck D, Labey L, Innocenti B, Parizel PM, Bellemans J. 2009. How precise can bony landmarks be determined on a CT scan of the knee? Knee. 16:358-65.

39. Wyler A, Bousson V, Bergot C, Polivka M, Leveque E, Vicaut E, Laredo JD. 2009. Comparison of MR-arthrography and CT-arthrography in hyaline cartilage-thickness measurement in radiographically normal cadaver hips with anatomy as gold standard. Osteoarthr Cartilage. 17:19-25.

40. Yamada Y, Toritsuka Y, Yoshikawa H, Sugamoto K, Horibe S, Shino K. 2007. Morphological analysis of the femoral trochlea in patients with recurrent dislocation of the patella using three-dimensional computer models. J Bone Joint Surg Br. 89B:746-751.

Chapter 3

A Statistical Shape Model of Trochlear Dysplasia of the Knee[2]

Trochlear dysplasia is known as the primary predisposing factor for patellar dislocation. Current methods to describe trochlear dysplasia are mainly qualitative or based on a limited number of discrete measurements. The purpose of this study is to apply statistical shape analysis to take the full geometrical complexity of trochlear dysplasia into account. Statistical shape analysis was applied on 20 normal and 20 trochlear dysplastic distal femurs models, including the cartilage. This study showed that the trochlea was anteriorized, proximalized and lateralized and that the mediolateral width and the notch width were decreased in the trochlear dysplastic femur compared to the normal femur. The first three principal components of the trochlear dysplastic femurs, accounting for 79.7% of the total variation, were size, sulcus angle and notch width. Automated classification of the trochlear dysplastic and normal femurs achieved a sensitivity of 85% and a specificity of 95%. This study shows that shape analysis is an outstanding method to visualise the location and magnitude of shape abnormalities. Improvement of automated classification and subtyping within the trochlear dysplastic group are expected when larger training sets are used.Classification of trochlear dysplasia, especially borderline cases may be facilitated by automated classification. Furthermore, the identification of a decreased notch width in association with an increased sulcus angle can also contribute to the diagnosis of trochlear dysplasia.

[2] This study is submitted for review: A. Van Haver, P. Mahieu, T. Claessens, H. Li, C. Pattyn, P. Verdonk, E.A. Audenaert. A Statistical Shape Model of Trochlear Dysplasia of the Knee. The Knee

3. 1. Introduction

TD is known as the primary predisposing factor for patellar dislocation (Dejour et al. 1994). Acute patellar dislocation is the second most common cause of traumatic hemarthrosis of the knee and accounts for approximately 3% of all knee injuries (Harilainen et al. 1988, Stefancin and Parker 2007). After the primary dislocation, the redislocation rate is high for conservative treatment, varying between 13 and 52% (Buchner et al. 2005). For different surgical treatments the redislocation rate is reported between 3.7 and 30% (Buchner et al. 2005, Shah et al. 2012). On long term, TD is also an important predisposing factor of PF arthritis (Allain et al. 2004).

To date, diagnosis, classification and treatment remain problematic, mainly due to the highly complex and variable geometrical presentation of TD. Various methods have been proposed to describe TD and to differentiate between normal and TD knees and between different classes of TD (Biedert and Bachmann 2009, Carrillon et al. 2000, Dejour et al. 1998, Dejour et al. 1994, Nelitz et al. 2013, Pfirrmann et al. 2000). These reports are mainly qualitative or based on a limited number of discrete measurements. To more realistically represent the complex shape of the trochlea, 3D computer models have been used to analyse the morphology of the TD femur (Biedert et al. 2011, Yamada et al. 2007). The morphological descriptions in these 3D studies however were still based on a relatively small set of discrete variables, not taking into account the full complexity of variation in geometry of the dysplastic knee as can be done by means of statistical shape modelling (SSM).

SSM has the potential to realistically describe anatomy and its variation in any population by conventional multivariate statistics of sets of corresponding landmarks representing the shape of the underlying structures. Unlike the methods used in previous studies, this technique has the potential for accurate description of distribution of anatomy in the population. Further, these models can be used to improve diagnosis, classification and treatment of specific medical conditions (Cootes et al. 1992). This is important in order to distinguish pathological from physiological shape variation. Given the lack of such model for TD, the objective of the current study was to provide a 3D statistical evaluation of the distal TD femur. Shape analysis was applied (1) to evaluate the location and magnitude of the differences between the average normal and TD femur, (2) to describe the leading modes of shape variation of TD femurs and (3) to perform an automated classification of normal and TD.

3. 2. Materials and Methods

3. 2. 1. Image acquisition and registration

For the TD group (TD group), 20 unmatched knees were included in the study (8 male patients, 12 female patients; mean age 29 years; age range 15 – 59 years). Selection was based on a history of recurrent patellar dislocation: Imaging records were evaluated for the presence of TD by two surgeons (PV & EA) and inclusion was defined upon consensus. For the control group, 20 unmatched knees were included with a normal anatomy of the PF joint (9 male patients, 11 female patients, mean age 30 years; age range 18 - 52 years). All cases were selected consecutively during a four year period (2008-2012).

To visualize and include the cartilage in the knee joint, arthro-CT scans were performed. All patients were scanned on a multidetector CT (Definition Flash, Siemens, Erlangen, Germany) after intra-articular injection of 10 to 15 cc iohexol 240 mg/ml (Omnipaque 240, GE Healthcare, Diegem, Belgium) under fluoroscopic guidance. Slice thickness was 1 mm. Patients were fixed in a supine position with 15° of knee flexion and the toes pointing straight up. The arthro-CT images were loaded in a 3D image processing software system (Mimics® 14.12, Materialise, Haasrode, Belgium) to create smooth 3D surface models of the knee bones including the cartilage. These 3D surface models were loaded in Matlab for SSA (MATLAB R2010b, The Mathworks, Inc., Natick, MA) (Figure 3.1).

Dense anatomical point correspondence was obtained using elastic registration of an isotropic template mesh consisting of 5453 vertices, based on the technique for non-rigid registration by Li et al. (Li et al. 2009).

After robust least squares superimposition (Procrustes transformation) of these homologous series of dense vertices, the morphological differences between the normal and TD distal femur models and within the TD femur models was established.

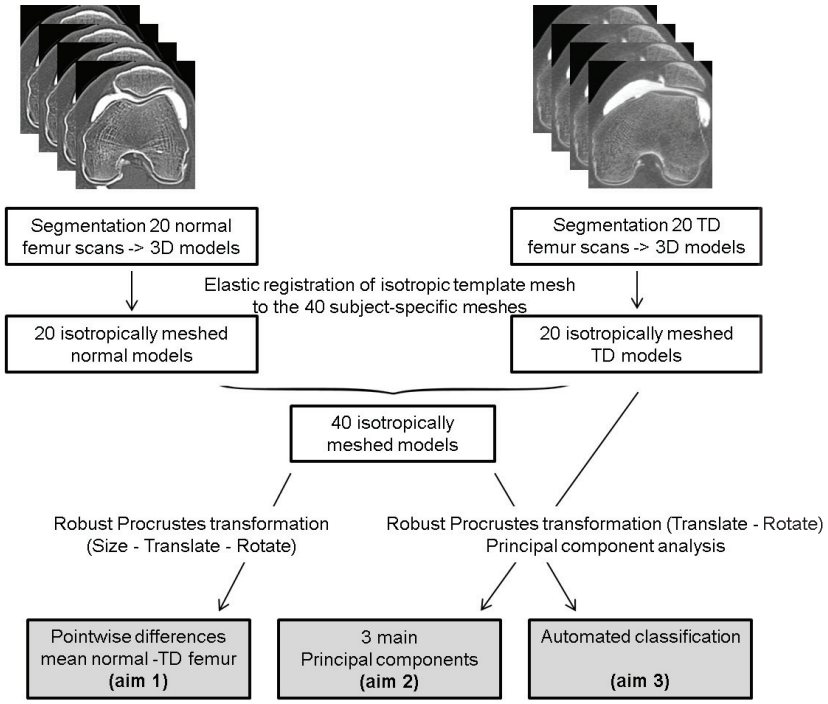

Figure 3.1 Schematic representation of the processing steps

It is important to note that the current sampling set contains femur models characterised by local dysmorphologies (e.g. a trochlear bump up to 6 mm), which can lead to alignment errors during the Procrustes transformation. These abnormalities are typically localized in a small area and do not extend over the whole region of interest. To account for general disturbance during alignment of the data sets by these local abnormalities, - the so-called pinocchio-effect - iterative exclusion of outliers at the 0.05 level was performed to obtain a robust alignment prior to the PCA (Claes et al. 2012).

3. 2. 2. Average difference between normal and trochlear dysplastic femur models

To investigate the differences in femoral bone geometry between the TD and normal femurs the mean shape of both femur sets was calculated and compared (Figure 3.2).

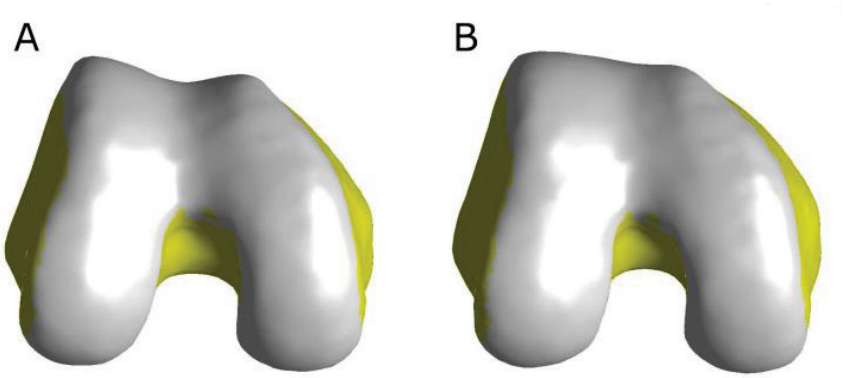

Figure 3.2 Mean shape of the normal femur (A) and TD femur (B): bone (yellow) and cartilage (white)

A distance map was calculated to describe the pointwise surface variation between the average TD and normal model was expressed by visualizing the magnitude and sense of vectors between the corresponding surface vertices. Local differences were visualised by displaying the contours of the average models in a mid-sagittal and axial cross-section of the models.

Differences between the two corresponded data sets were statistically evaluated by means of the Student's t-test at an alpha level for significance of 0.05.

3. 2. 3. Principal components of the trochlear dysplastic femur models

To describe shape variations within the TD group, PCA is applied on the corresponding vertices of the 20 non-resized TD surface meshes (Webb 2002). PCA consists of computing the statistically independent eigenvectors and eigenvalues of the data set. The eigenvectors (PCs) show global shape variations, called 'modes of variation' in a SSM. The associated eigenvalues indicate the amount of shape variance explained by that specific mode of shape variation. The eigenvectors are ordered according to their explained variance; eigenvectors with highest variance are placed first and those with low variance are placed last. The shape characteristics contained with each PC were visualised by plotting the shape corresponding to extreme values (that is, the mean value plus and minus 2.5 SD).

3. 2. 4. Shape model evaluation

To evaluate how well the model describes the overall TD population a "leave one out" assessment was performed. To do so, a SSM was constructed based on 19 bones, iteratively leaving one selected test bone out. Subsequently, the SSM was

fitted to the excluded bone and the goodness of fit of the SSM to describe a bone not included in the SSM was evaluated. As error measure the root mean square (RMS) distance was computed between the fitted sample and the corresponding vertices of the excluded bone. This procedure was repeated for all bones in the TD group and the normal group. The RMS errors for all femur models are an indication of the shape similarity between the left out sample and the training set.

3. 2. 5. Automated classification of the normal and trochlear dysplastic femur models

Notwithstanding the low number of included cases, an automated classification of the normal and TD femur models was attempted. Grouping of shape was based on the PCs of the complete, annotated training set of 40 femurs. It was first evaluated which PCs showed significant correlation with the clinical classification provided by the consensus of two senior orthopaedic experts (PV & EA). Consequently, it was evaluated if these components were successful in discriminating between the TD femur models and the normal models. To do so, linear discriminant analysis was applied to find a linear combination of the PCs which can separate the two classes. Sensitivity and specificity of the automated classification procedure were consequently determined by calculating the proportion of actual positives and actual negatives correctly identified by the SSM, with the clinical classification considered as the gold standard.

3. 3. Results

3. 3. 1. Average difference between normal and trochlear dysplastic femur models

Pointwise surface differences between the average TD and normal model are demonstrated by a distance map on the surface model of the average normal model in Figure 3.3. The average TD distal femur was heightened at the level of the central trochlear floor compared to the averaged normal distal femur. This elevation of the anterior trochlea was most pronounced in its proximal part, as demonstrated by the highlighted area in red indicating an anteriorization of up to 4.7 mm ($p < 0.001$) (Figure 3.3, Figure 3.4).

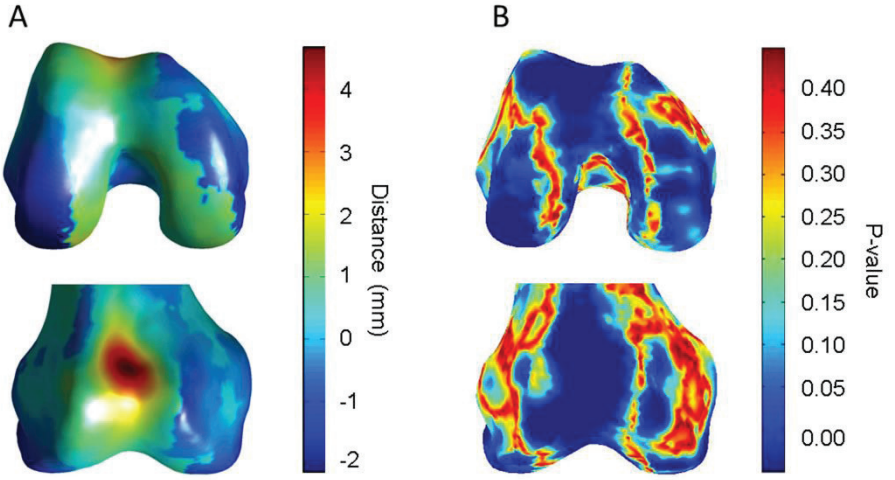

Figure 3.3 Pointwise distances (A) between the average normal and TD femur and the accompanying significance of these distances (p-values) (B) projected on the surface geometry of the average normal femur.

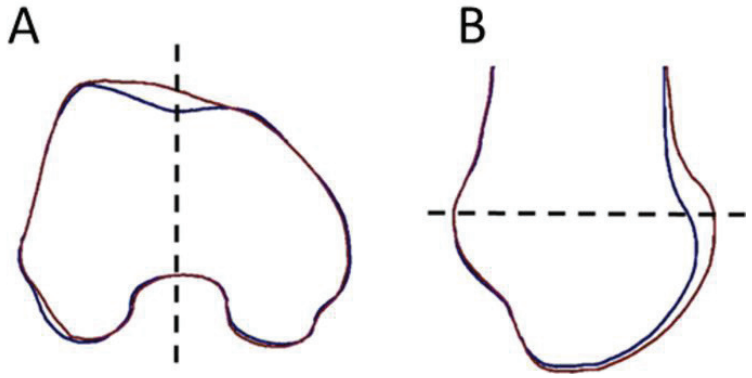

Figure 3.4 Axial (A) and mid-sagittal (B) contours of the mean normal femur (blue contour) and mean TD femur (red contour) demonstrating the large differences in the supratrochlear area

In addition, the trochlea was also proximalized and lateralized in the TD group compared to the normal group. Proximalization is demonstrated by the red coloured area proximal to the normal trochlea and lateralization is demonstrated by the blue area (indicating negative values) at the medial side of the trochlea and the green area (indicating positive values) at the lateral side of the trochlea.

On the distal view it can be observed that the average TD femur is smaller in the mediolateral direction as demonstrated by the blue areas at the outmost medial and lateral region ($p < 0.05$). The central parts of the medial and lateral condyle, which together comprise the notch, are bulkier in the average TD femur as demonstrated by the green coloured areas in the central part ($p < 0.05$).

3. 3. 2. Principal components of trochlear dysplastic femur models

The relative importance of each mode of shape variation - PC- is conventionally determined by the amount of variance within the population represented by each mode. The cumulative variance and the variance per mode are demonstrated in Figure 3.5. The three first PCs, which will be discussed in detail further in this study, describe together 79.7% of the observed population variance. Each of the remaining PCs described less than 3% of variance per mode (Figure 3.5).

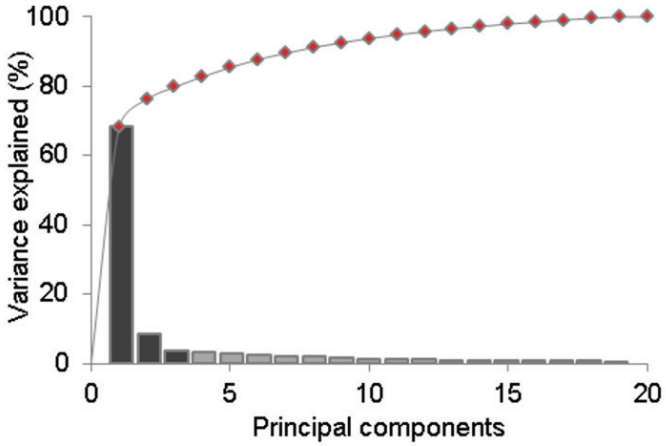

Figure 3.5 Cumulative variance (markers) and fraction of variance (bars) explained by principal components of the TD femur SSM. The dark colored bars represent the first three principal components

The PCs qualitatively describe the spatial distribution of global differences in the distal femur geometry within the TD group. In Figure 3.6 the shape variations along the first 3 modes of variation are visualized. It can be observed that the first PC, accounting for 68.0% of the variation, mainly concerns the size of the model. The second PC, which accounts for 8.2% of the variation concerns variation in the sulcus angle; the mean shape + 2.5 SD shows a convex trochlea with an anterior

prominence where the mean shape – 2.5 SD shows a rather normal concave trochlea with an apparently normal trochlear sulcus angle. The third PC accounts for 3.5% and shows mainly variation in the intercondylar notch width, but is clearly associated with variation in the anterior trochlea as well; with a smaller notch width, the anterior trochlea appears smaller in the mediolateral direction and the sulcus angle increases.

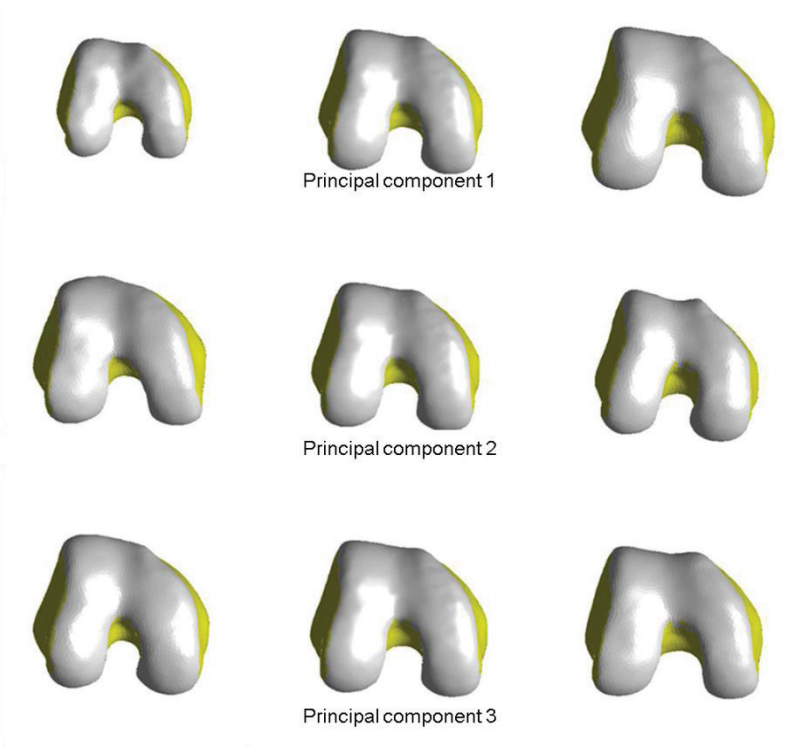

Figure 3.6 Mean shape of the TD femur varied by ± 2.5 SD along the first three principal components. Primary changes in geometry were respectively size, sulcus angle and notch width

3. 3. 3. Shape model evaluation

The RMS error of the SSM, using all PCs, averaged 1.3 mm for the TD knees and 1.2 mm for the normal knees (Figure 3.7).

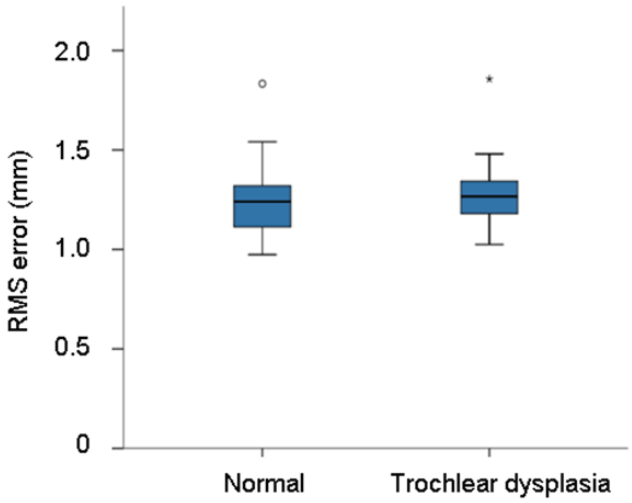

Figure 3.7 Box plot of the Root Mean Square error (RMS error) of the statistical shape model for the normal group and TD group, based on a leave-one-out validation test

3. 3. 4. Automated classification of the normal and trochlear dysplastic femur models

In the complete training set of 40 femur models, PC 2, 3 and 8 were significantly correlated with the clinical annotation dysplastic versus normal ($p < 0.05$). Automated classification with these significant components achieved a sensitivity of 85% and a specificity of 95%.

3. 4. Discussion

SSA is an outstanding method to visualise the location and magnitude of shape abnormalities of the mean TD femur. Furthermore, the three first shape modes, accounting for 79.7% of the shape variation of TD femurs were qualitatively described. In addition, automated classification of the normal and TD femur models was attempted.

Shape analysis showed significant differences between the shape of the average normal and TD femur. The largest differences were observed at the proximal trochlea. As expected, the central TD trochlea was substantially anteriorized compared to the normal trochlea, which is one of the key factors of TD (Dejour et al. 1994). Compared to earlier studies, the advantage of the current study is that the visual presentation of the differences between the normal and TD model provides a more complete and accurate evaluation of the morphological differences between

normal and TD femurs (Figure 3.3). By using the distance map it can easily be observed that the trochlear anteriorization is present in the complete central trochlea, but that the anteriorization gradually decreases towards the notch. In addition, the TD trochlea was clearly more proximally distributed. Yamaha et al. were the first to evaluate proximalization of the trochlear cartilage (Yamada et al. 2007). They suggested that the articular cartilage of the trochlea might be more proximally-distributed to allow contact with the articular cartilage of a high-riding patella, which is often associated with TD (Yamada et al. 2007). Adaptation of the trochlear shape to the patellar position was recently supported by an experimental animal study on growing rabbits (Huri et al. 2012). It was observed that lateralisation of the patella (obtained by releasing the medial soft tissue constraints) actually caused the development of a more flattened trochlea. With these observations, Huri et al. concluded that early reconstruction of the PF joint can help to prevent deterioration of the PF problems. The current study confirms that the TD trochlea is indeed distributed more proximally, but correlation tests with the patellar height were not performed. Less obvious, the TD model also demonstrated a lateral shift of the trochlea, which was also described by Yamada et al. (Yamada et al. 2007). Similar to the trochlear proximalization, trochlear lateralization might also be correlated with patellar lateralisation, but this was not tested in the current study. Other observed differences include a decreased mediolateral width, which supports earlier findings that the mediolateral/anteroposterior ratio is on average lower in the TD femur compared to the normal femur (Biedert and Bachmann 2009). Furthermore, the central parts of the medial and lateral condyle appear bulkier in the TD femur, which indicates a smaller notch width in TD femurs compared to the normal femurs.

In the second part of this study the first three PCs of the 20 TD femurs concerning the size, the sulcus angle and notch width, were investigated. As expected, the first component was the size, which is known to be the primary source of variability of nearly all biological systems (Fitzpatrick et al. 2011). In the current training set, size accounted for almost 70% of the total variability. The subsequent PCs described the actual shape variations of the TD femur, which have to our knowledge not been described yet. Not surprisingly, the second PC concerns the sulcus angle. The sulcus angle is closely related to the anteriorization of the central trochlea and trochlea depth and has been reported as one of the main factors of trochlear (Dejour et al. 1994). The third PC shows variation in the intercondylar notch width in associated with variation in the anterior trochlea; with a smaller notch width the sulcus angle increases. Variation in notch width has not often been discussed in the context of

TD. SSM of the normal PF joint have been developed by Fitzpatrick et al. (Fitzpatrick et al. 2011). The third PC in their model concerned the sulcus angle and though it was not discussed in their article, their results also demonstrated that smaller notch width was associated with larger sulcus angles. The current SSM suggests that sulcus angle variations (PC 2) can occur without variations in the notch width, but that variations in the notch width (PC 3) occur in a well-defined relation to the sulcus angle. Furthermore, the main shape variations within the TD femurs (sulcus angle and notch width) address the same regions as the main shape differences between the average normal and TD femur models.

Automated classification of the normal and TD femurs based on linear discriminant analysis of statically relevant PCs achieved a sensitivity of 85% and a specificity of 95%. These current results are -yet- not superior compared to manual methods, which may due to the current size of the training set. Measurements of the trochlear depth and trochlear facet asymmetry could differentiate TD knees from normal knees with a sensitivity of 100 % and a specificity of 96 % (Pfirrmann et al. 2000) and measurements of the lateral trochlear inclination angle could identify knees with patellar instability with a sensitivity of 93 % and a specificity of 87 % (Carrillon et al. 2000). However, no borderline cases were included in the control groups of the above mentioned studies; therefore it is unclear how good these discrete classifications will work for prospective series. Since classification in the current SSM method is based on a number of relevant shape variations instead of only one or two discreet measurements, SSM are more likely to be successful in classifying borderline cases. Furthermore, automated classification is assumed to improve when larger training sets are used.

Obviously, the small sample size is a limitation in this study. The sample size of the current study, however, was based on similar studies which did achieve robust results with almost half the sample size (Bredbenner et al. 2010). Clearly, TD is morphologically much more complex than other pathologies about the knee. A second limitation is that the cartilage thickness of the femur models was not analysed. In the current study the femur models included the cartilage because it has been demonstrated that the cartilage layer is thicker in the central part of the trochlea, hereby exacerbating the abnormal geometry of the trochlea (van Huyssteen et al. 2006). Future analysing of cartilage thickness can provide additional information on the shape of the subchondral bone as well as the thickness of the cartilage.

SSM provide an innovative and important step towards describing differences in knee joint geometry and have great potential to understanding and differentiating between normal and TD knees.

3. 5. Conclusions

This study shows that shape analysis is an outstanding method to visualise the location and magnitude of shape abnormalities. Classification of TD, especially borderline cases may be facilitated by automated classification. Furthermore, the identification of a decreased notch width in association with an increased sulcus angle may also contribute to the diagnosis of TD. Future studies on larger datasets however are designated.

References

1. Allain J, Dejour D, Argenson JN, Duparc F, Godefroy D, Gougeon F, Huten D, Jenny JY, Mertl P, Migaud H, et al. 2004. Isolated patello-femoral osteoarthritis. Rev Chir Orthop. 90:69-129.

2. Biedert R, Sigg A, Gal I, Gerber H. 2011. 3D representation of the surface topography of normal and dysplastic trochlea using MRI. Knee. 18:340-346.

3. Biedert RM, Bachmann M. 2009. Anterior-posterior trochlear measurements of normal and dysplastic trochlea by axial magnetic resonance imaging. Knee surgery, sports traumatology, arthroscopy : official journal of the ESSKA. 17:1225-30.

4. Bredbenner TL, Eliason TD, Potter RS, Mason RL, Havill LM, Nicolella DP. 2010. Statistical shape modeling describes variation in tibia and femur surface geometry between Control and Incidence groups from the Osteoarthritis Initiative database. J Biomech. 43:1780-1786.

5. Buchner M, Baudendistel B, Sabo D, Schmitt H. 2005. Acute traumatic primary patellar dislocation - Long-term results comparing conservative and surgical treatment. Clin J Sport Med. 15:62-66.

6. Carrillon Y, Abidi H, Dejour D, Fantino O, Moyen B, Tran-Minh VA. 2000. Patellar instability: Assessment on MR images by measuring the lateral trochlear inclination-initial experience. Radiology. 216:582-585.

7. Claes P, Daniels K, Walters M, Clement J, Vandermeulen D, Suetens P. 2012. Dysmorphometrics: the modelling of morphological abnormalities. Theor Biol Med Model. 9:

8. Cootes TF, Cooper DH, Taylor CJ, Graham J. 1992. Trainable Method of Parametric Shape-Description. Image Vision Comput. 10:289-294.

9. Dejour D, Reynaud P, Lecoultre B. 1998. Douleurs et instabilité rotulienne. Essai de classification. Médecin et Hygiène. 56:1466-1471.

10. Dejour H, Walch G, Nove-Josserand L, Guier C. 1994. Factors of patellar instability: an anatomic radiographic study. Knee surgery, sports traumatology, arthroscopy : official journal of the ESSKA. 2:19-26.

11. Fitzpatrick CK, Baldwin MA, Laz PJ, FitzPatrick DP, Lerner AL, Rullkoetter PJ. 2011. Development of a statistical shape model of the patellofemoral joint for investigating relationships between shape and function. J Biomech. 44:2446-52.

12. Harilainen A, Myllynen P, Antila H, Seitsalo S. 1988. The Significance of Arthroscopy and Examination under Anesthesia in the Diagnosis of Fresh Injury Hemarthrosis of the Knee-Joint. Injury. 19:21-24.

13. Huri G, Atay OA, Ergen B, Atesok K, Johnson DL, Doral MN. 2012. Development of femoral trochlear groove in growing rabbit after patellar instability. Knee surgery, sports traumatology, arthroscopy : official journal of the ESSKA. 20:232-8.

14. Li H, Adams B, Guibas LJ, Pauly M. 2009. Robust Single-View Geometry and Motion Reconstruction. Acm T Graphic. 28:

15. Nelitz M, Lippacher S, Reichel H, Dornacher D. 2013. Evaluation of trochlear dysplasia using MRI: correlation between the classification system of Dejour and objective parameters of trochlear dysplasia.

16. Pfirrmann CWA, Zanetti M, Romero J, Hodler J. 2000. Femoral trochlear dysplasia: MR findings. Radiology. 216:858-864.

17. Shah JN, Howard JS, Flanigan DC, Brophy RH, Carey JL, Lattermann C. 2012. A Systematic Review of Complications and Failures Associated With Medial Patellofemoral Ligament Reconstruction for Recurrent Patellar Dislocation. Am J Sport Med. 40:1916-1923.

18. Stefancin JJ, Parker RD. 2007. First-time traumatic patellar dislocation - A systematic review. Clin Orthop Relat R. 93-101.

19. van Huyssteen AL, Hendrix MRG, Barnett AJ, Wakeley CJ, Eldridge JDJ. 2006. Cartilage-bone mismatch in the dysplastic trochlea - An MRI study. J Bone Joint Surg Br. 88B:688-691.

20. Webb A. 2002. Statistical Pattern Recognition. Wiley.

21. Yamada Y, Toritsuka Y, Yoshikawa H, Sugamoto K, Horibe S, Shino K. 2007. Morphological analysis of the femoral trochlea in patients with recurrent dislocation of the patella using three-dimensional computer models. J Bone Joint Surg Br. 89B:746-751.

Chapter 4

The use of rapid prototyped implants to simulate knee joint abnormalities for in-vitro testing: a validation study with replica implants of the native trochlea[3]

To investigate the biomechanical effect of skeletal knee joint abnormalities, the authors propose to implant pathologically shaped rapid prototyped implants in cadaver knee specimens. This new method was validated by replacing the native trochlea by a replica implant on four cadaver knees with the aid of cadaver-specific guiding instruments. The accuracy of the guiding instruments was assessed by measuring the rotational errors of the cutting planes (on average 3.01° in extension and 1.18° in external/internal rotation). During a squat and open chain simulation the patella showed small differences in its articulation with the native trochlea and the replica trochlea, which could partially be explained by the rotational errors of the implants. This study concludes that this method is valid to investigate the effect of knee joint abnormalities with a replica implant as a control condition to account for the influence of material properties and rotational errors of the implant.

[3] This study is submitted for review: A. Van Haver, K. De Roo, M. De Beule, S. Van Cauter, L. Labey, P. De Baets, T. Claessens, P. Verdonk. The use of rapid prototyped implants to simulate knee joint abnormalities for in-vitro testing: a validation study with replica implants of the native trochlea Proceedings of the Institution of Mechanical Engineers, Part H: Journal of Engineering in Medicine.

4. 1. Introduction

Abnormal joint geometry frequently leads to abnormal joint function, disability and pain. Joint geometry can be evaluated by medical imaging and can be linked to clinical investigation of the patient.

Patients however often have a variety of bony and soft tissue abnormalities making it very hard to identify the primary factors causing the symptoms. Isolated research on geometrical abnormalities is thus quite difficult in an in-vivo population. In addition, investigation of certain parameters like the PF joint forces requires research methods which are too invasive and thus unethical to complete on living human subjects.

Cadaveric testing on the other hand allows for more invasive research but is limited in simulating abnormalities. Most cadaveric specimens have a normal geometry and no standardized procedure exists to simulate different abnormalities. To meet this limitation, we developed a new method to implant a 3D-printed pathological model in a cadaveric knee. This method allows us to investigate isolated abnormalities and define their influence on the (mal)function of the joint. With cadaver specific guiding instruments, a well-defined part of the cadaver bone is resected and replaced by a compatible but pathological implant containing the abnormality of interest.

Skeletal abnormalities are an important cause of abnormal joint function, disability and pain. Joint geometry can be visualized by medical imaging and can be linked to the medical history and the clinical examination of the patient. In the knee joint, dysplasia of the femoral trochlea has been reported as the primary factor in patellar instability (Dejour et al. 1994). The aetiology of patellar instability however is multifactorial; the patients usually have a variety of bony and soft tissue abnormalities (Dejour et al. 1994).

Therefore, to investigate the effect of isolated geometrical abnormalities on the kinematics, kinetics and stability of the PF joint, in-vitro experiments or computer simulations are more appropriate than an in-vivo analysis. Modifying the joint geometry while all other factors remain unaltered sets high technological requirements. Furthermore isolated joint modifications can also influence other concomitant factors/elements, such as the joint congruence and tightness of the soft tissues around the joint, which can also be a source of biomechanical deviations. Consequently, only few in vitro and in silico methods have been described to evaluate the joint geometry as an isolated factor. In-vitro experiments were performed on a knee rig to evaluate the kinematics and stability of the patella before

and after simulating TD. Cadaver specimens were altered by removing a wedge of bone to flatten the lateral trochlea (Senavongse and Amis 2005) and by lifting the articular cartilage to elevate the central groove (Amis et al. 2008). A two-dimensional transverse plane computer model was designed to evaluate the effect of an increased sulcus angle on the patellar stability, tilt and shift (Jafari et al. 2008). More recently, Fitzpatrick et al. used a SSM of normal knees to investigate the relation between the shape of the PF joint and the kinematics and kinetics (Fitzpatrick et al. 2011).

Especially in cadaver testing the possibilities to simulate skeletal abnormalities are limited. TD can be simulated on a normal cadaver specimen by conventional surgery, which is an adequate technique to compare the function of the normal knee joint and a surgically modified knee joint. TD however can occur in many variations: with or without the presence of a trochlear bump and with a shallow, flat or convex trochlea (Dejour et al. 1994). All these variations cannot be simulated by conventional surgery on the same cadaver.

To overcome this limitation, the authors suggest to physically create and implant different types of computer-aided rapid prototyped (RPT) models in cadaver specimens for experimental testing. The authors hypothesize that this method facilitates the investigation of isolated geometrical abnormalities in all their variations.

The aim of this study is (i) to describe this novel methodology of replacing the native anterior trochlea by a rapid prototyped trochlear implant and (ii) to validate this technique by comparing the geometry and the PF kinematics and kinetics of four cadaver knees before and after implantation of a RPT replica of the trochlea (hereafter referred to as replica implant).

4. 2. Materials and methods

Four unmatched fresh frozen cadaveric knees, both male and female (aged 75 – 85 years) were thawed at room temperature. Before medical images were obtained, a water-soluble X-ray contrast medium (Iodixanol, Visipaque, GE Healthcare, London, UK) was injected in the knee joint to visualize the cartilage. The knees were scanned with a Toshiba/Aquilion helical multislice computed tomography (CT) scanner (Toshiba Medical Systems, Otawara, Japan). The slice interval was 0.5 mm, the image matrix was 512 × 512 pixels and the pixel size was 0.728 mm. The CT images showed trochlear cartilage damage in cadaver knee 1. The other three

cadaver knees showed no abnormalities. The arthro-CT data of the cadaveric knees were loaded in a 3D image processing software system (Mimics 14.12, Materialise, Haasrode, Belgium) to reconstruct the femoral bones including the cartilage and to design the trochlear implants and the custom guiding instruments.

4. 2. 1. Design of the replica implants

After reconstruction of the 3D femur model, the cutting plane is defined. This plane is the interface where the cadaveric femur model and the implant model meet. It will be used to design the implant as well as the guiding instruments to cut the cadaveric trochlea. The plane (Figure 4.1) is defined manually parallel to the PCL (1) and intersects the femur proximally at the level of the supra-trochlear shaft (2) and distally just anterior to the notch (3), assuring contact with the patella from 0 to 60° of knee flexion.

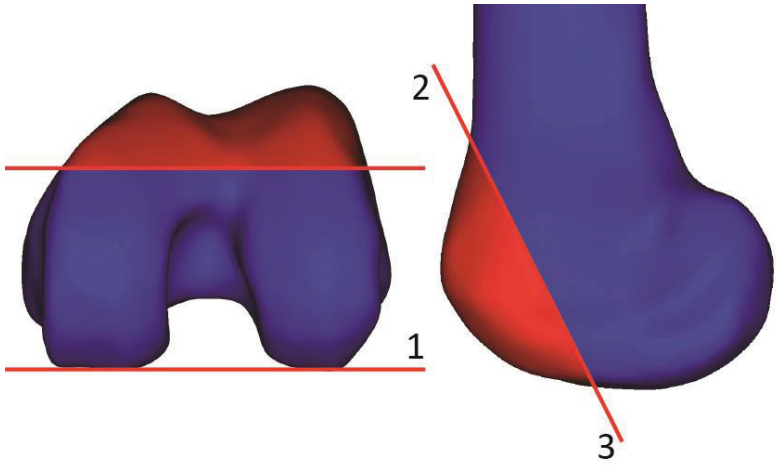

Figure 4.1 Orientation of the cutting plane. The blue model represents the cadaver femur, the red model represents the replica implant (knee 1)

In the design of the replica implant, the loss of bone caused by the saw blade was taken into account. Therefore, a layer of 1.2 mm (equivalent to the thickness of the saw blade) is added at the contact area of the 3D trochlea to compensate for the bone loss.

4. 2. 2. Design of the guiding instruments

To ensure correct orientation of the surgical saw blade when resecting the cadaveric trochlea, cadaver-specific guiding instruments were designed to fit precisely on the

anterior part of the distal femur Figure 4.2. The guiding instrument is featured with a number of inspection holes allowing for monitoring its position on the bone.

At the lateral side of the instrument a guiding block guides the surgical saw blade in a correct position through the cadaveric femur bone (Figure 4.2).

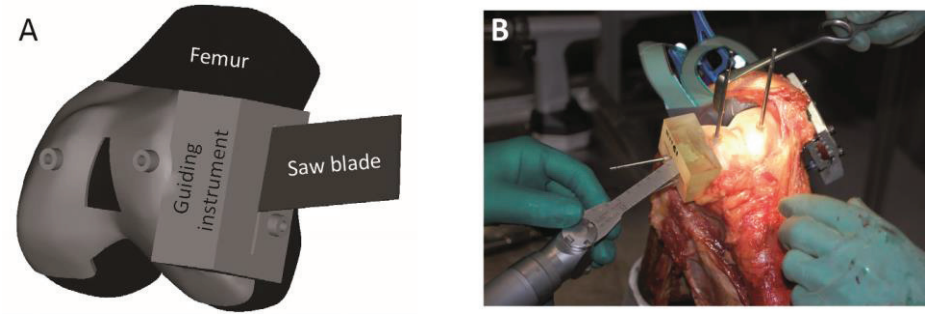

Figure 4.2 Guiding instrument to resect the cadaveric trochlea: 3D model (a) and intraoperative image (b)

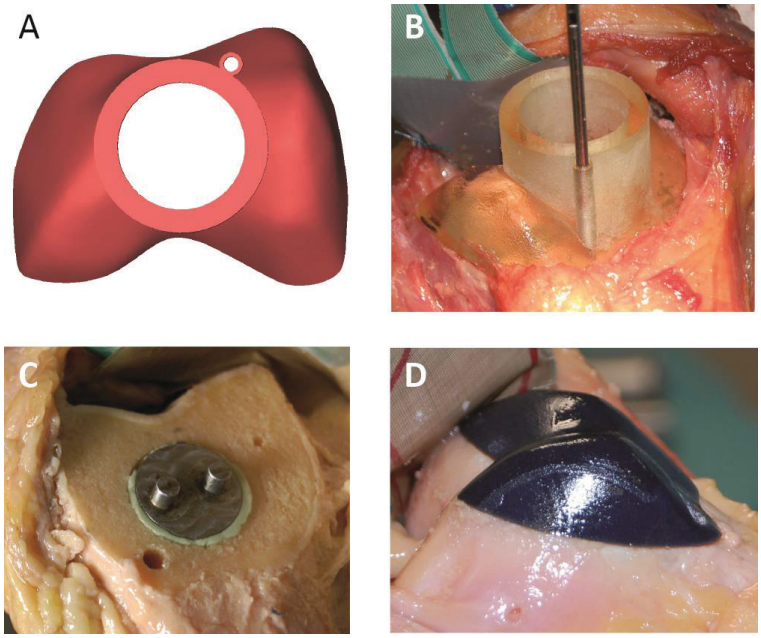

Figure 4.3 Guiding instrument to ream a socket for the fixation tool (A, B), placement of the implant on the fixation tool (C, D)

Pinholes are created at the anterior and lateral side to fix the guiding instrument on the bone with four orthopaedic screws. When the trochlear bone is resected, a fixation component is cemented in the trabecular bone (VersaBond, Smith & Nephew Inc., Memphis, TN). This device permits easy replacement of one implant by another between the test sessions. To accurately place this component, a socket is reamed in the surface of the trabecular bone with a second guiding instrument (Figure 4.3).

The biconvex patellar reamer (Genesis II, Smith & Nephew, Inc., Memphis, TN) with a diameter of 26 mm perfectly fits in the cylindrical guide with a diameter of 27 mm.

4. 2. 3. Rapid prototyping of the implants and guiding instruments

The material properties of the implant should mimic the properties of the in-vivo trochlea as closely as possible. The trochlear cartilage articulates with the patellar cartilage. It is exposed to a wide range of loads up to 10 times the body weight and has excellent frictional and load bearing properties (Kuster et al. 1997, Reilly and Martens 1972). Increased loads in the PF joint provoke an increase of the PF contact area (Hehne 1990, Matthews et al. 1977). By increasing the contact area, the contact forces are distributed and the peak stresses on the cortical bone underneath are reduced. This mechanism is most likely attributable to the soft nature of cartilage. For this reason hardness was selected as the principal material property of the outer layer of the implants. The hardness of cartilage is found to be between 80 and 90 shore A (Spahn et al. 2007), the hardness of cortical bone between 80 and 90 shore D (Wahnert et al. 2011). Other material properties of cartilage and cortical bone are listed in Table 4.1.

Table 4.1 Material properties of cartilage and cortical bone (Ateshian and Wang 1995, Choi et al. 1990, Froimson et al. 1997, Jurvelin et al. 2003, Spahn et al. 2007, Wahnert et al. 2011)

Property	*Cartilage*	*Cortical bone*
Shore hardness	80-90 Shore A	80-90 Shore D
Young's modulus (MPa)	0.6	15400 - 16000
Aggregate modulus (MPa)	0.6	
Poisson ratio	0-0.2	0.5
Friction coefficient	0.002-0.02	

Because of the complex geometry of the pathological implant, rapid prototyping (RPT) was considered as the most appropriate method to manufacture the implants. More specifically, a multi material 3D Connex350™ printer (Objet Ltd., Rehovot,

Israel) was selected. This 3D printer can jet two materials simultaneously, which allows printing the virtually reconstructed cortical bone and cartilage in one single model with a very high resolution: the horizontal layers are built up with a thickness of 0.028 mm. After building the layers, the material is exposed to UV radiation to obtain a glossy, smooth and more planar surface. The implants were printed with a rubberlike photopolymer with a shore A value of 80-90 for the cartilage part (DM_9885/9785) and with a shore A value of 90-100 for the bony part (DM_9895/9795). Both materials are a combination of a flexible resin TangoBlackPlus and a hard resin VeroWhitePlus. Their material properties are listed in Table 4.2 (Objet Ltd., Rehovot, Israel).

Given the complex shape of the guiding instruments, RPT was again selected as the best method for manufacturing. The guiding instruments were printed with the Objet Eden350V printer (Objet Ltd., Rehovot, Israel) with a layer thickness of 0.016 mm. The selected material was a translucent acrylic-based photo polymer (FullCure 720), which facilitates monitoring of the saw blade position and orientation.

Table 4.2 Material properties of the RPT implant (Objet Ltd., Rehovot, Israel)

Property	*ASTM*	*Implant*	
		Cartilage	*Cortical bone*
Shore hardness (Shore A)	Scale A	80-90	90-100
Tensile strength (MPa)	D-412	6	20
Elongation at break (%)	D-412	55	30
Tensile tear resistance (Kg/cm)	D-624	26	46

4. 2. 4. Validation of the replica implants and guiding instruments

Accuracy of the replica implants and guiding instruments

The accuracy of the implants in the cadaver is determined by geometrical and positioning errors of the implants and guiding instruments. Geometrical errors can occur at each stage of the process, from the acquisition of CT slices to the segmentation, the manufacturing and finishing process. Though the accuracy of the models is dependent on the scanner type, scanning parameters and reconstruction settings, we accept an error of 0.15 mm for the implant design in the current study based on literature values (Allen et al. 2010, Rathnayaka et al. 2012). The accuracy of the manufacturing and finishing process of the Connex printer is reported to be between 0.10 and 0.30 mm (Objet Ltd., Rehovot, Israel).

Positioning errors can be caused by inaccuracy or insufficiency of the guiding instruments and can be evaluated by comparing the planned cutting plane with the actual cutting plane. Post-operative CT-scans of the cadaver specimen were performed to visualise the actual cutting plane. The angle between both planes was measured in the axial plane (internal/external rotation error) and sagittal plane (flexion/extension rotation error) in Mimics. The angle was defined positive in the axial plane when the actual cutting plane was rotated externally with respect to the planned cutting plane. In the sagittal plane the angle was defined positive when the actual cutting plane showed more flexion compared to the planned cutting plane. The distance between the planes was calculated and visualized in the open-source program pyFormex (http://pyformex.org).

Effect of the replica implants on the patellofemoral kinematics and kinetics

The impact of the geometrical and positioning errors and the influence of the RPT material properties were estimated by repeating identical experimental tests before and after the placement of a replica implant. The replica implant and cadaver-specific guiding instruments were manufactured for four cadaver knees. After fixing frames with four infrared reflective markers to femur, tibia and patella, the knees were mounted in the Smith & Nephew test rig (Victor et al. 2009) to perform a squat simulation (between 20-80° knee flexion) and an open chain extension simulation (between 5-65° knee flexion). The PF kinematics and kinetics were continuously monitored by a Vicon system (Vicon, Oxford, UK) and a pressure sensor which was fixed between the patella and the femur (Tekscan, South Boston, MA, USA). The PF rotation, tilt and mediolateral translation were analysed according to Belvedere et al. (Belvedere et al. 2007). Lateral tilt, internal rotation of the patellar apex and medial translation were defined as positive (Figure 4.4).

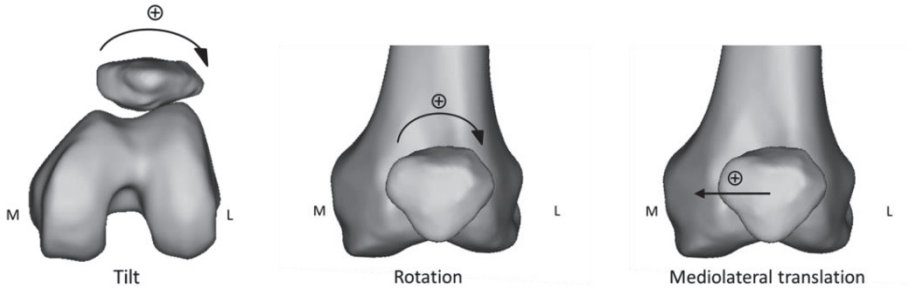

Figure 4.4 Patellofemoral kinematics

To demonstrate how well the kinematics and kinetics of the replica implants correlate with those of the native knees, paired samples correlation tests were performed. Bland-Altman plots were created to visualise the differences between the native knee and replica implant. To investigate if the differences were randomly distributed, paired samples correlation tests were performed between the mean values ([Native + Replica]/2) and the differences (Native - Replica) of the parameters.

To investigate to what extent the variation in differences between the native knee and replica implant can be explained by the rotational errors in the cutting plane, linear regression analysis was performed with the differences in kinematic and kinetic parameters as dependent variables and the rotational errors as independent variables.

4. 3. Results

4. 3. 1. Accuracy of the replica implant placement in the cadaver

Post-operative CT scans were performed to define the actual cutting plane. These images showed that the contour of the 3D replica is perfectly in line with the contour of the cadaver femur (Figure 4.5).

The rotational errors between the planned and the actual cutting plane were evaluated in Mimics in the axial and sagittal plane and are listed in Table 4.3.

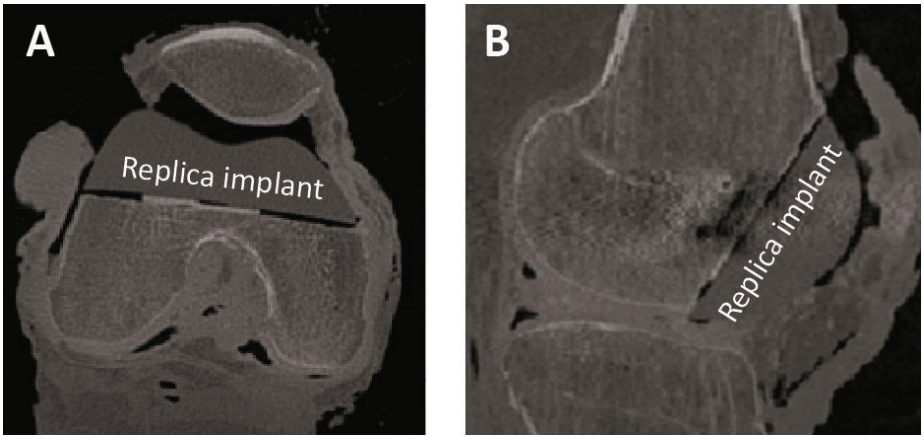

Figure 4.5 Post-operative CT scan: axial and sagittal view on the cutting plane.

Table 4.3 Rotational error between the planned and actual cutting plane for each knee and the mean absolute errors (±SD)

	Axial (°)	*Sagittal (°)*
Knee 1	-1.88	-3.97
Knee 2	1.16	-2.71
Knee 3	-1.35	-2.74
Knee 4	-0.36	-2.63
Mean (± SD)	1.18 (± 0.63)	3.01 (± 0.64)

In the axial plane, the mean absolute rotational error was small (1.18 ± 0.63°), the actual cutting plane was rotated internally in three knees and externally in one knee compared to the planned cutting plane. The rotational error in the sagittal plane was larger (3.01 ± 0.64°) and occurred systematically in extension.

The distance between the planned and the actual cutting plane was calculated in pyFormex and is represented by a colour plot on the anterior surface of the trochlea of knee 4, positioned on the actual cutting plane (Figure 4.6).

The maximal positive distance was located in the distal area of the trochlea and the maximal negative distance was located in the proximal area (Table 4.4).

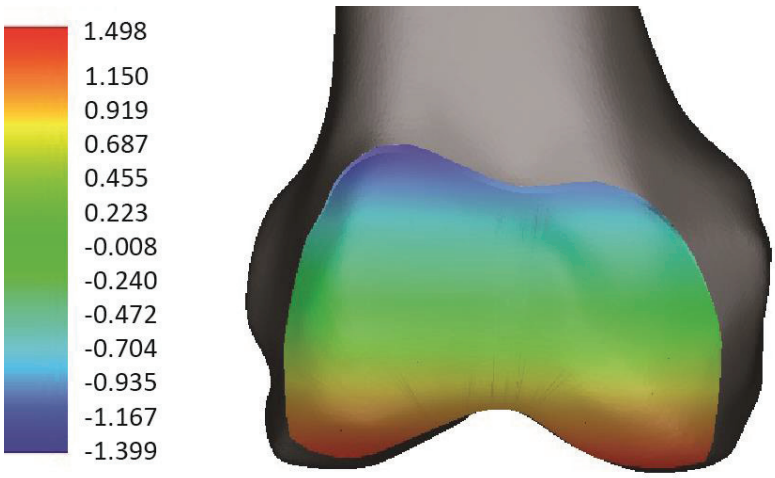

Figure 4.6 Implanted trochlea of knee 4 with a colour plot representing the distance (in mm) between the planned and actual cutting plane

Table 4.4 Maximal distance between the planned and actual cutting plane

	Proximal (mm)	*Distal (mm)*
Knee 1	-2.59	2.46
Knee 2	-0.14	2.82
Knee 3	-1.51	1.32
Knee 4	-1.40	1.50
Mean (±SD)	-1.41(±1.00)	2.03 (±0.73)

4. 3. 2. Effect of the replica implants on the patellofemoral kinematics and kinetics

All parameters in the open chain and squat simulation demonstrated significant correlations between the native and replica condition (Table 4.5).

The PF tilt, rotation and mediolateral translation showed a small mean difference (< 0.5° and < 0.5 mm) between the native and replica condition, except for the mediolateral translation during the squat simulation, where the patella shifted on average 3.8 mm less medially in the replica condition compared to the native condition (

Figure 4.7).

Table 4.5 Paired samples correlations (r) between the native knee and replica condition and between the average ([native + replica]/2) and the difference (native - replica). Statistically significant correlations ($p < 0.05$) are indicated by (*)

	Squat		*Open chain*	
	Native vs Replica	Average vs Difference	Native vs Replica	Average vs Difference
Rotation	0.992*	-0.577*	0.996*	-0.367*
Tilt	0.970*	0.472*	0.965*	0.580*
ML translation	0.953*	0.810*	0.532*	-0.216
Contact area	0.977*	-0.008	0.938*	-0.205
Contact pressure	0.915*	-0.552*	0.877*	-0.541*

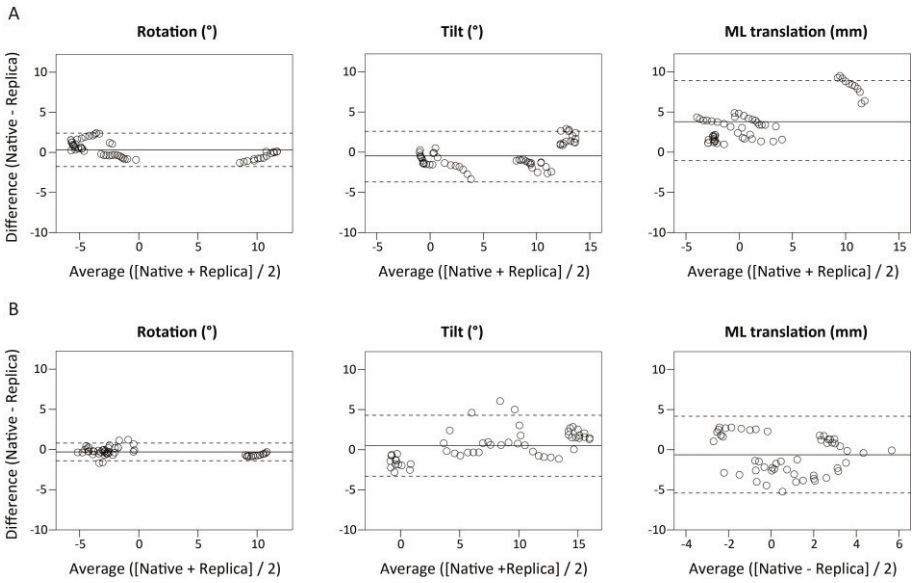

Figure 4.7 Bland-Altman plots for the kinematic parameters of the four knees during the squat (panel A) and open chain (panel B) simulation with average differences (solid lines) and ± 2 SD (dashed lines). The dots represent the patellar rotation, tilt and mediolateral translation with respect to the femur during the squat and open chain with an interval of 5° of knee flexion

The differences were randomly distributed for the mediolateral translation in the open chain simulation (Table 4.5). All other parameters showed a systematic variation of the differences with the mean: with increased mean internal rotation, lateral tilt and medial translation of the patella, the difference between the native and replica condition was significantly smaller (or more negative) for rotation and larger for tilt and mediolateral translation (

Figure 4.7, Table 4.5).

The PF contact area and contact pressure showed relatively small mean differences between the replica and the native condition. During the open chain simulation the mean difference was 12.5 mm^2 for the contact area and -0.05 MPa for the contact pressure. During the squat simulation the mean difference was 6.3 mm^2 for the contact area and 0.01 MPa for the contact pressure (

Figure 4.8). The differences in contact area were randomly distributed and the differences in contact pressure are smaller (more negative) when the mean contact pressure increases (

Figure 4.8, Table 4.5).

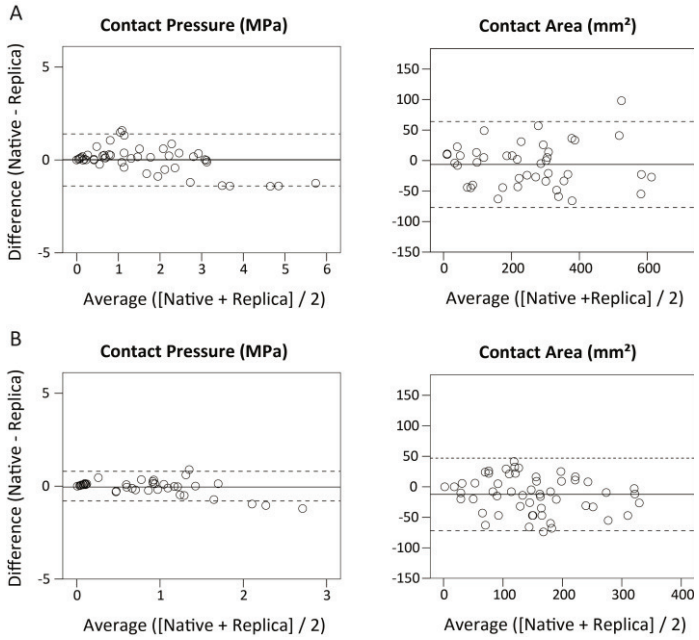

Figure 4.8 Bland-Altman plots for kinetic parameters of the four knees during the squat (panel A) and open chain (panel B) simulation with average differences (solid lines) and ± 2 SD (dashed lines). The dots represent the patellofemoral contact pressure and contact area during the squat and open chain with an interval of 5° of knee flexion

For the differences between the native and replica condition in the squat simulation linear regression showed that the variation in differences in patellar rotation, patellar mediolateral translation and PF contact pressure could be explained by the rotational errors of the cutting plane for respectively 33% ($p < 0.001$), 50% ($p < 0.001$) and 31% ($p < 0.001$). The variation in differences in patellar tilt and PF contact area could not be explained by the rotational errors of the cutting plane.

For the differences between the native and replica condition in the open chain simulation linear regression showed that the variation in differences in patellar tilt, patellar mediolateral translation and PF contact pressure could be explained by the rotational errors of the cutting plane for respectively 50% ($p < 0.001$), 79% ($p < 0.001$) and 35% ($p < 0.001$). The variation in differences in patellar rotation and PF contact area could not be explained by the rotational errors of the cutting plane.

4. 4. Discussion

This study shows that the proposed method allows physical simulation of skeletal geometries by RPT for experimental purposes.

Correct placement of the trochlear implants in the cadaver however is critical for the PF rotation, tilt, mediolateral translation, contact area and contact pressure. In orthopaedics, it is generally accepted that rotational errors in the axial and sagittal plane should be within 3° (Jenny et al. 2005). In procedures with standard guiding instruments (intramedullary or extramedullary rods that can be aligned along bone axes under visual alignment), only 70–85% of cases are placed within these boundaries (Jenny et al. 2005). For the cadaver-specific pathological implants custom made guiding instruments based on arthro-CT images were manufactured. CT scans are considered to be the ultimate tool to define the bony surface (Chauhan et al. 2004, Victor et al. 2009). But this technique is no longer accurate when articular cartilage irregularities are present (Tibesku et al. 2012). Therefore arthro-CT scans were performed to assure accurate definition of both bone and cartilage. Nevertheless, for the first knee, which showed irregularly damaged cartilage, the rotational error in the sagittal plane was higher than the threshold of 3°. This could be due to the fact that the contrast fluid was not dispersed evenly in the entire knee joint, making it necessary to interpolate the cartilage thickness in the regions where the contrast fluid was missing.

Rotational errors of the cutting plane may lead to under- or overstuffing, maltracking of the patella, a decrease of the PF contact areas and concomitantly an increase of the PF contact pressures (Siston et al. 2005, Verlinden et al. 2010), which was confirmed in the current study. Despite the high correlations between the native and replica condition for all measured parameters, the variation in differences in most of the investigated parameters between both conditions could at least partly be explained by the rotational errors of the cutting planes. Therefore, when investigating the influence of a pathological geometry, the pathological condition should be compared to a replica condition instead of the native condition to rule out the influence of the confounding effect of rotational errors.

Besides the rotational errors, the material properties of the implants can also affect the behaviour of the model in the cadaver experiments. To date, not all the material properties of the RPT material are provided by the supplier. Potentially important properties of the RPT materials, namely the friction coefficient, Young's modulus

and Poisson's ratio should be further investigated by performing additional material testing.

These rotational errors and differences in material properties are not an issue in the earlier studies of Amis and colleagues, where the articulating material is preserved (Amis et al. 2008, Senavongse and Amis 2005). The current method however allows simulating an unrestricted variety of geometrical characteristics, inherent to the appearance of TD. Moreover, the proposed method allows future testing of multiple abnormalities by replacing one type of trochlear implant by another on one single cadaver specimen.

4. 5. Conclusions

This study shows that skeletal geometry can be simulated by 3D-modelling and RPT. The influence of the material properties and possible rotational errors of the implants can be countered by using a replica implant as a control condition instead of the native condition. Simulating a variety of isolated joint deformities can lead to better understanding of the specific biomechanical effects of the deformities.

References

1. Allen BC, Peters CL, Brown NAT, Anderson AE. 2010. Acetabular Cartilage Thickness: Accuracy of Three-Dimensional Reconstructions from Multidetector CT Arthrograms in a Cadaver Study. Radiology. 255:544-552.

2. Amis AA, Oguz C, Bull AMJ, Senavongse W, Dejour D. 2008. The effect of trochleoplasty on patellar stability and kinematics - A biomechanical study in vitro. J Bone Joint Surg Br. 90B:864-869.

3. Ateshian GA, Wang HQ. 1995. A Theoretical Solution for the Frictionless Rolling-Contact of Cylindrical Biphasic Articular-Cartilage Layers. J Biomech. 28:1341-1355.

4. Belvedere C, Catani F, Ensini A, de la Barrera JLM, Leardini A. 2007. Patellar tracking during total knee arthroplasty: an in vitro feasibility study. Knee Surg Sport Tr A. 15:985-993.

5. Chauhan SK, Scott RG, Breidahl W, Beaver RJ. 2004. Computer-assisted knee arthroplasty versus a conventional jig-based technique - A randomised, prospective trial. J Bone Joint Surg Br. 86B:372-377.

6. Choi K, Kuhn JL, Ciarelli MJ, Goldstein SA. 1990. The Elastic-Moduli of Human Subchondral, Trabecular, and Cortical Bone Tissue and the Size-Dependency of Cortical Bone Modulus. J Biomech. 23:1103-1113.

7. Dejour H, Walch G, Nove-Josserand L, Guier C. 1994. Factors of patellar instability: an anatomic radiographic study. Knee surgery, sports traumatology, arthroscopy : official journal of the ESSKA. 2:19-26.

8. Fitzpatrick CK, Baldwin MA, Laz PJ, FitzPatrick DP, Lerner AL, Rullkoetter PJ. 2011. Development of a statistical shape model of the patellofemoral joint for investigating relationships between shape and function. J Biomech. 44:2446-52.

9. Froimson MI, Ratcliffe A, Gardner TR, Mow VC. 1997. Differences in patellofemoral joint cartilage material properties and their significance to the etiology of cartilage surface fibrillation. Osteoarthr Cartilage. 5:377-386.

10. Hehne HJ. 1990. Biomechanics of the Patellofemoral Joint and Its Clinical Relevance. Clin Orthop Relat R. 73-85.

11. Jafari A, Farahmand F, Meghdari A. 2008. The effects of trochlear groove geometry on patellofemoral joint stability - a computer model study. P I Mech Eng H. 222:75-88.

12. Jenny JY, Clemens U, Kohler S, Kiefer H, Konermann W, Miehlke RK. 2005. Consistency of implantation of a total knee arthroplasty with a non-image-based navigation system - A case-control study of 235 cases compared with 235 conventionally implanted prostheses. J Arthroplasty. 20:832-839.

13. Jurvelin JS, Buschmann MD, Hunziker EB. 2003. Mechanical anisotropy of the human knee articular cartilage in compression. Proc Inst Mech Eng H. 217:5.

14. Kuster MS, Wood GA, Stachowiak GW, Gachter A. 1997. Joint load considerations in total knee replacement. J Bone Joint Surg Br. 79B:109-113.

15. Matthews LS, Sonstegard DA, Henke JA. 1977. Load Bearing Characteristics of Patello-Femoral Joint. Acta Orthop Scand. 48:511-516.

16. Rathnayaka K, Momot KI, Noser H, Volp A, Schuetz MA, Sahama T, Schmutz B. 2012. Quantification of the accuracy of MRI generated 3D models of long bones compared to CT generated 3D models. Med Eng Phys. 34:357-363.

17. Reilly DT, Martens M. 1972. Experimental Analysis of Quadriceps Muscle Force and Patello-Femoral Joint Reaction Force for Various Activities. Acta Orthop Scand. 43:126-&.

18. Senavongse W, Amis AA. 2005. The effects of articular, retinacular, or muscular deficiencies on patellofemoral joint stability - A biomechanical study in vitro. J Bone Joint Surg Br. 87B:577-582.

19. Siston RA, Patel JJ, Goodman SB, Delp SL, Giori NJ. 2005. The variability of femoral rotational alignment in total knee arthroplasty. J Bone Joint Surg Am. 87A:2276-2280.

20. Spahn G, Kahl E, Klinger HM, Muckley T, Gunther M, Hofmann GO. 2007. Mechanical behavior of intact and low-grade degenerated cartilage. Biomed Tech. 52:216-222.

21. Tibesku CO, Innocenti B, Wong P, Salehi A, Labey L. 2012. Can CT-based patient-matched instrumentation achieve consistent rotational alignment in knee arthroplasty? Arch Orthop Traum Su. 132:171-177.

22. Verlinden C, Uvin P, Labey L, Luyckx JP, Bellemans J, Vandenneucker H. 2010. The influence of malrotation of the femoral component in total knee replacement on the mechanics of patellofemoral contact during gait AN IN VITRO BIOMECHANICAL STUDY. J Bone Joint Surg Br. 92B:737-742.

23. Victor J, Van Doninck D, Labey L, Innocenti B, Parizel PM, Bellemans J. 2009. How precise can bony landmarks be determined on a CT scan of the knee? Knee. 16:358-65.

24. Victor J, Van Glabbeek F, Vander Sloten J, Parizel PM, Somville J, Bellemans J. 2009. An experimental model for kinematic analysis of the knee. J Bone Joint Surg Am. 91 Suppl 6:150-63.

25. Wahnert D, Hoffmeier KL, Stolarczyk Y, Frober R, Hofmann GO, Muckley T. 2011. Evaluation of a Customized Artificial Osteoporotic Bone Model of the Distal Femur. J Biomater Appl. 26:451-464.

Chapter 5

The impact of trochlear dysplasia on the patellofemoral kinematics, contact and stability: a cadaver study with rapid prototyped joint deformities[§]

Trochlear dysplasia appears in different geometrical variations. The Dejour classification is widely used to grade the severity of trochlear dysplasia and to decide on treatment. It has however not been investigated yet how different classes of trochlear dysplasia affect the patellofemoral biomechanics. The purpose of this study is to investigate 1) the impact of trochlear dysplasia on patellofemoral biomechanics and 2) if different types of trochlear dysplasia have a different impact on patellofemoral biomechanics. Trochlear dysplasia was simulated in four cadaveric knees by replacing the native trochlea by different types of custom-made rapid prototyped implants. For each knee one implant was designed to replicate the native trochlea and four implants were designed to simulate four types of trochlear dysplasia. The knees were subjected to a squat simulation, an open chain extension simulation and a patellar stability test. The patellofemoral kinematics, contact area, contact pressure and stability were compared between the control group (replica implants) and the trochlear dysplastic group and between the subgroups of trochlear dysplasia. The patellofemoral joint in the trochlear dysplastic group showed increased internal rotation, lateral tilt and lateral translation, increased contact pressures, decreased contact areas and decreased stability compared to the control group. Within the trochlear dysplastic group, the implants graded as Dejour type D showed the largest deviations for the kinematical parameters and the implants graded as Dejour type B and D showed the largest deviations for the patellofemoral contact areas and pressures. Patellofemoral kinematics, contact area, contact pressure and

[§] This study is submitted for review: A. Van Haver, K. De Roo, M. De Beule, L. Labey, P. De Baets, D. Dejour, T. Claessens, P. Verdonk. The impact of trochlear dysplasia on the patellofemoral kinematics, contact and stability: a cadaver study with rapid prototyped joint deformities. The American Journal of Sports Medicine

stability are significantly affected by trochlear dysplasia. Off all types of trochlear dysplasia, the models characterised with a pronounced trochlear bump showed the largest deviations in patellofemoral biomechanics.

5. 1. Introduction

Dysplasia of the femoral trochlea is currently universally accepted as the primary factor in patellar instability (Arendt and Dejour 2013, Dejour et al. 1994). TD is a geometrical abnormality of the shape and depth of the trochlear groove mainly at its proximal part, where the patella engages into the trochlea. It may lead to PF maltracking, increased contact pressures, patellar instability and isolated PF arthritis (Amis et al. 2008, Dejour et al. 1990, Grelsamer et al. 2008, Pfirrmann et al. 2000). Classification of TD to assess the severity or to advice on treatment is an important topic in PF research. The most commonly used classification system is the four-grade Dejour classification (Dejour et al. 1998). The four Dejour classes are defined on true lateral radiographs and axial CT or MR scans: type A is characterised by the crossing sign and a fairly shallow trochlea, type B by the crossing sign, a trochlear spur and a flat or convex trochlea, type C by the crossing sign, a double contour representing a hypoplastic medial condyle, asymmetry of trochlear facets and a convex lateral facet and type D by the crossing sign, a supratrochlear spur, a double-contour sign, asymmetry of the trochlear facets and a cliff pattern (Dejour et al. 1998). It has been investigated if the four Dejour classes reflect differences in objective morphological characteristics of the PF joint, the incidence of PF arthritis and the outcome of trochleoplasty (Allain et al. 2004, Fucentese et al. 2011, Grelsamer et al. 2008, Nelitz et al. 2013, Zaffagnini et al. 2010). Thus far, it has not been possible to investigate if the four Dejour classes also reflect differences in PF biomechanics. Few in-vitro experiments have been performed to evaluate the PF biomechanics in TD knees versus normal knees. Amis and colleagues simulated TD by removing a wedge of bone to flatten the lateral trochlea (Senavongse and Amis 2005) and by lifting the articular cartilage to elevate the central groove (Amis et al. 2008). These surgical techniques were successful to demonstrate significant differences in patellar stability and tracking between normal and TD knees.

The aim of this study was (i) to investigate the impact of TD on the PF biomechanics and (ii) to investigate if different types of TD have a different impact on the PF biomechanics. This study applied a novel validated method to replace the original cadaver trochlea by different types of custom made rapid prototyped (RPT)

implants for experimental testing (Van Haver et al., unpublished data, 2013). The authors hypothesize that this method facilitates the investigation of isolated TD in all its variations.

5. 2. Materials and methods

5. 2. 1. Cadaver specimens

Four unmatched fresh frozen cadaveric knees, two male and two female (aged 75-85 years) were thawed at room temperature. Passive optical reflective markers were rigidly attached to the femur, tibia, and patella before arthro-CT images were obtained. Cadaver knee 1 showed trochlear cartilage damage and cadaver knee 4 showed moderate dysplasia of the trochlea (characterised by a trochlear bump of 4.4 mm). The other cadaver knees showed no abnormalities.

5. 2. 2. Trochlear implants

To evaluate the effect of the trochlear morphology on PF biomechanics a validated method to simulate bony deformities was applied (Van Haver et al., unpublished data, 2013). Five different types of custom trochlear implants were manufactured for each cadaver specimen with RPT. A multi material 3D Connex350™ printer (Objet Ltd., Rehovot, Israel) printed the cartilage layer with a shore A value of 80-90, the rest of the implant was printed with a shore A value of 90-100. The first type of implant was a replica of the trochlear shape of the cadaver and the four other implants contained different dysplastic trochlear shapes, based on arthro-CT scans of four TD patients classified as Dejour type A, B, C and D. All patients had a history of recurrent patellar dislocation and showed a variation of geometrical abnormalities of the trochlea. The arthro-CT data of the cadaveric and patient knees were loaded in 3D image processing software (Mimics 14.12, Materialise, Haasrode, Belgium) for segmentation and 3D reconstruction of the femoral bones.

Based on the patients' arthro-CT scans, cadaver specific trochlear implants were manufactured containing different morphological types of TD. The patient-based implants were designed to encompass the geometrical characteristics of the pathology of the patients and at the same time fit the cadaver specimens perfectly. To this end, the patient femur models were scaled and positioned to match the cadaveric femur model (Figure 5.1). During the positioning of the pathological 3D femur models, special attention was given to the rotational alignment because malrotation of the femur can result in maltracking of the patella, a decrease of the PF

contact areas and, concomitantly, an increase of PF contact pressures (Siston et al. 2005, Verlinden et al. 2010). Furthermore, care was taken that the most anterior parts of the trochlea of both models coincided to avoid over- or understuffing of the PF joint.

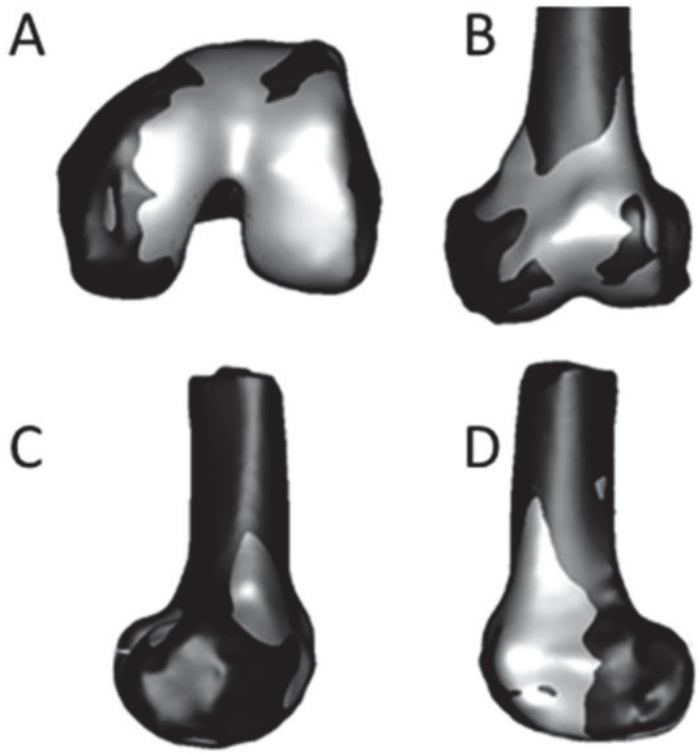

Figure 5.1 Rescaling and repositioning of a pathological femur model (grey) on the cadaveric femur model (black). Distal (A), frontal (B), medial (C) and lateral view (D)

After scaling and positioning the pathological 3D femur model, the cutting plane is defined. This plane is the interface where the cadaveric femur model and the implant model meet. The plane will be used to design the replica and patient-based implant as well as the guiding instruments to cut the cadaveric trochlea. The cutting plane (Figure 5.2) is defined parallel to the PCL (1) and intersects the femur proximally at the level of the supra-trochlear shaft (2) and distally just anterior to the notch (3), assuring contact of the patella with the trochlear implant from 0 to 60° of knee flexion.

After identifying this cutting plane, the cadaver femur model can be combined with a patient trochlea model. To assure a perfectly smooth fit, a transition zone of

approximately 1 cm is selected in the area where the trochlea makes contact with the cadaver. In this transition zone manual remeshing and smoothing is applied without altering the cadaver model and without altering the pathological characteristics of the trochlea.

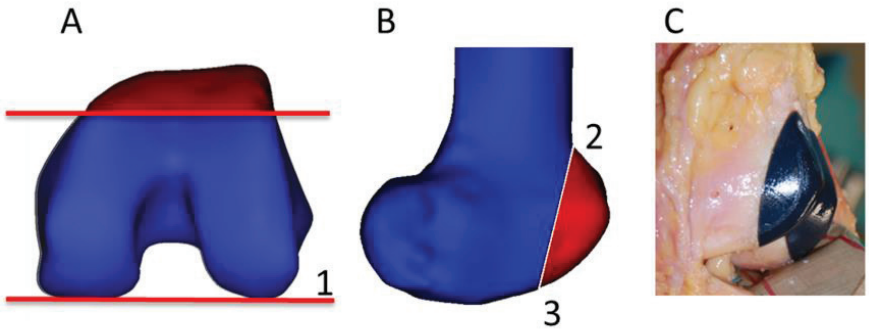

Figure 5.2 3D models (A and B) and picture (C) of the cadaver femur with trochlear implant: The cutting plane is defined parallel to the posterior condylar line (1), proximal to the anterior trochlea (2) and anterior to the notch (3)

In the design of the replica and patient-based implants, the loss of bone caused by the saw blade was compensated by adding a layer of 1.2 mm at the contact area of the trochlear implant.

Because of the complex geometry of the patient-based implant, RPT was considered as the most appropriate method to manufacture the custom implants and guiding instruments.

5. 2. 3. Morphology and classification of the modified cadaver knees

Each of the four cadaver knees was experimentally tested with one replica implant and four patient-based implants. Combining the four knees with the five types of implants resulted in 20 different models.

The 20 modified cadaver knees were subjected to evaluation according to the four-grade Dejour classification by two senior surgeons (DD& PV). Each of the modified cadaver knees was assigned to one of the four Dejour classes upon consensus. It was expected that all four native knees would be classified as normal, but cadaver knee four was graded as type A. No other morphological abnormalities of the PF joint were observed in the four native knees.

Although it was possible to visually identify the original trochlear morphology of the patient knees in the modified cadaver knees (Figure 5.3), the modified cadaver knees were not always classified as the same type of TD as the original patient knee by 2 experienced orthopaedic surgeons. This was mainly caused by the positioning method of the 3D femur models of the cadaver and patient (described in section 2.2); when the distal femoral condyles are optimally positioned to replace the cadaver trochlea by the patient trochlea as shown in Figure 5.1, the femur with the smallest shaft diameter will show the largest anterior offset and vice versa. This strategy was applied to avoid PF overstuffing, which can be a possible cause of medial tracking as described by Amis and colleagues (Amis et al. 2008).

Of the 20 modified cadaver knees, three knees were classified as normal (15%), seven as type A (35%), three as type B (15%), five as type C (25%) and two as type D (10%).

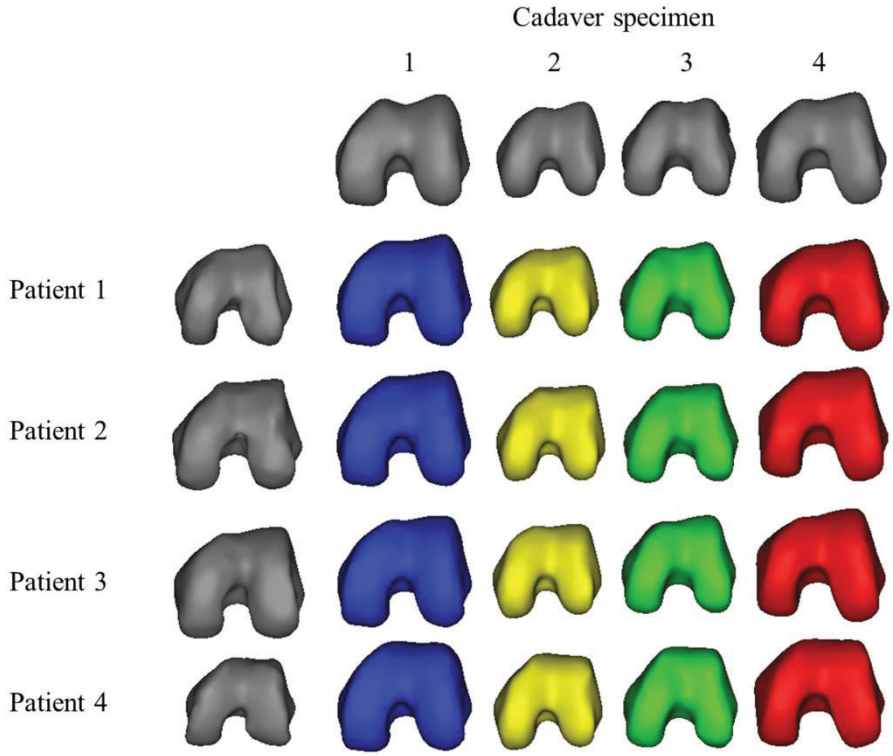

Figure 5.3 Bottom view on the 20 3D models. The four original patient knees and cadaver knees are represented in grey. The colored models consist of the distal femur of the cadaver combined with the anterior trochlea of the patient. Each modified cadaver is represented by another color.

5. 2. 4. Measurement of the patellofemoral kinematics and contact pressure and area

PF kinematics have been shown to be different in open versus closed chain exercises and in weight-bearing versus non-weight-bearing exercises. Moreover, patellar maltracking is reported to be more pronounced in non-weight-bearing open chain exercises (Doucette and Child 1996, Powers et al. 2003). Therefore the effect of the different trochlear shapes was evaluated during a squat simulation (from 35 to 75° knee flexion) as well as an open chain extension simulation (from 65 to 5° knee flexion). Though it is well accepted that lateral subluxation occurs during the last 20-30° of knee extension (Doucette and Child 1996, Powers 2000, Varadarajan et al. 2010), it was not possible to obtain higher extension positions during the squat simulation as the knee could be pulled in hyperextension, which would damage the specimen.

A knee rig, based on the Oxford Knee Rig, was used to simulate a squat movement and an open chain extension movement (Figure 5.4) (Victor et al. 2009).

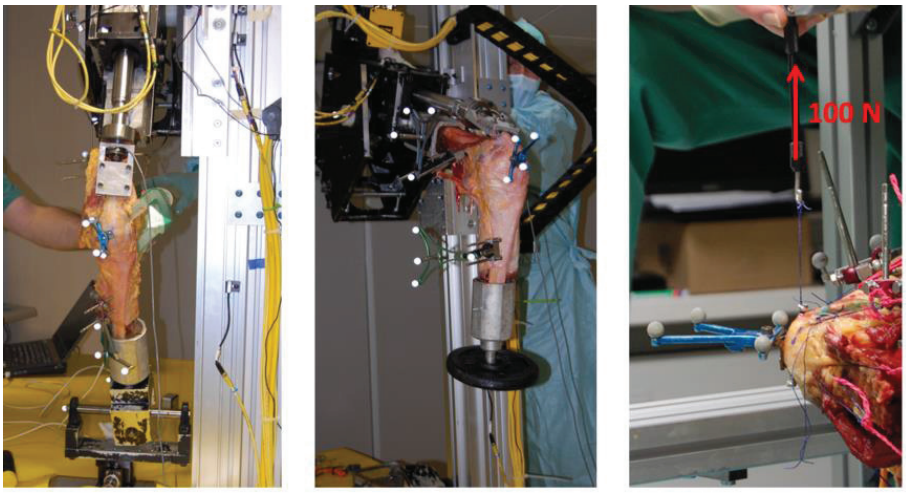

Figure 5.4 Test rigs to evaluate the patellofemoral kinematics, contact area and contact pressure (squat and open chain simulation) and to evaluate the patellofemoral stability (patellar stability rig)

The motion of femur, tibia and patella was recorded by six calibrated infrared cameras (MX40+ Vicon Motion Systems, Los Angeles, CA, USA) and the PF tilt, rotation and mediolateral translation were defined according to Belvedere et al. (Belvedere et al. 2007) The PF contact area and mean pressure were recorded by a calibrated K-scan 4000 pressure sensor (Tekscan, South Boston, MA, USA).

Since the cadaver specimens show substantial size differences as demonstrated by Figure 5.3, the mediolateral translation and the PF contact area were normalized by multiplying the translation with the rescaling factor and by multiplying the contact area by the squared rescaling factor described in section 2.3.

5. 2. 5. Measurement of the patellofemoral stability

The lateral and medial stability of the patella was quantified by recording the mediolateral translation of the patella caused by applying a force of 100 N in the lateral and medial direction (Figure 5.4). It was assumed that the patella would not reach its ultimate lateral or medial position before achieving the maximum force of 100 N.

A stability rig, partially based on the stability rig described by Senavongse et al. was used to evaluate the effect of the different trochlear shapes on the patellar stability in different knee flexion angles (Senavongse et al. 2003).

The stability rig consisted of a frame in which the knee specimen was positioned horizontally with the lateral side of the knee on top. The femur was rigidly fixed and the distal tibia was positioned in an open cylindrical container, which was attached to the rig in a circular track around the knee flexion-extension axis. With this container the knee was sequentially fixed in 10, 20, 30, 45 and 60° of knee flexion while all other degrees of freedom of the tibial and patellar motion were left unconstrained.

A total load of 175 N was applied to the quadriceps tendons and 30 N was applied on the iliotibial band (ITB) by hanging a series of calibrated weights according to the physiological cross-sectional areas and directions of the muscles relative to the femoral axis as indicated in Table 5.1 (Bull et al. 1999, Farahmand et al. 1998, Merican et al. 2009).

In order to displace the patella laterally and medially from its stable neutral position, a force of 100 N was applied manually to a screw in the most medial and most lateral border of the patella. This force was monitored by a digital dynamometer.

Table 5.1 Direction and distribution of weights attached to the tendons of the quadriceps (vastus lateralis longus (VLL), vastus lateralis obliquus (VLO), vastus medialis longus (VML), vastus medialis obliquus (VMO), rectus femoris + vastus intermedius (RF+VI)) and iliotibial band (ITB)

	Load direction angles		**Load distribution**	
VLL	14° lateral		33%	57.75 N
VLO	35° lateral	33° posterior	9%	15.75 N
VML	15° medial		14%	24.50 N
VMO	47° medial	44° posterior	9%	15.75 N
RF+VI			35%	61.25 N
ITB		6° posterior	100%	30.00 N

The PF kinematics were recorded analogous to the kinematics during the squat and open chain simulation. The mediolateral position of the patella in its stable neutral position and in its ultimate medial and lateral position (after applying 100 N medially and laterally) was normalized for size differences.

5. 2. 6. Preparation of the cadaver specimens

Prior to the experiments, the specimens were thawed at room temperature over 24 hours. The femur and tibia were rigidly fixed with polymethylmethacrylate in two containers, taking the physiologic valgus angle into account.

To place the trochlear implants, a custom-made guiding instrument was fitted on the articular surface of the distal femur (as described in section 4.2.2., see Figure 4.2, Figure 4.3). Care was taken to place the instrument in the best fitting and most stable position. Monitoring of the position was facilitated by the transparent material and perforations in the guiding instruments (Van Haver et al., unpublished data, 2013). The instrument was then fixed with pins at the anterior and lateral side. After fixation, an oscillating saw blade was guided through the lateral slot in the instrument to remove the femoral trochlea. When the guiding instrument and the trochlea were removed from the distal femur, a second guiding instrument was used to ream a cylindrical socket in the surface of the trabecular bone of the femur. In this socket, a fixation component was cemented to enable easy replacement of one trochlear implant by another during the experimental tests. After placing the implants, the knee joint was closed with a Vicryl 2 suture (Ethicon NV, Johnson&Johnson, Sommerville, NJ, USA).

5. 2. 7. Statistics

A two-way ANOVA for unequal sample sizes was conducted to examine the effect of TD on the PF kinematics, contact area and pressure and patellar stability. Analyses were first done for the TD models (TD group) versus the normal models (control group). Subsequently, analyses were done for the different subgroups, containing one or more groups. If significant differences between the subgroups were found, Tukey post-hoc tests were performed for pairwise comparisons.

5. 3. Results

5. 3. 1. Effect on the patellofemoral kinematics

Squat

During the squat simulation the mean patellar tracking showed progressive external rotation, lateral tilt and lateral translation with increasing knee flexion from 35° to 75° (Figure 5.5). The patellae showed more internal rotation ($p< 0.001$) and lateral tilt ($p = 0.016$) in the TD group compared to the control group. For the mediolateral translation, the patellae showed on average more lateral tracking in the TD group compared to the control group, but this difference was not significant ($p = 0.246$). Between the four Dejour classes analyses of the kinematics showed no specific differences.

Open chain

During the open chain extension simulation the mean patellar tracking in the control group showed a progressive internal rotation, medial tilt and medial translation with increasing knee extension from 65 to 25° and no rotation, a lateral tilt and lateral translation from 25 to 5° of knee flexion (Figure 5.5). The patella was consistently more internally rotated ($p<0.001$), laterally tilted ($p < 0.001$) and more laterally positioned ($p < 0.001$) in the TD group compared to the control group.

Tukey post testing revealed that type D showed more internal rotation ($p = 0.001$) and more lateral tilt ($p = 0.049$) compared to type A, B, C. For the mediolateral translation, no difference was observed between type D and type A, B, C ($p = 0.848$).

5. 3. 2. Effect on the patellofemoral contact pressure and area

Squat

During the squat simulation the mean PF contact pressure and area increased with knee flexion from 35 to 75°. The contact pressure was on average higher in the TD group ($p = 0.028$) while the contact area was on average lower in the TD group ($p < 0.001$) compared to the control group (Figure 5.5). Analysis of the four different classes revealed that type B and D showed higher PF contact pressures ($p = 0.002$) and lower PF contact areas ($p = 0.006$) compared to type A and C.

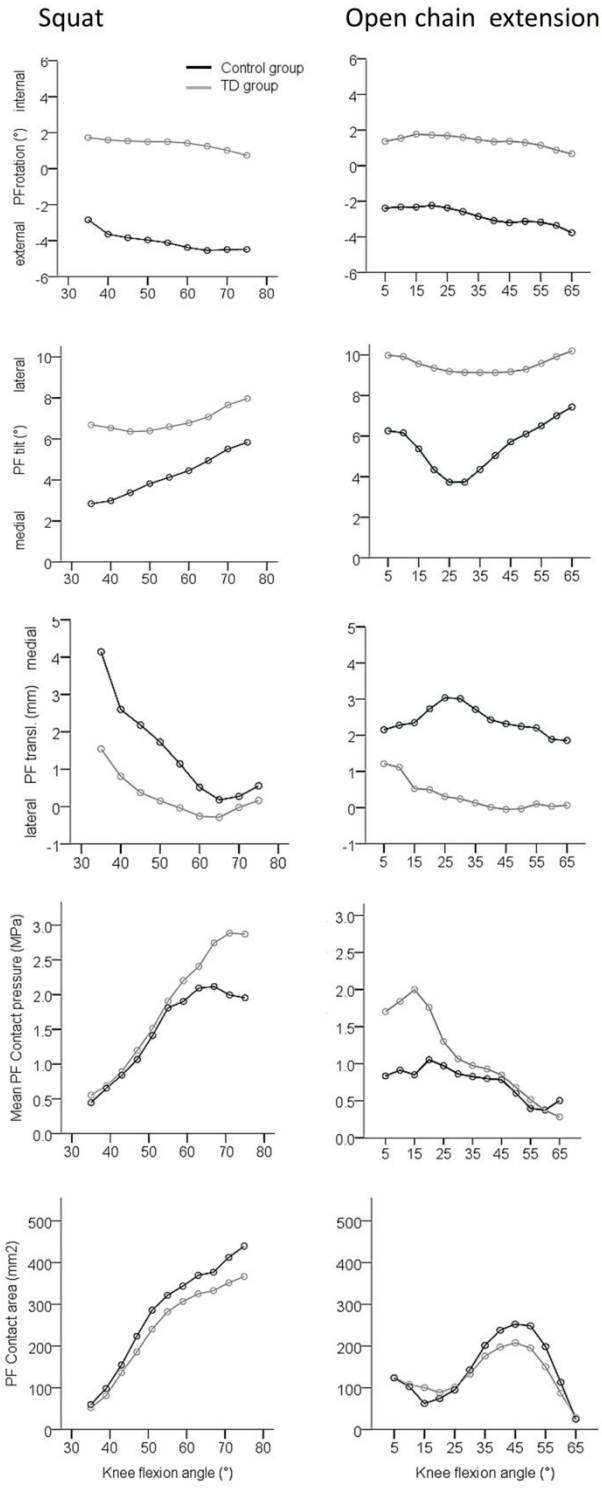
Squat
Open chain extension
Control group
TD group
PFrotation (°)
internal
external
PF tilt (°)
lateral
medial
PF transl. (mm)
medial
lateral
Mean PF Contact pressure (MPa)
PF Contact area (mm2)
Knee flexion angle (°)
Knee flexion angle (°)

Figure 5.5 Patellofemoral rotation, tilt, mediolateral translation, contact pressure and contact area during the squat simulation and open chain extension simulation as a function of knee flexion for the control group and TD group

Open chain

During the open chain extension simulation the mean PF contact pressure increased with knee extension from 65 to 15° and decreased beyond 15° of knee flexion. The contact area increased from 65 to 45° of knee flexion and decreased beyond 45° of knee flexion. The contact pressure was on average higher in the TD group ($p = 0.001$) while the contact area was on average lower in the TD group ($p < 0.002$) compared to the control group (Figure 5.5). Analysis of the four different classes revealed that type B and D showed higher PF contact pressures ($p < 0.001$) and higher PF contact areas ($p < 0.001$) compared to type A and C.

5. 4. Effect on the patellofemoral stability

The neutral position of the patella tended to be more lateral in the TD group compared to the control group (on average 4 mm, $p = 0.384$) (Figure 5.6). After applying 100 N in the lateral direction, the patella shifted on average 3 mm more lateral in the TD group compared to the control group ($p = 0.007$). The largest difference (4 mm) in displacement between the normal and TD group was observed at 20° of knee flexion ($p = 0.093$). The final mediolateral position was on average 7 mm more lateral in the TD group compared to the control group ($p = 0.031$).

Applying 100 N on the patella in the medial direction did not demonstrate significant different between the control and TD group.

For the four different Dejour classes, the analysis of the patellar stability in the lateral and medial direction showed no significant differences between the four types.

However, the neutral patellar position was on average 3 mm more lateral in type B and D compared to type A and C ($p = 0.144$) and the patellar position after applying 100 N to the lateral side was on average 2 mm more lateral in type B and D compared to type A and C ($p = 0.075$).When applying 100 N in the medial direction, the patellar position was on average 2.2 mm less medial in type B and D compared to type C and D ($p = 0.057$).

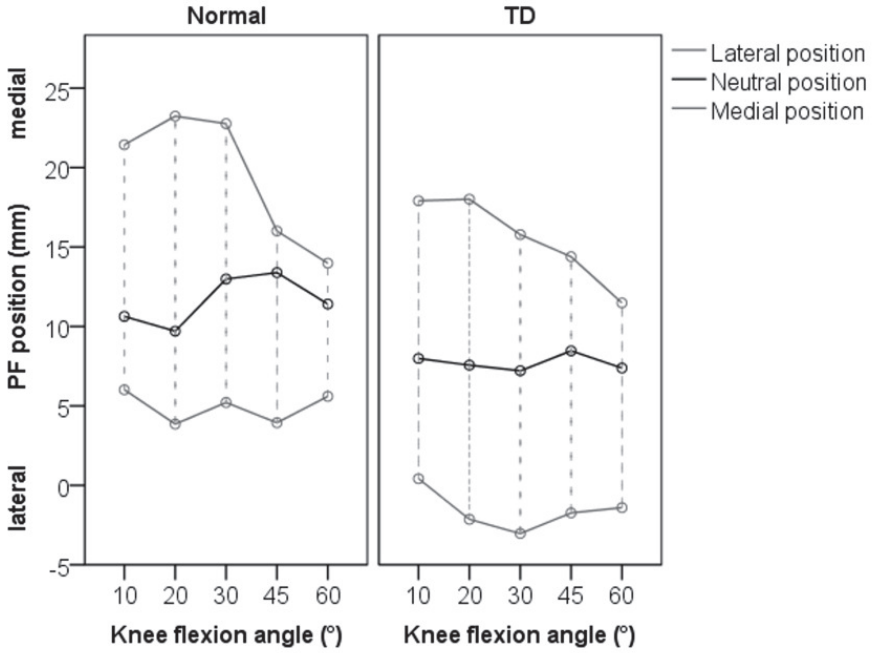

Figure 5.6 Results of the patellar stability test for control group and the trochlear dysplastic group (TD). Patellofemoral mediolateral position in rest (Neutral position) and after applying 100 N on the patella in the medial direction (Medial position) and lateral direction (Lateral position) as a function of knee flexion angle.

5. 5. Discussion

This new research method, using RPT implants to simulate TD, showed that TD has a significant impact on the PF biomechanics and that TD knees characterized by a trochlear bump perform worse than the other types. Dejour type D showed the strongest deviation in terms of PF kinematics. Dejour type B and D showed the strongest deviation in terms of PF contact. Further differentiation in the biomechanical behaviour according to the four Dejour classes was not possible.

The differences in PF kinematics, contact area, contact pressure and stability between the TD group and control group were highly significant. Earlier studies by Amis and colleagues are in line with the current results, except for the mediolateral tracking of the patella in the TD group. Amis and colleagues observed that the

patellae in the TD knees tended to move medially compared to the normal knees, which was probably due to tightening of the medial retinacular restraints caused by the elevation of the central groove in the earlier study (Amis et al. 2008). In the current study care was taken to avoid excessive anterior elevation of the trochlea. Consequently, the medial retinaculum was not tightened, but the trochlear bump was sometimes less pronounced than initially intended (as described in section 2.3).

Classification of TD is an important topic in PF research and, up to date, the four-grade Dejour classification is the most widely used classification system to grade the severity of TD. Nevertheless, differences in PF biomechanics in-between the four Dejour classes have to our knowledge not been investigated before. Several important findings are based on this four-grade classification, but recently the observer reliability of the classification has been questioned and a more reliable two-grade classification was proposed by grading Dejour type A as low grade and grouping type B, C and D as high grade TD (Lippacher et al. 2012). This alternative grouping is supported by two studies, showing that only type A could be morphologically distinguished from type B, C and D by applying the Dejour classification as well as by applying morphological cut-off values (Lippacher et al. 2012, Nelitz et al. 2013). Based on their findings, the authors concluded that the Dejour classification is useful in discriminating low-grade (type A) from high-grade (type B, C and D) TD. According to Lippacher et al. this is an important distinction for clinical purposes because prognosis and treatment mainly depend on the severity of TD (Lippacher et al. 2012).

Notwithstanding the superior observer reliability of this two-grade classification, other studies, including the current study, do not seem to support that the two-grade classification (separating type A from type B, C and D) is the most appropriate grouping in terms of prognosis and treatment. The only significant predictor of a better outcome after sulcus-deepening trochleoplasty was the presence of a supratrochlear spur or bump, which resulted in a more restricted indication of this technically demanding procedure for type D and severe type B, while TD type A, C and mild type B are advised to be treated with other techniques (Dejour et al. 2013, Dejour and Saggin 2010, Fucentese et al. 2011). Furthermore it has been shown that isolated PF arthritis is particularly associated with TD in the presence of a supra trochlear bump (Dejour type B and D) (Allain et al. 2004, Grelsamer et al. 2008, Zaffagnini et al. 2010).

The current experimental study shows that TD knees with a distinct trochlear bump show more severe biomechanical deviations.

Deviations in the PF kinematics were significantly more severe in type D compared to type A, B and C during the open chain extension simulation. Similar differences were also observed but were not significant during the squat simulation. This difference between open chain and squat confirms earlier indications of in-vivo research that open chain exercises are more provocative for patellar maltracking than closed chain exercises (Doucette and Child 1996, Powers et al. 2003). In the current study, the patella was more externally rotated and laterally tilted in type D compared to the other types. Previous studies on patient populations have shown that lateral patellar tilt, measured statically on axial images, is highly correlated with the severity of TD (Dejour and Le Coultre 2007, Dejour et al. 1998). This significant correlation was not found in the current study. Possible explanations are the associated abnormalities which are often present in patient TD populations and which were excluded from the current study. Possible concomitant causes of increased lateral tilt include vastus medialis muscle weakness (Novejosserand and Dejour 1995), tightness of the lateral retinaculum, laxity of the medial retinaculum (Arendt and Dejour 2013).

Deviations in the PF contact pressure and area were significantly more severe in Dejour type B and D compared to type A and C; type B and D showed significantly smaller contact areas and higher contact pressures compared to type A and C. These findings confirm and explain results of in-vivo studies relating TD to isolated PF arthritis and to the outcome of trochleoplasty. Isolated PF arthritis is highly associated with TD, particularly in the presence of a supra trochlear spur (Dejour type B and D) (Allain et al. 2004, Grelsamer et al. 2008, Zaffagnini et al. 2010). It is assumed that the prominence of the proximal trochlea causes an increase of the PF compression in knee flexion like a reverse Maquet effect (Grelsamer et al. 2008, Zaffagnini et al. 2010). This explanation is also believed to be the reason for the better outcome of trochleoplasty in type B and D (Fucentese et al. 2011). The current study shows experimental evidence that the PF contact pressures are indeed substantially increased in type B and D.

The reduced PF stability in the TD group was most pronounced at 20° of knee flexion, which agrees with previous research (Senavongse and Amis 2005). The PF stability showed no significant differences among the four classes, however type B and D showed on average a more lateral position before and after applying 100 N to the patella.

This in-vitro study has some inherent limitations. The Dejour classification was used to grade the TD models. An important consequence of the poor observer agreement

for the four separate Dejour classes is the possibility that study results based on the four-grade classification, including the results of the current study, might be biased to some grouping incorrectness. In addition, TD was simulated without altering the patellar articular shape nor the patellar height, leading to potential mismatch of the PF joint. Amis et al. already discussed that this mismatch is justified because the lateral patellar facet stays in contact with the trochlea, while the medial facet lifts of off the trochlear surface, which is actually similar to clinical situations (Amis et al. 2008). Furthermore, as in other in-vitro studies the used test set-ups have well-known restrictions which can affect the kinematics and stability of the patella. An important restriction in the stability rig is that the patellar rotation and tilt are influenced by the applied lateral and medial load. Ideally, the patella load should only be imposed in the mediolateral direction, which could be achieved by cementing a ball-bearing in the centre of the patella (Senavongse et al. 2003). Nevertheless, the current set-up provided an important indication of the patellar stability. Finally, another limitation is the limited number of tested knees and the unequal number of tested cases in each of the four TD groups (type A, B, C and D). Therefore, statistical analysis for unequal sample size was performed.

Despite these limitations, the current experimental study shows that TD knees with a distinct trochlear bump demonstrated consistently more severe biomechanical deviations. In clinical settings, the Dejour classification identifies TD with a trochlear bump as type B and D. An unsolved problem however is the observer agreement of this classification (Lippacher et al. 2012). Recently, Dejour et al. brought the problem of undiagnosed or underestimated TD to the attention (Dejour et al. 2013). Their study indicated that missed high grade dysplasia (defined as type B and D) may lead to ill-fated treatment of patellar dislocation. In addition, contradictory suggestions have been made on the classification; further differentiation of the four classes is sometimes used in relation to treatment decision (mild and severe type B). On the other hand, grouping of type B, C and D was proposed to improve observer agreement. These findings indicate that further research on trochlear shape variations is warranted.

5. 6. Conclusions

The use of rapid prototyped models of joint deformities allowed to investigate the biomechanical impact of different types of TD on the PF kinematics, contact and stability.

This study shows an important experimental indication that TD knees with a pronounced trochlear bump (Dejour type B and D) are more prone to PF arthritis caused by increased PF compression. For the same reason, this study supports earlier hypotheses that the better outcome of trochleoplasty in knees with a supratrochlear bump is at least partly due to a larger unloading effect of the sulcus deepening in these types compared to other types of TD. Currently, these types with a supratrochlear bump are graded as Dejour type B and D. Improvement of observer agreement, however, is necessary for more accurate grading.

References

1. Allain J, Dejour D, Argenson JN, Duparc F, Godefroy D, Gougeon F, Huten D, Jenny JY, Mertl P, Migaud H, et al. 2004. Isolated patello-femoral osteoarthritis. Rev Chir Orthop. 90:69-129.

2. Amis AA, Oguz C, Bull AMJ, Senavongse W, Dejour D. 2008. The effect of trochleoplasty on patellar stability and kinematics - A biomechanical study in vitro. J Bone Joint Surg Br. 90B:864-869.

3. Arendt EA, Dejour D. 2013. Patella instability: building bridges across the ocean a historic review. Knee Surg Sport Tr A. 21:279-293.

4. Belvedere C, Catani F, Ensini A, de la Barrera JLM, Leardini A. 2007. Patellar tracking during total knee arthroplasty: an in vitro feasibility study. Knee Surg Sport Tr A. 15:985-993.

5. Bull AMJ, Andersen HN, Basso O, Targett J, Amis AA. 1999. Incidence and mechanism of the pivot shift - An in vitro study. Clin Orthop Relat R. 219-231.

6. Dejour D, Byn P, Ntagiopoulos PG. 2013. The Lyon's sulcus-deepening trochleoplasty in previous unsuccessful patellofemoral surgery. Int Orthop. 37:433-439.

7. Dejour D, Le Coultre B. 2007. Osteotomies in patello-femoral instabilities. Sports Med Arthrosc. 15:39-46.

8. Dejour D, Reynaud P, Lecoultre B. 1998. Douleurs et instabilité rotulienne. Essai de classification. Médecin et Hygiène. 56:1466-1471.

9. Dejour D, Saggin P. 2010. The sulcus deepening trochleoplasty-the Lyon's procedure. Int Orthop. 34:311-316.

10. Dejour H, Walch G, Neyret P, Adeleine P. 1990. Dysplasia of the Femoral Trochlea. Rev Chir Orthop. 76:45-54.

11. Dejour H, Walch G, Nove-Josserand L, Guier C. 1994. Factors of patellar instability: an anatomic radiographic study. Knee surgery, sports traumatology, arthroscopy : official journal of the ESSKA. 2:19-26.

12. Doucette SA, Child DD. 1996. The effect of open and closed chain exercise and knee joint position on patellar tracking in lateral patellar compression syndrome. J Orthop Sport Phys. 23:104-110.

13. Farahmand F, Senavongse W, Amis AA. 1998. Quantitative study of the quadriceps muscles and trochlear groove geometry related to instability of the patellofemoral joint. J Orthopaed Res. 16:136-143.

14. Fucentese SF, Zingg PO, Schmitt J, Pfirrmann CW, Meyer DC, Koch PP. 2011. Classification of trochlear dysplasia as predictor of clinical outcome after trochleoplasty. Knee surgery, sports traumatology, arthroscopy : official journal of the ESSKA. 19:1655-61.

15. Grelsamer RP, Dejour D, Gould J. 2008. The pathophysiology of patellofemoral arthritis. Orthop Clin N Am. 39:269-+.

16. Lippacher S, Dejour D, Elsharkawi M, Dornacher D, Ring C, Dreyhaupt J, Reichel H, Nelitz M. 2012. Observer Agreement on the Dejour Trochlear Dysplasia Classification A Comparison of True Lateral Radiographs and Axial Magnetic Resonance Images. Am J Sport Med. 40:837-843.

17. Merican AM, Kondo E, Amis AA. 2009. The effect on patellofemoral joint stability of selective cutting of lateral retinacular and capsular structures. J Biomech. 42:291-296.

18. Nelitz M, Lippacher S, Reichel H, Dornacher D. 2013. Evaluation of trochlear dysplasia using MRI: correlation between the classification system of Dejour and objective parameters of trochlear dysplasia.

19. Novejosserand L, Dejour D. 1995. Quadriceps Dysplasia and Patellar Tilt in Objective Patellar Instability. Rev Chir Orthop. 81:497-504.

20. Pfirrmann CWA, Zanetti M, Romero J, Hodler J. 2000. Femoral trochlear dysplasia: MR findings. Radiology. 216:858-864.

21. Powers CM. 2000. Patellar kinematics, part II: The influence of the depth of the trochlear groove in subjects with and without patellofemoral pain. Phys Ther. 80:965-973.

22. Powers CM, Ward SR, Fredericson M, Guillet M, Shellock FG. 2003. Patellofemoral kinematics during weight-bearing and non-weight-bearing knee extension in persons with lateral subluxation of the patella: A preliminary study. J Orthop Sport Phys. 33:677-685.

23. Senavongse W, Amis AA. 2005. The effects of articular, retinacular, or muscular deficiencies on patellofemoral joint stability - A biomechanical study in vitro. J Bone Joint Surg Br. 87B:577-582.

24. Senavongse W, Farahmand F, Jones J, Andersen H, Bull AMJ, Amis AA. 2003. Quantitative measurement of patellofemoral joint stability: force-displacement behavior of the human patella in vitro. J Orthopaed Res. 21:780-786.

25. Siston RA, Patel JJ, Goodman SB, Delp SL, Giori NJ. 2005. The variability of femoral rotational alignment in total knee arthroplasty. J Bone Joint Surg Am. 87A:2276-2280.

26. Varadarajan KM, Freiberg AA, Gill TJ, Rubash HE, Li GA. 2010. Relationship Between Three-Dimensional Geometry of the Trochlear Groove and In Vivo Patellar Tracking During Weight-Bearing Knee Flexion. J Biomech Eng-T Asme. 132:

27. Verlinden C, Uvin P, Labey L, Luyckx JP, Bellemans J, Vandenneucker H. 2010. The influence of malrotation of the femoral component in total knee replacement on the mechanics of patellofemoral contact during gait AN IN VITRO BIOMECHANICAL STUDY. J Bone Joint Surg Br. 92B:737-742.

28. Victor J, Van Glabbeek F, Vander Sloten J, Parizel PM, Somville J, Bellemans J. 2009. An experimental model for kinematic analysis of the knee. J Bone Joint Surg Am. 91 Suppl 6:150-63.

29. Zaffagnini S, Dejour D, Arendt EA. 2010. Patellofemoral pain, instability, and arthritis clinical presentation, imaging, and treatment. Springer-Verlag. xii, 331 p.

Chapter 6

General discussion and future prospects

The relation between trochlear dysplasia and patellar dislocation has been discussed for over a century (Isermeyer 1967). The vast evolution in imaging resulted in a more detailed description of trochlear dysplasia with specific anatomical signs like the trochlear bump and crossing sign (Dejour et al. 1994, Malghem and Maldague 1989). Patellar dislocation has received a lot of attention in anatomical and biomechanical studies leading to an increased understanding of the problem, but also to an increased acknowledgement of its complexity. Besides the trochlear shape many other (skeletal and soft tissue) factors can be involved in the mechanism of patellar dislocation. This complexity is expressed by the impressive number (+100) of surgical techniques (Andrish 2008) described in literature and the ongoing debate on when to apply which technique. Up to date there is no agreement on the clinical and radiographic indications to alter the trochlear shape (Arendt and Dejour 2013, Dejour et al. 2013). The current policy is that trochleoplasty is justified in trochlear dysplasia Dejour type B and D.

This work was focused on the anatomy of trochlear dysplasia and its impact on the patellofemoral joint. In the first morphological part of this work the geometrical characteristics of the distal trochlear dysplastic femur were investigated on 3D surface models and in the second biomechanical part the effect of different types of trochlear dysplasia was investigated in a series of cadaver experiments.

Despite the unsolved problem of accurately classifying the geometrical variations, this work shows empirical evidence that the presence of a trochlear bump is a key provocative factor for severely disturbed patellofemoral kinematics and increased contact pressures. Clinically, this implies that the presence of a trochlear bump is an important factor in the development of early patellofemoral arthritis. In addition, these findings also explain the better outcome for trochleoplasty in trochlear dysplasia Dejour type B and D (both characterised by a trochlear bump).

6. 1. Morphological part

6. 1. 1. Discussion

In the morphological part of this work the distal femur was investigated with a landmark-based analysis and a SSA. The observations in both methods are largely concordant with each other. It can however not be concluded that the second study confirms the findings of the first one, since both studies are applied on the same dataset. The first study provides quantitative characteristics of the TD distal femur, while the second study provides a more global and informative analysis of the distal femur shape.

As expected, both morphological studies show that the anterior trochlea is the most affected region of the TD distal femur. This is obviously not a novel finding, but the applied methodology is novel and counters several issues that can flaw morphological measurements. First, in the current study the largest femur model was 35% larger than the smallest femur model. This clearly has implications on the cut-off values which are commonly used to diagnose TD. A second issue was mismatch of subchondral bone and cartilage. It is well-known and well-documented that the shape of the articulating cartilage does not always match the shape of the subchondral bone, especially in TD femurs. Thirdly, working with 3D models eliminates possible misalignment errors that can occur during imaging.

In addition to the abnormalities in the trochlear region, the TD distal femur appeared to have a lower mediolateral/anteroposterior ratio and a smaller notch width compared to normal femurs. PCA showed that a smaller notch width appeared in association with an increased trochlear sulcus angle. Though these changes outside the trochlear region are not assumed to contribute directly to patellar instability, they appear to be highly related to TD.

It is important to note that both methods are useful. The landmark based analysis provides discrete measurements for each femur which can easily be interpreted, while the SSA provides more global and more complex information, which can be used for describing the main modes of shape variation and for automated classification and clustering.

Automated classification of normal and TD distal femurs was achieved with a sensitivity of 85% and a specificity of 95%. The results obtained with the current PCA are not superior to non-automated methods. It is expected that sensitivity and specificity of automated classification will improve with increasing sample size.

Classification of different variations of TD is an ongoing discussion. The Dejour classification is the most widely used classification, but neither qualitative nor quantitative assessments on 2D or on 3D images succeeded to obtain optimum observer agreement. Grading of TD is important to assess the patient's risk for early PF arthritis and to decide if surgical modification of the trochlear shape is warranted. Statistical shape analyses might provide an alternative method to cluster different types of TD. Larger sample size however is required for reliable clustering.

6. 1. 2. Clinical relevance

In clinical practice and in morphological studies, it is important to take the size of the patient's knee into account, especially when defining and applying cut-off values for diagnostic or therapeutic reasons.

Measuring on 3D models offers some advantages, like taking the full geometry, size differences and alignment errors into account. In clinical settings however, time-consuming generation of 3D models can be an important drawback to work with 3D models, but future improvements of automatic and semi-automatic segmentation will probably overcome this current drawback.

Despite the small sample size, the SSA demonstrated promising prospects to improve classification of TD.

6. 1. 3. Limitations

The main limitation of these morphological studies is the small sample size. Forty knees were included, which is a rather small number, especially for SSA.

Furthermore, the 3D surface models included the cartilage, but the cartilage thickness itself was not investigated.

The arthro-CT images did not show the full shaft of the femur. Therefore, the orientation of the longitudinal axis of the femur had to be estimated, which might have led to measurement inaccuracies.

In addition, 3D processing steps and manual landmark definition may also have led to accuracy errors.

6. 2. Biomechanical part

6. 2. 1. Discussion

In the biomechanical part of this work a new method to investigate the biomechanical impact of osseous abnormalities was first validated and then applied to simulate TD. RPT was used to manufacture cadaver-specific guiding instruments and different types of cadaver-specific trochlear implants. To our knowledge this is the first experimental study which investigated the impact of different types of TD.

The validation study showed that replacing the native trochlea by a rapid prototyped replica induces moderate changes in PF biomechanics. This is not surprising since the material properties of the implant are not identical to the properties of cartilage. In addition, the guiding instruments can induce a rotational error, which can also be a source of altered biomechanics. Therefore this research method is considered to have great potential to investigate osseous abnormalities, provided that the native condition is not used a control condition. Instead, a replica of the native geometry should be used.

The shape of the pathological implants was based on medical images of patients who suffered from recurrent patellar dislocations. Four patients were selected, each showing a different type of TD. Consequently, the trochlear shape was sized and remodelled at the edges to assure a smooth fit with the cadaver.

Inserting the pathological implants in the otherwise normal knees resulted in a simulation of TD without any other associated abnormalities or injuries, which is an artificial situation. In in-vivo situations, the patient is usually affected by multiple abnormalities at the level of the bones and at the level of the soft tissues. This dissertation however only focussed on the morphology and biomechanical effect of TD. The rationale behind this choice was to create a situation in which the isolated effect of TD could be investigated. Therefore, all other anatomical structures of the knee were left unaltered. Investigating the influence of other abnormalities was beyond the scope of this dissertation.

The TD shape of the implants significantly affected the PF kinematics, contact pressures, contact areas and stability. Especially the presence of a trochlear bump had a major impact on the PF biomechanics. These observations are in line with, and provide evidence for the findings of earlier clinical studies showing that patients with TD type B and D have a higher risk to develop osteoarthritis and a better outcome of trochleoplasty.

6. 2. 2. Clinical relevance

The results of the biomechanical study provide evidence that patients with a pronounced supratrochlear bump are prone to severely increased contact pressures and on long term to PF osteoarthritis. Therefore this study supports that trochleoplasty is indeed justified in TD with a pronounced bump.

Currently, TD with a supratrochlear bump is graded as Dejour type B and D. Improvement of observer agreement, however, is necessary for more accurate grading. The results of this study show that new classifications should not only demonstrate a superior reliability, but should also be relevant for clinicians to decide on treatment.

6. 2. 3. Limitations

This in-vitro study is a simulation of very complex in-vivo mechanisms. The knee is a coupled mechanical system in which a change to one part of the system affects the other parts. Simulating isolated abnormalities is thus a relative concept.

In addition, the cadaver-specific characteristics (e.g. the tension of the MPFL) also influenced the results of this study.

Further, not all material properties of the rapid prototyped implants are documented by the supplier. Additional material testing should be done to investigate these properties.

In this study only the most relevant parameters for patellar dislocation were investigated. Given the complex interactions in the knee joint, it may well be possible that tibiofemoral biomechanics are altered as well. This was however beyond the scope of the current study.

After performing the experiment, the 3D models were evaluated by blinded observers. The models were graded with the Dejour classification, which has shown a rather low reliability. Therefore the current results might be biased to some grouping incorrectness.

6. 3. Future prospects

In this dissertation, only a small number of knees was included, no other abnormalities besides TD and no treatment methods were investigated.

Increasing the sample size of the SSM could improve automated classification of normal and TD knees and might also succeed in clustering TD femurs, which could improve grading of TD.

Grading TD remains an important research topic in literature. To date, the Dejour classification is still accepted as the most appropriate classification to grade TD. It is important for future classifications that the classes reflect differences in morphology as well as differences in biomechanics. The PF kinematics, contact areas, contact pressures and stability data obtained in the biomechanical study may subsequently be used to evaluate if new classifications reflect differences in PF biomechanics.

The current SSA and biomechanical study did not analyse abnormalities other than TD.

In the SSA, evaluating the patellar shape and position would add important information to the current study. It has been stated that patella alta and tilt are associated with TD. In addition it has also been suggested that patellar maltracking or patella alta might lead to overgrowth of the distal femoral physis, thereby causing TD (Tardieu et al. 2006) and that the articular cartilage of the trochlea might be more proximally-distributed to allow contact with the articular cartilage of a high-riding patella (Yamada et al. 2007). Adaptation of the trochlear shape to the patellar position was recently also supported by an experimental animal study on growing rabbits (Huri et al. 2012). It was observed that lateralisation of the patella (obtained by releasing the medial soft tissue constraints) actually caused the development of a more flattened trochlea. If these hypotheses are true, one would expect to find a high correlation between the patellar shape and position and the trochlear shape. Given the geometrical complexity of these bones, SSA could be applied to analyse the relation between patella and trochlea.

Biomechanical studies on patella alta have already been performed, but have not yet been investigated in association with TD. It has been shown that isolated patella alta mainly increases the contact pressures in deep flexion (Luyckx et al. 2009). Patients with TD and patella alta however frequently demonstrate PF arthritis equivalent with increased pressures in early flexion. Simulating patella alta in combination with TD might increase our understanding of their interaction.

The MPFL also receives a lot of attention in literature on patellar dislocation. In recurrent dislocation this ligament is usually ruptured. Reconstruction of the MPFL has evolved towards a popular technique because of its relatively low risk and technical difficulty on one hand and because of its good results regarding patellar

stability on the other hand. It has been stated however that isolated MPFL reconstruction is not considered the best solution if TD or patella alta are present (Dejour et al. 2013). Moreover, it was stated that a normal trochlea with a deep groove and an elevated lateral facet are necessary for the MPFL to provide stability (Arendt et al. 2002, Bicos et al. 2007). In the presence of a trochlear bump, isolated reconstruction of the medial soft-tissues the patella would be subjected to firm medial stabilisation and medial tilt, which could lead to undesirable impingement between the patella and the trochlear prominence and subsequently increased contact pressures (Dejour et al. 2013).

In the current study the MPFL was not ruptured, which corresponds with an intact or reconstructed ligament. Severely increased contact pressures were indeed noted in the current study in test cases with a pronounced trochlear bump.

Testing knees with a ruptured MPFL combined with a trochlear bump could show to what extent this ligament contributes to the increased contact pressures. Following the statements of Dejour, Arendt and Bicos (Arendt et al. 2002, Bicos et al. 2007, Dejour 2013), it would be expected that the combined presence of a trochlear bump and a ruptured MPFL would result in lower pressures compared to the current study. Conversely, given the function of the MPFL, it can also be expected that the combination of TD and ruptured MPFL would lead to more disturbed patellar stability and kinematics compared to the results of the current study..

In addition to simulating abnormalities, this new method also opens perspectives to investigate the effect of treatment methods, like trochleoplasty.

Though deepening of the trochlea in Dejour type B and D is supported by clinical studies and by the current experimental study, it remains a difficult procedure with varying degrees of success. Potential complications include the risk of arthrofibrosis, post-operative pain and PF arthritis. To what extent and in what way these complications are related to the geometrical characteristics of the trochleoplasty is unknown. Thus far, the outcome of trochleoplasty has not been reported or investigated in light of geometrical characteristics of the pre-and post-operative trochlea. The experimental method described in chapter 5 and 6 can be used to simulate the preoperative and postoperative condition of patients treated with trochleoplasty. This way, the geometrical characteristics of the pathological condition and the performed surgery can be related to objective parameters like the PF kinematics, contact area, contact pressure and stability. Such analysis might help surgeons to better understand the success (or the lack of success) of trochleoplasty.

As outlined throughout this dissertation, the aetiology of patellar dislocation is multifactorial and complex and so is its treatment. This dissertation only focussed on the morphology and biomechanical effect of TD. Other anatomical structures of the knee were left unaltered, even though it is well known that they have an important influence on patellar biomechanics as well. Therefore, investigating isolated abnormalities was not the final goal, it is rather the beginning.

References

1. Andrish J. 2008. The management of recurrent patellar dislocation. Orthop Clin N Am. 39:313-+.

2. Arendt EA, Dejour D. 2013. Patella instability: building bridges across the ocean a historic review. Knee Surg Sport Tr A. 21:279-293.

3. Arendt EA, Fithian DC, Cohen E. 2002. Current concepts of lateral patella dislocation. Clin Sport Med. 21:499-+.

4. Bicos J, Fulkerson JP, Amis A. 2007. Current concepts review - The medial patellofemoral ligament. Am J Sport Med. 35:484-492.

5. Dejour D, Byn P, Ntagiopoulos PG. 2013. The Lyon's sulcus-deepening trochleoplasty in previous unsuccessful patellofemoral surgery. Int Orthop. 37:433-439.

6. Dejour H. 2013. The patellofemoral joint and its historical roots: the Lyon School of Knee Surgery. Knee surgery, sports traumatology, arthroscopy : official journal of the ESSKA. 13.

7. Dejour H, Walch G, Nove-Josserand L, Guier C. 1994. Factors of patellar instability: an anatomic radiographic study. Knee surgery, sports traumatology, arthroscopy : official journal of the ESSKA. 2:19-26.

8. Huri G, Atay OA, Ergen B, Atesok K, Johnson DL, Doral MN. 2012. Development of femoral trochlear groove in growing rabbit after patellar instability. Knee surgery, sports traumatology, arthroscopy : official journal of the ESSKA. 20:232-8.

9. Isermeyer H. 1967. Über die pathologische Luxation der Patella. Arch Klin Chir. 8:23.

10. Luyckx T, Didden K, Vandenneucker H, Labey L, Innocenti B, Bellemans J. 2009. Is there a biomechanical explanation for anterior knee pain in patients with

patella alta? Influence of patellar height on patellofemoral contact force, contact area and contact pressure. J Bone Joint Surg Br. 91B:344-350.

11. Malghem J, Maldague B. 1989. Depth Insufficiency of the Proximal Trochlear Groove on Lateral Radiographs of the Knee - Relation to Patellar Dislocation. Radiology. 170:507-510.

12. Tardieu C, Glard Y, Garron E, Boulay C, Jouve JL, Dutour O, Boetsch G, Bollini G. 2006. Relationship between formation of the femoral bicondylar angle and trochlear shape: Independence of diaphyseal and epiphyseal growth. Am J Phys Anthropol. 130:491-500.

13. Yamada Y, Toritsuka Y, Yoshikawa H, Sugamoto K, Horibe S, Shino K. 2007. Morphological analysis of the femoral trochlea in patients with recurrent dislocation of the patella using three-dimensional computer models. J Bone Joint Surg Br. 89B:746-751.

List of figures

List of tables

Appendix A

Ghent Knee Rig: Pilot validation study on a quasi-static weight-bearing knee rig[5]

This study presents a pilot study on a quasi-static knee rig designed to investigate the influence of pathologies and surgical interventions on the patellofemoral kinetics of cadaveric knees. The knee rig allows cadaveric knees to flex and extend under a simulated body weight by transmitting a force to the quadriceps tendon. During the squat simulation, the ground reaction force stays within physiological values. Before using this device to answer clinical questions, two knee-specimens were tested to assess the repeatability of the rig. Four repeated flexion-extension cycles were performed under a simulated body weight of 700 N, with an isolated force on the quadriceps tendon up to 2700 N and with a ground reaction force close to 350 N. The resulting patellofemoral contact area shifted from distal to proximal during knee flexion. From 20 to 60° degrees of knee flexion the mean contact area and pressure increased respectively from 80.2 ± 3.3 to 349.5 ± 10.1 mm2 and from 0.9 ± 0.2 to 5.9 ± 0.7 MPa. The transmitted force on the quadriceps tendon, the ground reaction force and the patellofemoral contact area and pressure were continuously measured and showed a relative variability of respectively 1.6%, 2.4%, 2.8% and 3.2%. The presented knee rig shows a good repeatability which allows us to use this knee rig to quantify the influence of anatomical changes on the patellofemoral contact area's and pressures during a squat simulation.

[5] This study is published as A. Van Haver, K. De Roo, T. Claessens, M. De Beule, P. Verdonk, P. De Baets. Pilot validation study on a quasi-static weight-bearing knee rig. Proceedings of the Institution of Mechanical Engineers, Part H: Journal of Engineering in Medicine (2013) 227 (3): 229-233

A.1. Introduction

In-vitro testing of the human knee continues to be an important research method in orthopedic biomechanics. First of all in-vitro experiments allow us to test isolated conditions or treatments on one single knee specimen which rules out inter-specimen variations (Woo et al. 2006). Secondly, a number of interesting parameters such as the contact pressures inside the knee joint can only be accurately obtained during in-vitro experiments.

Two main categories of knee rigs are reported in literature, the well-known and widely used (quasi-) static Oxford type rigs and the dynamic robotic knee testing systems (Varadarajan KM 2009). The original Oxford Knee Rig was introduced in 1978 (Bourne 1978) and refined and copied several times (Petersilge et al. 1994, Shoemaker et al. 1993, Zavatsky 1997). In some Oxford Knee Rigs, as in our proposed knee rig, the flexion-extension position is controlled by applying a load on the quadriceps tendon (F_Q) (Patil et al. 2005, Zavatsky 1997).

Although many knee rigs have been described, according to Muller et al (2009) only few studies applied physiological muscle loading and realistic ground reaction forces (F_{GR}) (Muller et al. 2009). Knee biomechanics however, can be considerably changed by the loading conditions, even though the shapes of the kinematic profiles remain unaltered (Muller et al. 2009). Furthermore, since our research is focussed on the PF joint forces, loading conditions are important to account for cartilage deformation that may occur with load (Besier et al. 2005).

In this paper we present a pilot study on a quasi-static Oxford type weight-bearing knee rig in which the flexion-extension position is continuously altered by F_Q. This F_Q reaches physiological values up to 2700 N while the F_{GR} stays within a realistic range of 300 – 400 N. Given the low speed (2.75 mm/s) of the actuator acting as F_Q we consider the movement to be quasi-static.

The purpose of this study is to investigate the repeatability of the knee rig by calculating the relative variability of F_Q, F_{GR} and the PF contact area and pressure. This repeatability test is essential for using the proposed knee rig for future research on the PF joint forces in cadaveric knees.

A.2. Methods

A.2.1. Test set-up

The mechanical construction of the presented knee rig consists of a vertical frame with a hip and ankle assembly (Figure A.1). The hip assembly (A) allows the femur to perform a flexion–extension and an internal-external rotation. Two vertical supports (B) guide the hip assembly up and down, enabling the knee to flex and extend smoothly. The ankle assembly (C) allows the tibia to perform a flexion–extension, varus–valgus and internal–external rotation. The knee is thus free to move in its six degrees of freedom. In addition, two sliding platforms (D) between the ankle assembly and the supporting table allow the ankle to slide in the medio-lateral and antero-posterior direction. The ankle movements can be constrained or unconstrained.

We simulated a physiological body weight of 700 N by setting the weight above hip height to 275 N (i.e. body weight above hip height on one leg in bipedal stance, calculated according to de Leva (de Leva 1996)). This weight can be varied to approach the cadaver-specific values. Above the hip assembly a displacement controlled electrical actuator (Parker Hannifin, Nijvel, Belgium) (E) is mounted on two horizontal profiles. The actuator creates an extensor moment about the knee joint by transmitting the force to the quadriceps tendon through a steel cable. The cable is guided as closely as possible to the shaft of the femur by two pulleys (F), simulating a Q-angle between 8° and 30° (Conlan et al. 1993, Mizuno et al. 2001). A tendon clamp (G) attaches the cable to the tendons of the RF and the VI. In between the actuator and the cable an uniaxial force sensor (Sensy, loadcell 5932, Jumet, Belgium) is mounted to register the applied force on the quadriceps tendon. Other sensors were implemented to quantity F_{GR} (Sensy, loadcell 2962, Jumet, Belgium) and the flexion angle of the femur (Active sensors, RP5110-350 rotary potentiometer, Dorset, UK).

The knee flexion angle β can be calculated from the flexion angle of the femur (α), the length of the femur (l_{femur}) and tibia (l_{tibia}) and the optional anterior-posterior displacement of the mechanical ankle (y) with the following formula:

$$\beta = \alpha + \arcsin\left(\frac{l_{femur}.sin(\alpha) - y}{l_{tibia}}\right)$$

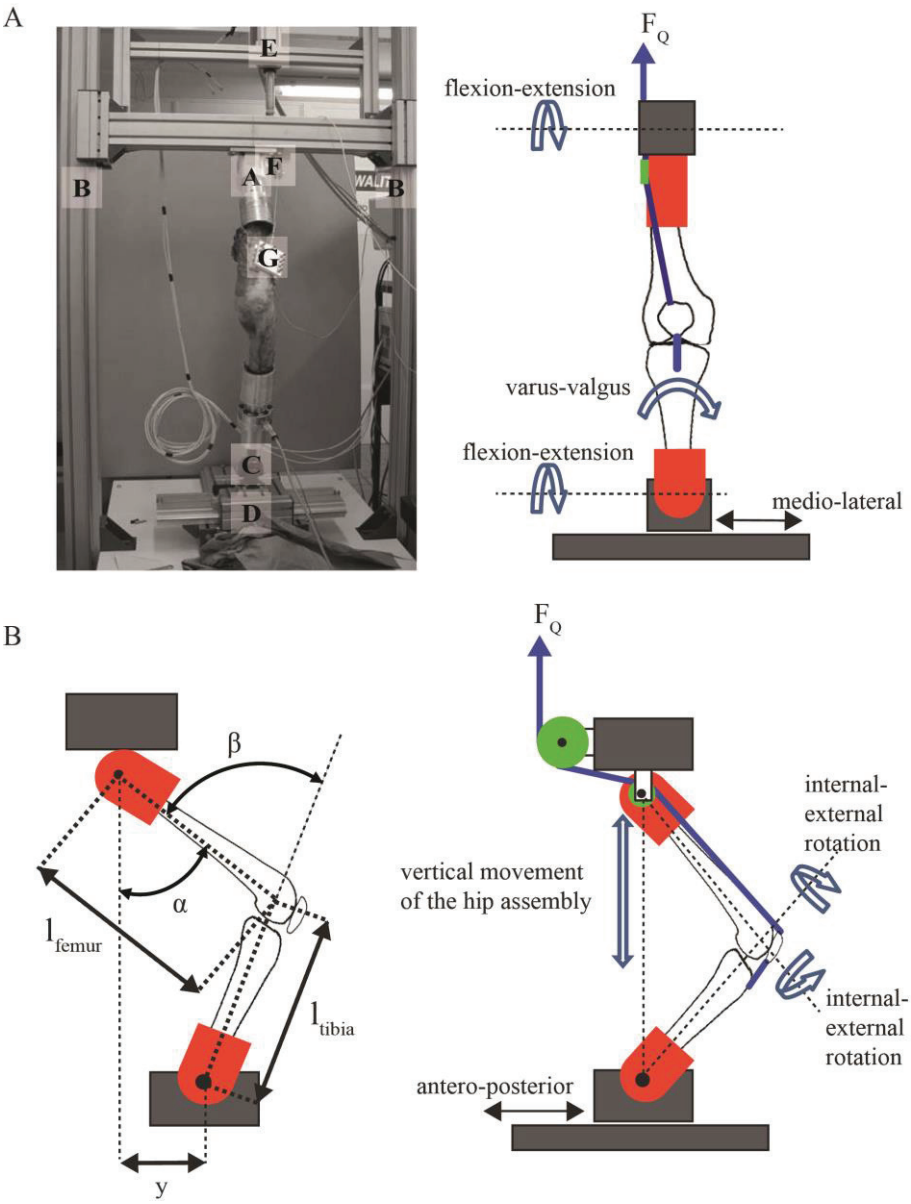

Figure A.1 Knee Rig. Frontal view (a); A = hip assembly, B = vertical profiles, C = ankle assembly, D = sliding platforms, E = actuator, F = pulley, G = tendon clamp. Sagittal view (b); α = hip angle, β = knee flexion angle, y = antero-posterior displacement of the ankle assembly, l_{femur} = femur length, l_{tibia} = tibia length, F_Q = Force on the quadriceps tendon

The contact pressure distribution and area in the PF joint are measured with a 5051 I-scan pressure sensitive film (Tekscan Inc., South Boston, MA, USA).

Prior to testing, the range of motion, simulated body weight, speed of the actuator and ankle position are determined. During the test, F_Q, F_{GR}, the flexion angle of the femur and the PF contact area and pressures are continuously measured.

A.2.2. Materials and test protocol

Two cadaveric knees (K1 and K2, both embalmed with a mixture of formol, phenol and thymol) were tested on the presented knee rig at room temperature. Arthro-CT scans were made prior to testing to ensure that no bony abnormalities were present. Each knee was amputated through the tibia and fibula at 23 cm from the ankle joint and through the femur at 14 cm from the hip joint, according to the distance to the respective mechanical joint. The cadaver bones were connected with the mechanical hip and ankle by embedding the free ends of the dissected bones in aluminum cylinders, which can easily be mounted in the knee rig. When the femoral bone was embedded, the natural valgus alignment of the femur was respected. The quadriceps muscle was dissected to clamp the tendons of the RF and VI together. The pressure film was inserted in the PF joint through a lateral parapatellar incision as described by Ostermeier (Ostermeier et al. 2007) and was attached on the articulating surface of the patella using a topical two-octylcyanoacrylate tissue adhesive, Dermabond® (Ethicon NV, Johnson & Johnson, Somerville, NJ, USA). Prior to closing the incision with single stitches to restore physiological conditions, the contour of the articulating surface of the patella was digitized on the pressure film, so that potential noise outside the patellar surface could be discarded.

For this study, the mechanical ankle was positioned under the mechanical hip in the anterior-posterior direction and slightly medial to allow the natural valgus angle of the knee. The actuator acted with a constant speed of 2.75 mm/s. K1 was tested with a knee flexion range from 20 to 60° flexion, while K2 was tested from 35 to 60° of flexion because of cadaver specific limitations. Four uninterrupted flexion-extension cycles were recorded for each specimen.

The mean F_{GR} ± SD during the four cycles was calculated for each knee. The maximal F_Q was analyzed separately for the flexion and extension phase, because the extension phase requires a considerably higher force than the flexion phase. The resulting PF contact area and pressure were analysed as a function of the knee angle.

To demonstrate the repeatability of the test rig we quantified the variation of F_{GR}, F_Q and the PF contact area and pressure within each knee as the coefficient of variation (CV). The mean CV is calculated as the mean value of the CVs of K1 and K2.

A.3. Results

Measurements of F_Q and F_{GR} (K1) are shown in Figure A.2. The mean F_{GR} was 339 ± 9 N for K1 and 373 ± 10 N for K2, these results approximate the sum of the weight above hip height, the cadaver specimen and the mechanical ankle. F_Q reached a maximum value at the deepest knee flexion angle and was systematically higher during the extension phase compared to the flexion phase. During the flexion phase the peak F_Q was 1332 ± 33 N for K1 and 1487 ± 16 N for K2. During the extension phase the peak F_Q was 2680 ± 68 N for K1 and 2656 ± 17 N for K2.

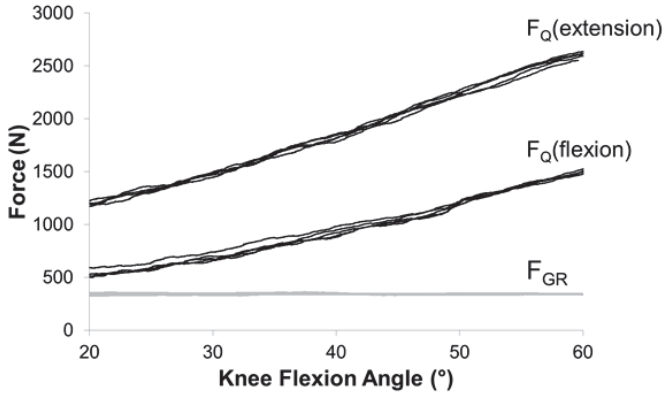

Figure A.2 Force on the quadriceps tendon (F_Q) and the ground reaction force (F_{GR}) in function of the knee flexion angle (Knee 1)

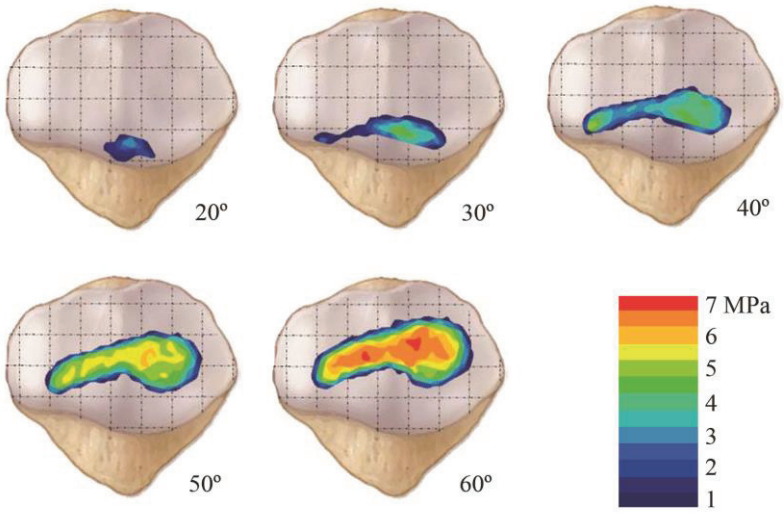

Figure A.3 Pressure distribution of knee 1 at 20, 30, 40, 50 and 60° of knee flexion during the extension phase

The contact area on the patella shifted from distal to proximal with deeper knee flexion, which is demonstrated in the Tekscan frames of K1 (Figure A.3). From 20 to 60° degrees of knee flexion the mean contact area and pressure increased respectively from 80.2 ± 3.3 to 349.5 ± 10.1 mm^2 and from 0.9 ± 0.2 to 5.9 ± 0.7 MPa. The difference between the extension phase and the flexion phase is shown in Figure A.2, Figure A.4 and Figure A.5.

The mean relative variability was 2.4% for F_{GR}, 1.6% for F_Q (1.8% during flexion and 1.4% during extension), 2.8% for the contact area and 3.2% for the contact pressure.

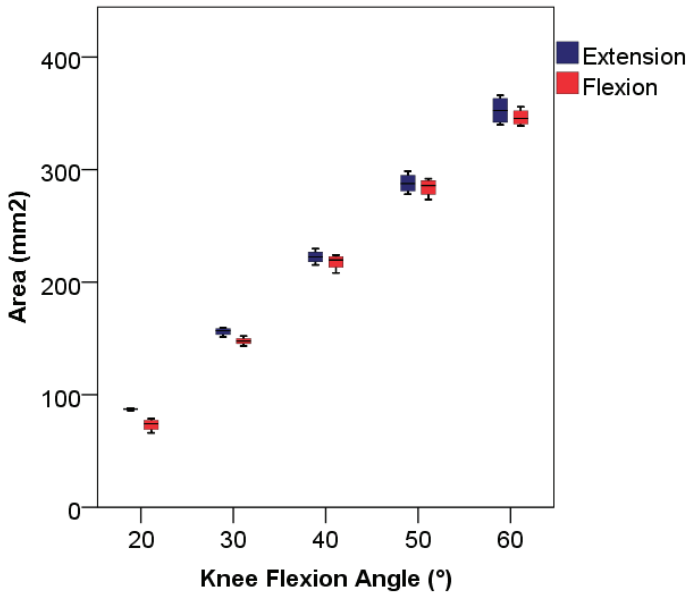

Figure A.4 Mean (± SD) patellofemoral contact area at 20, 30, 40, 50 and 60° of knee flexion during the flexion and extension phase (Knee 1)

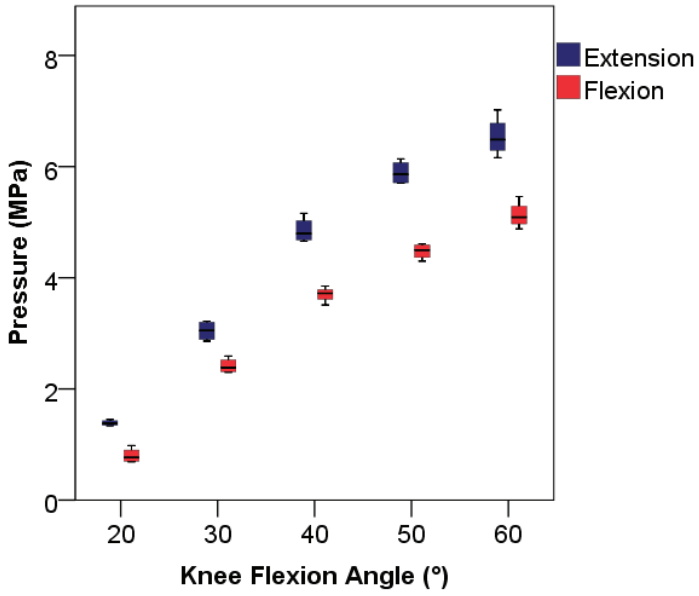

Figure A.5 Mean (± SD) patellofemoral contact pressure at 20, 30, 40, 50 and 60° of knee flexion during the flexion and extension phase (Knee 1)

A.4. Discussion

This pilot study on a limited number of specimens demonstrates that F_Q and F_{GR} are within the physiological range and that all measured parameters show a low variability; the repeatability of the test rig is proven to be good.

The PF contact forces measured in this study however are presumably higher than in in-vivo circumstances because 1) the simulated body weight is applied solely through the F_Q and the patella tendon (Mason et al. 2008), 2) the ankle and hip assembly are aligned on a fixed vertical line (Mason et al. 2008) and 3) embalmed cadaveric specimen have stiffer soft tissues compared to fresh frozen specimen (Viidik and Lewin 1966).

It must be taken into account that these factors will not be changed when testing anatomical variations or surgical treatments on cadaveric knees. This test rig will only quantify the effect of the anatomical changes or surgical treatments on the PF kinetics of cadaveric knees. Out of these quantifications we expect to achieve useful insights in PF joint forces.

References

1. Besier TF, Draper CE, Gold GE, Beaupre GS, Delp SL. 2005. Patellofemoral joint contact area increases with knee flexion and weight-bearing. J Orthopaed Res. 23:345-350.

2. Bourne R, Goodfellow, J. W. and O'Connor, J. J. 1978. A functional analysis of various knee arthroplasties. Trans. orthop. Res. Soc. . 24:

3. Conlan T, Garth WP, Lemons JE. 1993. Evaluation of the Medial Soft-Tissue Restraints of the Extensor Mechanism of the Knee. J Bone Joint Surg Am. 75A:682-693.

4. de Leva P. 1996. Adjustments to Zatsiorsky-Seluyanov's segment inertia parameters. J Biomech. 29:1223-1230.

5. Mason JJ, Leszko F, Johnson T, Komistek RD. 2008. Patellofemoral joint forces. J Biomech. 41:2337-2348.

6. Mizuno Y, Kumagai M, Mattessich SM, Elias JJ, Ramrattan N, Cosgarea AJ, Chao EYS. 2001. Q-angle influences tibiofemoral and patellofemoral kinematics. J Orthopaed Res. 19:834-840.

7. Muller O, Lo J, Wunschel M, Obloh C, Wulker N. 2009. Simulation of force loaded knee movement in a newly developed in vitro knee simulator. Biomed Tech. 54:142-149.

8. Ostermeier S, Holst M, Bohnsack M, Hurschler C, Stukenborg-Colsman C, Wirth CJ. 2007. Dynamic measurement of patellofemoral contact pressure following reconstruction of the medial patellofemoral ligament: An in vitro study. Clin Biomech. 22:327-335.

9. Patil S, Colwell CW, Ezzet KA, D'Lima DD. 2005. Can normal knee kinematics be restored with unicompartmental knee replacement? J Bone Joint Surg Am. 87A:332-338.

10. Petersilge WJ, Oishi CS, Kaufman KR, Irby SE, Colwell CW. 1994. The Effect of Trochlear Design on Patellofemoral Shear and Compressive Forces in Total Knee Arthroplasty. Clin Orthop Relat R. 124-130.

11. Shoemaker SC, Adams D, Daniel DM, Woo SL. 1993. Quadriceps Anterior Cruciate Graft Interaction - an in-Vitro Study of Joint Kinematics and Anterior Cruciate Ligament Graft Tension. Clin Orthop Relat R. 379-390.

12. Varadarajan KM HR, Johnson T, et al. 2009. Can in vitro systems capture the characteristic differences between the flexion–extension kinematics of the healthy and TKA knee? Med Eng Phys. 31:899-906.

13. Viidik A, Lewin T. 1966. Changes in tensile strength characteristics and histology of rabbit ligaments induced by different modes of postmortal storage. Acta Orthop Scand. 37:141-55.

14. Woo SLY, Abramowitch SD, Kilger R, Liang R. 2006. Biomechanics of knee ligaments: injury, healing, and repair. J Biomech. 39:1-20.

15. Zavatsky AB. 1997. A kinematic-freedom analysis of a flexed-knee-stance testing rig. J Biomech. 30:277-280.

Appendix B

Landmarks, Planes and Measurements

B.1. Landmarks

Twelve landmarks on the femur for rescaling (figure 2.1)

- Femoral Medial Epicondyle (FME): the most anterior and distal osseous prominence over the medial aspect of the medial femoral condyle (LaPrade et al. 2007, Victor et al. 2009, Victor et al. 2009)

- Femoral Medial Sulcus (FMS): depression on the bony surface slightly proximal and posterior to FME (LaPrade et al. 2007, Victor et al. 2009)

- Femoral Lateral Epicondyle (FLE): the most anterior and distal osseous prominence over the lateral aspect of the lateral femoral condyle (LaPrade et al. 2003, Victor et al. 2009)

- Femoral Medial Condyle Posterior (FMCP): the most posterior point of the medial condyle on the 3D model of the femur, aligned along the longitudinal axis of the femur[6]

- Femoral Lateral Condyle Posterior (FLCP): the most posterior point of the lateral condyle on the 3D model of the femur, aligned along the longitudinal axis of the femur[6]

[6] Because the CT scan only captured the knee joint, the longitudinal axis of the femur was estimated by drawing 2 circles on a sagittal view through the shaft of the femur as described by Biedert et al. 1. Biedert RM, Netzer P, Gal I, Sigg A, Tscholl PM. 2011. The lateral condyle index: a new index for assessing the length of the lateral articular trochlea as predisposing factor for patellar instability. Int Orthop. 35:1327-1331.

- Femoral Medial Condyle Distal (FMCD): the most distal point of the medial condyle on the 3D model of the femur, aligned along the longitudinal axis of the femur[6]

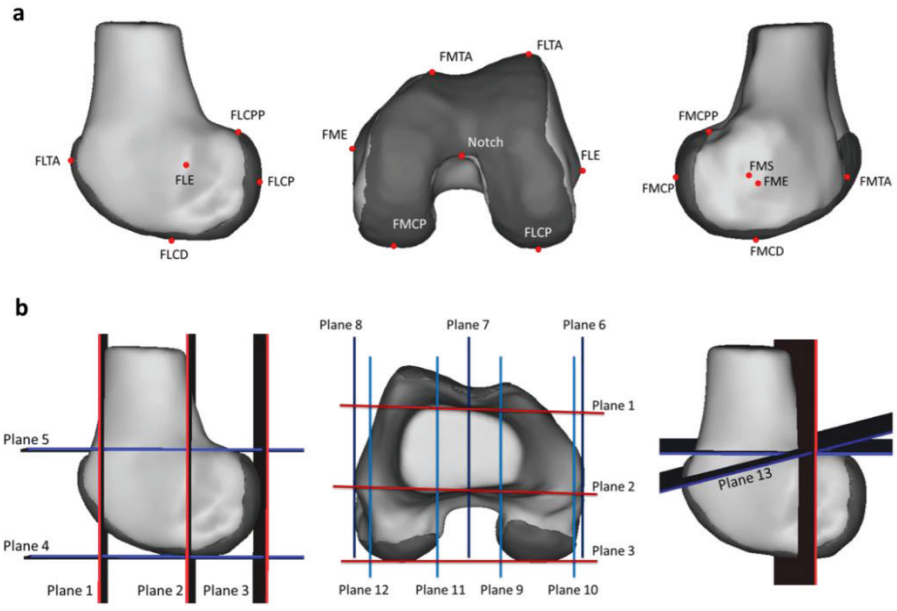

Figure 2.1 3D model of a distal femur composed of bone (light grey) and cartilage (dark grey). Panel a: Location of the 12 landmarks used for Procrustes rescaling: lateral, distal and medial view on the femur. Panel b: Reference planes to evaluate the morphometric parameters in the anteroposterior (left and middle figure), mediolateral (middle figure) and proximodistal (left figure) direction and an auxiliary plane (right figure) to evaluate trochlear depth (details on the landmarks and planes are listed in Appendix B)

- Femoral Lateral Condyle Distal (FLCD): the most distal point of the lateral condyle on the 3D model of the femur, aligned along the longitudinal axis of the femur[6]

- Femoral Medial Trochlea Anterior (FMTA): the most anterior point of the medial trochlea on the 3D model of the femur, aligned along the longitudinal axis of the femur[6]

- Femoral Lateral Trochlea Anterior (FLTA): the most anterior point of the lateral trochlea on the 3D model of the femur, aligned along the longitudinal axis of the femur[6]

- Femoral Medial Condyle Posterior Proximal (FMCPP): the most proximal point of the cartilage on the posterior medial condyle, aligned along the longitudinal axis of the femur[6]

- Femoral Lateral Condyle Posterior Proximal (FLCPP): the most proximal point of the cartilage on the posterior lateral condyle, aligned along the longitudinal axis of the femur[6]

- Notch: the most anterior point in the middle of the femoral notch on a caudal to cranial view of the femur, aligned along the longitudinal axis of the femur[6]

Additional landmarks

Femur

- Deepest point on the trochlea along a plane subtended 15° from the perpendicular to the tangent of the posterior femoral cortex (Dejour et al. 1994)

- Highest point on the trochlea along a plane subtended 15° from the perpendicular to the tangent of the posterior femoral cortex (Dejour et al. 1994)

- Proximal Edge of the trochlear cartilage (PE) (Yamada et al. 2007)

- Femoral Medial Condyle Internal Point (FMCIP): most lateral point of the cartilage of the medial condyle in the axial view of the notch

- Femoral Medial Condyle External Point (FMCEP): most medial point of the cartilage of the medial condyle in the axial view of the notch

- Femoral Lateral Condyle Internal Point (FLCIP): most medial point of the cartilage of the lateral condyle in the axial view of the notch

- Femoral Lateral Condyle External Point (FLCEP): most lateral point of the cartilage of the lateral condyle in the axial view of the notch

- Femoral lateral trochlea: the most anterior point of the lateral trochlea in the axial slice of the femoral lateral condyle posterior

- Femoral medial trochlea: the most anterior point of the medial trochlea in the axial slice of the femoral lateral condyle posterior

- Trochlear deepest point: the deepest point of the trochlea in the axial slice of the femoral lateral condyle posterior
- Trochlear most prominent point: most prominent point of the trochlear groove

Patella

- Patella Lateral point (PL): most lateral point of the articular surface of the patella
- Patella Medial point (PM): most medial point of the articular surface of the patella
- Patella Superior point (PS): most superior point of the articular surface of the patella
- Patella Inferior point (PI): most inferior point of the articular surface of the patella
- Patella ridge: point on the border of the medial and lateral facet of the patella

Tibia

- Tuberositas tibiae
- Most anterior point of the tibial articulating surface of the tibia

B.2. Planes (figure 2.1)

- Plane 1: Anterior sTEA plane: plane tangent to the anterior cortex, parallel to the sTEA
- Plane 2: Posterior sTEA plane: plane tangent to the posterior cortex, parallel to the sTEA
- Plane 3: PCL plane: plane through FMCP and FLCP and parallel to the longitudinal axis of the femur[6]

- Plane 4: Distal condylar plane: plane through FMCD and FLCD and perpendicular to the longitudinal axis of the femur[6]
- Plane 5: Proximal condylar plane: plane through FMCPP and FLCPP and perpendicular to the longitudinal axis of the femur[6]
- Plane 6: Medial plane: plane through FME, parallel to FAAx and perpendicular to PCL
- Plane 7: Notch plane: plane through the notch , parallel to FAAx and perpendicular to PCL
- Plane 8: Lateral plane: plane through FLE, parallel to the longitudinal axis of the femur[6] and perpendicular to PCL
- Plane 9: Internal Medial condyle plane: plane through FMCIP, parallel to the longitudinal axis of the femur[6] and perpendicular to PCL
- Plane 10: External Medial condyle plane: plane through FMCEP, parallel to the longitudinal axis of the femur[6] and perpendicular to PCL
- Plane 11: Internal Lateral condyle plane: plane through FLCIP, parallel to the longitudinal axis of the femur[6] and perpendicular to PCL
- Plane 12: External Lateral condyle plane: plane through FLCEP, parallel to the longitudinal axis of the femur[6] and perpendicular to PCL
- Plane 13: Trochlear depth plane: plane subtended 15° from the perpendicular to the tangent of the posterior femoral cortex to measure the trochlear depth as defined by Dejour et al. (Dejour et al. 1994)

B.3. Measurements

Characteristics of trochlear dysplasia

- Trochlear depth (mm): Distance between the highest and deepest point of the trochlea measured perpendicular to plane 3
- Sulcus angle (°): The angle formed by the intersection of the medial and lateral trochlear facets measured in the axial slice of FLCP
- Lateral inclination angle of the trochlea (°): The angle between the PCL and a line along the lateral facet measured in the axial slice of FLCP

- Medial inclination angle of the trochlea (°): The angle between the PCL and a line along the medial facet measured in the axial slice of FLCP
- Trochlear bump (mm): The distance between plane 1 and the most prominent point of the trochlear groove
- Trochlear cartilage height (mm): The distance between plane 4 and PE
- Caton-Deschamps index (-): The ratio of the distance between PIP and most anterior point of the tibial articulating surface to the length of the articular surface of the patella
- Lateral patellar displacement (mm): The distance from PMP to the perpendicular to plane 3, passing through the most anterior point of the medial condyle
- Patellar tilt (°): The angle between the patellar width line (line between PLP and PMP) and PCL
- Asymmetry trochlear facets (%): Percentage of the medial to the lateral trochlear facet length (medial facet/lateral facet * 100)
- Asymmetry patellar facets (%): Percentage of the medial to the lateral patellar facet length (medial facet/lateral facet length * 100)

Morphometric characteristics

- Medial femur: Distance between the FMTA and plane 3
- Medial trochlea: Distance between FMTA and plane 1
- Medial posterior condyle: Distance between the FMCP and plane 2
- Lateral femur: Distance between FLTA and plane 3
- Lateral trochlea: Distance between FLTA and plane 1
- Lateral posterior condyle: Distance between FLCP condyle and plane 2
- Medial condyle: Distance between FMCPP and plane 4
- Lateral condyle: Distance between FLCPP and plane 4

- Distal femur: Distance between FLE and plane 6
- Medial condyle: Distance between FMCIP and plane 10
- Lateral condyle: Distance between FLCIP and plane 12
- Notch width: Distance between FMCIP and plane 11

References

1. Biedert RM, Netzer P, Gal I, Sigg A, Tscholl PM. 2011. The lateral condyle index: a new index for assessing the length of the lateral articular trochlea as predisposing factor for patellar instability. Int Orthop. 35:1327-1331.

2. Dejour H, Walch G, Nove-Josserand L, Guier C. 1994. Factors of patellar instability: an anatomic radiographic study. Knee surgery, sports traumatology, arthroscopy : official journal of the ESSKA. 2:19-26.

3. LaPrade RE, Engebretsen AH, Ly TV, Johansen S, Wentorf FA, Engebretsen L. 2007. The anatomy of the medial part of the knee. J Bone Joint Surg Am. 89A:2000-2010.

4. LaPrade RF, Ly TV, Wentorf FA, Engebretsen L. 2003. The posterolateral attachments of the knee - A qualitative and quantitative morphologic analysis of the fibular collateral ligament, popliteus tendon, popliteofibular ligament, and lateral gastrocnemius tendon. Am J Sport Med. 31:854-860.

5. Victor J, Van Doninck D, Labey L, Innocenti B, Parizel PM, Bellemans J. 2009. How precise can bony landmarks be determined on a CT scan of the knee? Knee. 16:358-65.

6. Victor J, Wong P, Witvrouw E, Sloten JV, Bellemans J. 2009. How isometric are the medial patellofemoral, superficial medial collateral, and lateral collateral ligaments of the knee? The American journal of sports medicine. 37:2028-36.

7. Yamada Y, Toritsuka Y, Yoshikawa H, Sugamoto K, Horibe S, Shino K. 2007. Morphological analysis of the femoral trochlea in patients with recurrent dislocation of the patella using three-dimensional computer models. J Bone Joint Surg Br. 89B:746-751.

Curriculum Vitae

Personal details

Name: Annemieke Van Haver

Birth: 29/12/1976

Marital status: Married, two children

Email: mvhaver@hotmail.com

Studies

Bachelor in Physiotherapy: University College Ghent (1998)

Master in Physical Education and Movement Sciences (magna cum laude): Ghent University (2002)

Master after Master Biomedical and Clinical Engineering techniques (cum laude): University Leuven (2004)

Professional career

Physiotherapy: in private practices in Belgium and Italy (1998-2004)

Clinical Research Associate: sites in Belgium and Switzerland (2005-2008)

PhD student: University College Ghent (2008-2013)

Publications, indexed in SCI

A. Van Haver, K. De Roo, M. De Beule, S. Van Cauter, E. Audenaert, T. Claessens and P. Verdonk. Semi-automated landmark-based 3D analysis reveals new morphometric characteristics in the trochlear dysplastic femur. Knee Surgery, Sports Traumatology, Arthroscopy DOI: 10.1007/s00167-013-2573-1 (published online on 19 June 2013)

A. Van Haver, K. De Roo, T. Claessens, M. De Beule, P. Verdonk and P. De Baets (2013) Pilot validation study on a quasi-static weight-bearing knee rig. Part H, Journal of Engineering in Medicine. 227 (3): 229-233

S. Van Cauter, M. De Beule, **A. Van Haver** , P. Verdonk and B. Verhegghe (2012) Automated extraction of the femoral anatomical axis for determining the intramedullary rod parameters in total knee arthroplasty. International journal for numerical methods in biomedical engineering. 28(1): 158-169

Submitted for review:

A. Van Haver, K. De Roo, M. De Beule, S. Van Cauter, L. Labey, T. Claessens and P. Verdonk. Replicating joint geometries with rapid prototyping for in-vitro experimental testing: a validation study. Part H, Journal of Engineering in Medicine

A. Van Haver, K. De Roo, M. De Beule, S. Van Cauter, L. Labey, T. Claessens and P. Verdonk. The impact of trochlear dysplasia on the patellofemoral kinematics, contact and stability: a cadaver study with rapid prototyped joint deformities. The American Journal of Sports Medicine

A. Van Haver, P. Mahieu, T. Claessens, P. Verdonk, L. Hao, C. Pattyn and E. Audenaert. A statistical shape model of trochlear dysplasia of the knee. The Knee

F. Dewaele, AF. Kalmar, E. Baert, **A. Van Haver**, G. Hallaert, F. De Mets, L. Cardon, B. Vandersmissen, L. Williams, JP. Kalala Okito, K. Pameleire, K. Vonck, J. Caemaert and D. Van Roost. Trendelenburg position in the treatment of extreme cerebellar slump. Journal of Neurosurgery

Conference contributions

A. Van Haver, P. Mahieu, T. Claessens, P. Verdonk, EA Audenaert (2013) Landmark-based 3D analysis of Trochlear Dysplasia. CORS 2013 (accepted)

A. Van Haver, K. De Roo, M. De Beule, S. Van Cauter, E. Audenaert, T. Claessens, P. Verdonk (2013) A Statistical Shape Model of Trochlear Dysplasia of the Knee. CORS 2013 (accepted)

P. Verdonk, **A. Van Haver**, K. De Roo, E. Audenaert and T. Claessens (2013) Semi-Automated 3D Analysis Reveals New Morphological Differences Between Normal And Trochleodysplatic Knees. ISAKOS

A. Van Haver, T. Claessens, M. De Beule, S. Van Cauter, P. Verdonk (2012) Simulating bony deformities in the knee joint with rapid prototyping: a validation study. 5th PMI conference, Proceedings.

S. Van Cauter, M. De Beule, **A. Van Haver** , P. Verdonk and B. Verhegghe (2011) Automated extraction of the femoral anatomical axis for planning intramedullary rod alignment. 24th annual congress of the international society for technology in arthroplasty, Abstracts.

S. Van Cauter, M. De Beule, **A. Van Haver**, P. Verdonk and B. Verhegghe (2011) Automated extraction of the femoral shaft axis and its distal entry point from full and reduced 3D models

Proceedings of the III ECCOMAS thematic conference on computational vision and medical image processing: VipIMAGE 2011. p.57-61

A. Van Haver, J. Quintelier, M. De Beule, P. De Baets and P. Verdonk (2010) Patellofemoral contact during simulated weight bearing squat movement: a cadaveric study. PMI conference, 4th International, Proceedings.

A. Van Haver, J. Quintelier, P. Verdonk, F. Almqvist, M. De Beule and P. De Baets (2010) Patellofemoral contact during squat simulation on cadaveric knees. Sustainable Construction and design N. 1. p.4-11

A. Van Haver, P. Verdonk, M. De Beule and P. De Baets (2010) Simulated weight bearing squat movement: patellofemoral measurements on cadaveric specimens. Belgian Day on Biomedical Engineering, 9th conference, Abstracts.

A. Van Haver, J. Quintelier, P. Verdonk, F. Almqvist, M. De Beule and P. De Baets (2010) Patellofemoral contact during squat simulation on cadaveric knees. IFMBE proceeedings. 29. p.639-642

A. Van Haver, J. Quintelier, P. De Baets, M. De Beule and P. Verdonk (2010) Patellofemoral contact areas during simulated weight bearing squat. European Society of Biomechanics, 17th Congress, Abstracts.

J. Quintelier, **A. Van Haver**, P. De Baets, P-J De Roo and F. Almqvist (2009) Dynamic analysis of knee biomechanics on cadaveric specimens. International Society of Biomechanics, 22nd Congress, Abstracts.